Author:
Bruno, Vito Domenico

Title:
Development and characterisation of a porcine closed chest model of acute myocardial infarction for cells, drugs, and tissue engineering applications.

Development and characterisation of a porcine closed-chest model of acute myocardial infarction for cells, drugs, and tissue engineering applications.

Vito D. Bruno, Bsc, PhD

A dissertation submitted to the University of Bristol in accordance with the requirements for the award of the degree of MD in the Faculty of Medicine

Supervisors: Prof. Raimondo Ascione

Dr. Tom Johnson

Prof. Sadeeh Suleiman

Bristol Medical School, Translational Health Science

November 2020

Word count: 22161

ABSTRACT

Background: Myocardial infarction (MI) is a major cause of death and disability worldwide with 20% and 45% mortality at 1- and at 5-year respectively. Following MI several detrimental changes are known to occur in the myocardium and a better understanding of these changes would be beneficial for the prevention and treatment of the disease. The aim of this research project was to develop and characterize a large animal model of closed-chest balloon MI with ischaemia-reperfusion injury for diagnostic and therapeutic purposes.

Methods: From November 2016 to March 2018, a closed-chest MI model using percutaneous coronary occlusion was performed in 65 Yorkshire swine. This thesis reports the clinical, haemodynamic, and biochemical parameters related to the model. In addition, this thesis reports the findings cardiac magnetic resonance (CMR) studies performed in the acute and chronic phase after MI.

Results: In total, 65 experiments were performed. Overall experiment-related mortality was 6.1% with 40% of the animals demonstrating malignant arrhythmia during the induction of MI. Longer periods of coronary occlusion (90 minutes vs 60 minutes) resulted in a higher incidence of complications and mortality rate. The average scar size by CMR in the acute phase was 20.70±7.24 grams (as percentage of LV mass = 21.61±7.58 %) at early CMR, and at chronic time point was 8.38±3.5 grams (as percentage of LV mass = 7.93±3.36 %). The left ventricular function (LVEF) decreased significantly at early CMR with a mean value of 43.21±8.62 %. The mean value of cardiac troponin I four hours after MI was 87.47 ± 48.62 ng/ml.

Conclusion: With this work we have been able to develop a reliable and highly reproducible model of acute MI in large animal. The model is affected by a very low failure rate, produces a consistent myocardial scar, and can be used for multiple therapeutic and diagnostic purposes in MI.

FOREWORD

I declare that the work in this dissertation was carried out in accordance with the requirements of the University's Regulations and Code of Practice for Research Degree Programmes and that it has not been submitted for any other academic award. Except where indicated by specific reference in the text, the work is the candidate's own work. Work done in collaboration with, or with the assistance of, others, is indicated as such. Any views expressed in the dissertation are those of the author.

SIGNED: ..... DATE: .....

Signed:
Vito D. Bruno

ACKNOWLEDGMENT

First and foremost, I would like to express my sincere gratitude to my supervisor Prof. Raimondo Ascione for his continuous support of my MD project: he has provided important guidance in all parts of this project, from the design of the study, to the development of the model, data collection, analysis and support with thesis writing. My sincere gratitude goes to him for the substantial effort applied to sustain my progress in this innovative and exciting research field.

I would also like to extend my gratitude to Dr. Tom Johnson: he has been a really valuable trainer guiding me throughout the development of the model and providing me the confidence needed to engage in percutaneous techniques in which I did not have experience. Dr Johnson is a great supervisor and a very knowledgeable cardiologist who has always made himself available for advice and suggestions.

I also would like to express my gratitude to Prof. Saadeh Suleiman. His massive experience in the cardiovascular research field has been an important source of knowledge and he has been a good adviser throughout the project.

Special thanks to Prof. Sarah George, who also looked after me during this project with strong support and critical advice.

I would also like to thank the members of Prof. Ascione's group: Dr Eva Sammut, Mr. Daniel Baz Lopez, Dr Hugo van Oostrom, and Dr Julia Deutsch for their precious support. A special thanks to the TBRC team - without the great support of the entire team at TBRC, this project would not have been possible.

I am truly thankful to my wife Serena and my children Giovanni and Aurora, who patiently supported me during this project and encouraged me to continue even in the difficulties - this thesis is dedicated to them.

PUBLICATIONS AND PRESENTATIONS

The following publications and presentations have arisen from the work undertaken as part of this study to date:

Publications:

D.S. Mansell*, **V.D. Bruno***, E. Sammut, A. Chiribiri, T. Johnson, I. Khaliulin, D. Baz Lopez, H.S. Gill, K.H. Fraser, M. Murphy, T. Krieg, M.S. Suleiman, S. George, R. Ascione, A.N. Cookson. Regional changes in myocardial strain predict ventricular remodelling after myocardial infarction in a large animal model. Submitted to Scientific Reports on March 2020. * indicates co-first authorship

Abstract presentation:

V.D. Bruno, D. Baz Lopez, H Lin, M.S. Suleiman, E. Sammut, A. Cookson, C. Soeller, H.S.Gill, T. Johnson, R. Ascione. Characterization of myocardial injury and extracellular matrix remodeling in a model of porcine closed-chest acute balloon myocardial infarction. 2018 Annual Meeting of the Society of Cardiothoracic Surgery in Great Britain and Ireland. Glasgow 18-20 March 2018.

V.D. Bruno, D. Baz Lopez, E. Sammut, T.W. Johnson, R. Ascione. mRNA expression of Ankyrin-B is associated with ventricular mass reduction after myocardial infarction. 2020 Annual Research Meeting, Society of Cardiothoracic Surgery in Great Britain and Ireland. 7 November 2020.

VD. Bruno[1], E. Sammut, H. Van Oostrom, D. Baz Lopez, D. Odunmbaku-Mansell, M. Murphy, T. Krieg, G. Chanoit, A. Cookson, T W. Johnson, R. Ascione. 2020 Annual Research Meeting, Society of Cardiothoracic Surgery in Great Britain and Ireland. 7 November 2020.

D. Baz Lopez, **V.D.Bruno**, E. Sammut, T.W.Johnson, R.Ascione. Warburg effect in the damaged heart: Transcriptional analysis of glucose and OXPHOS relevant genes. 2020 Annual Research Meeting, Society of Cardiothoracic Surgery in Great Britain and Ireland. 7 November 2020.

Grant Applications:

V.D.Bruno, E. Sammut, T. Johnson, R. Ascione. Establishing global registries of approved research in large animals. Submitted to NC3Rs project grant on the 8/1/2020.

V.D.Bruno, S. George, R.Ascione. Combined tacrolimus and metilprednisolone to reduce scar size after acute myocardial infarction: preclinical proof of concept in an advanced porcine model. Submitted to Heart Research UK Novel and Emerging Technologies (NET) grant. Submitted in October 2020 and invited for full application (deadline 8th January 2021).

TABLE OF CONTENTS

LIST OF TABLES

LIST OF ILLUSTRATION

GLOSSARY OF ABBREVIATION

5SD:	5 standard deviation
ALT:	Aspartate Transaminase
ACT:	Activated clotting time
AP:	Antero-posterior
ASPA:	Animals (Scientific Procedures) Act 1986
BNP:	Brain (B-type) natriuretic peptide
BZ:	Borderzone
CK:	Creatine Kinase
CMR:	Cardiac Magnetic Resonance
cTn:	Cardiac Troponin
cTnI:	Cardiac Troponin I
cTnT:	Cardiac Troponin T
SBP:	Systolic Blood pressure
DBP:	Diastolic Blood pressure
CAD:	Coronary Artery Disease
CHD:	Chronic Heart Disease
CPR:	Cardio-Pulmonary Resuscitation
DC:	Direct Current
ECG:	Electrocardiogram
ECSR:	Endocardial Circumferential Strain Rate
FWHM:	Full Width Half Maximum
HF:	Heart Failure

H/R: Hypoxia Reperfusion

HR: Heart Rate

IHF: Ischaemic Heart Failure

I/R: Ischaemia Reperfusion

IV: Intravenous

JL: Judkin Left

kg: Kilogram

LAO: Left anterior oblique

LCA: Left coronary artery

LDA: Left anterior descending

LVEF: Left Ventricular Ejection Fraction

LVEDD: Left Ventricular End Diastolic Diameter

LVESD: Left Ventricular End Systolic Diameter

LVEDDi: Left Ventricular End Diastolic Diameter (indexed to BSA)

LVESDi: Left Ventricular End Systolic Diameter (indexed to BSA)

MI: Myocardial Infarction

MRI: Magnetic Resonance Imaging

NHS: National Healthcare System

OM: Obtuse Marginal

PPCI: Primary Percutaneous Coronary Intervention

PPL: Procedure Project License

RAO: Right anterior oblique

RCA: Right coronary artery

ROI:	Region of Interest
SE:	Standard Error
SD:	Standard deviation
SMCR:	Society for Cardiovascular Magnetic Resonance
TBRC:	Translational Biomedical Research Centre
TTE:	Transthoracic Echocardiogram
TOE:	Trans-oesophageal Echocardiogram
US:	Ultrasound

Chapter I. INTRODUCTION

Section 1.01 Background

Myocardial infarction (MI) represents the death of cardiac myocytes due to myocardial ischaemia typically triggered by coronary atherosclerotic disease[1]. The result is a demand-supply imbalance whereby available blood supply cannot meet myocardial demand. Narrowing of the lumen of a coronary artery may culminate in a complete blockage due to activated inflammation in the vascular wall/atherosclerotic plaque[2]. There are many predisposing factors to MI including family history/ genetic predisposition, poor diet, lack of exercise, hypercholesterolaemia, hypertension, diabetes mellitus, ageing, male gender, smoking, stress, and obesity[3].

(a) Myocardial infarction

Myocardial infarction is a major cause of death and disability worldwide [4] and it is amongst the most important causes of morbidity and mortality in the United States leading to more than $11 billion in annual hospitalization costs[5]. Among patients older than 45 years who have had an MI, the incidence of recurrent MI or fatal coronary heart disease within 5 years ranges from 17-20%, with similar figures for heart failure with a projected increased cost of almost 100% by 2030[6]. The incidence of MI can be used as a proxy for the prevalence of coronary artery disease (CAD) in that population[4]. An estimated 16.5 million Americans ≥ 20 years of age have coronary heart disease (CHD) with an overall prevalence of 6.3% in US adults (7.4% for males and 5.3% for females)[6]. The partial or complete epicardial coronary occlusion due to the presence of vulnerable plaques is the most common cause of MI and accounts for about 70% of the related lethal events[7].

The advent of primary percutaneous coronary intervention (PPCI) has reduced the incidence of death following MI[8]. However, with improved survival, more patients are left with significant scarring of the myocardium that can be associated with ischaemic heart failure (IHF) associated with poor quality of life and reduced life expectancy[9]. Myocardial changes associated with IHF include cardiomyocyte loss, cell necrosis and/or apoptosis, matrix remodeling and replacement fibrosis (Figure 1).

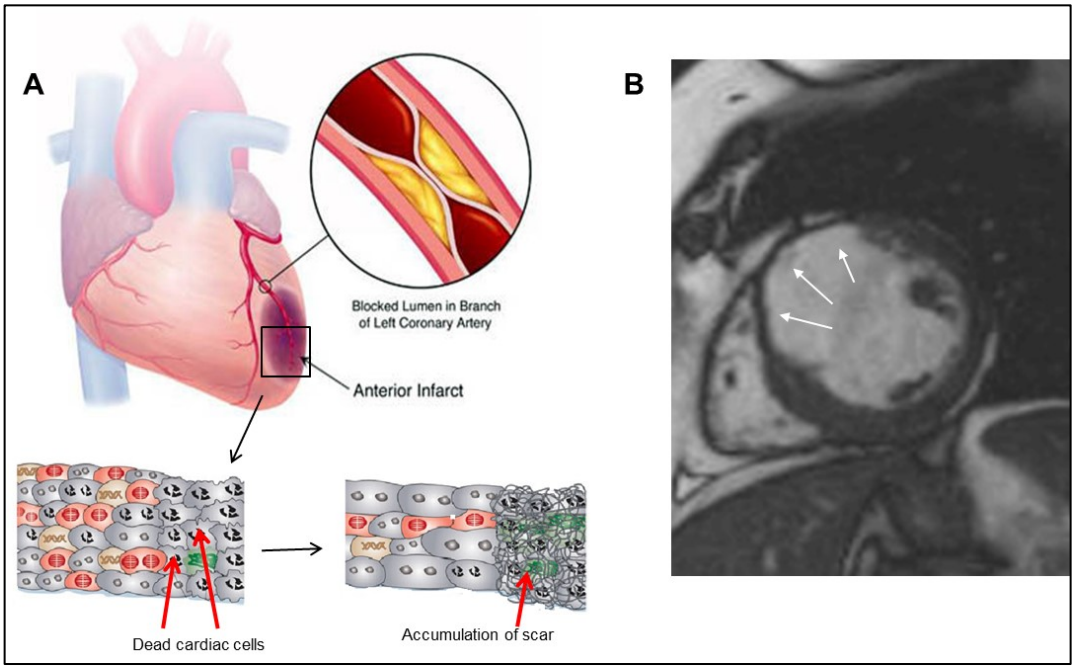

Figure 1. ***A****: Schematic representation of an anterior acute MI (upper panel) and associated myocardial changes (lower panels) with dead cells (grey cells) presence of fibroblasts (green cells) and replacement fibrosis;* ***B****: Cardiac magnetic resonance imaging showing a short-axis view of the mid left ventricle with extensive antero-apical wall scarring/thinning (white arrows)..*

Ischaemic heart failure following acute MI (AMI) afflicts about 30 million people worldwide, with >1.2 million admissions every year in USA/EU[10], >70,000 annual deaths in the UK, and 20% and 45% mortality at 1- and at 5-year respectively[11].

There are only few medical/device IHF therapies are available, which have been associated only with modest clinical benefits, emphasising that more effective IHF treatments and relevant preclinical models are desperately needed for patients with IHF. Regenerative therapies have so far focused on using different cell types to replace the lost myocardial cells after MI, but so far these studies have been scarce with variable efficacy[12,13]. Following MI several detrimental changes occur in the myocardium. For example, myocardial ooedema post-AMI triggers myocardial stiffness[14] and interstitial fibrosis[15]. In addition, inflammation contributes to myocardial damage and death after AMI[16–19]. A better understanding of these changes has led more recently to the research community focusing on developing new treatments that may be able to modulate the inflammatory, proliferative and maturation/scarring phases following AMI (

Figure 2) as alternative approaches.

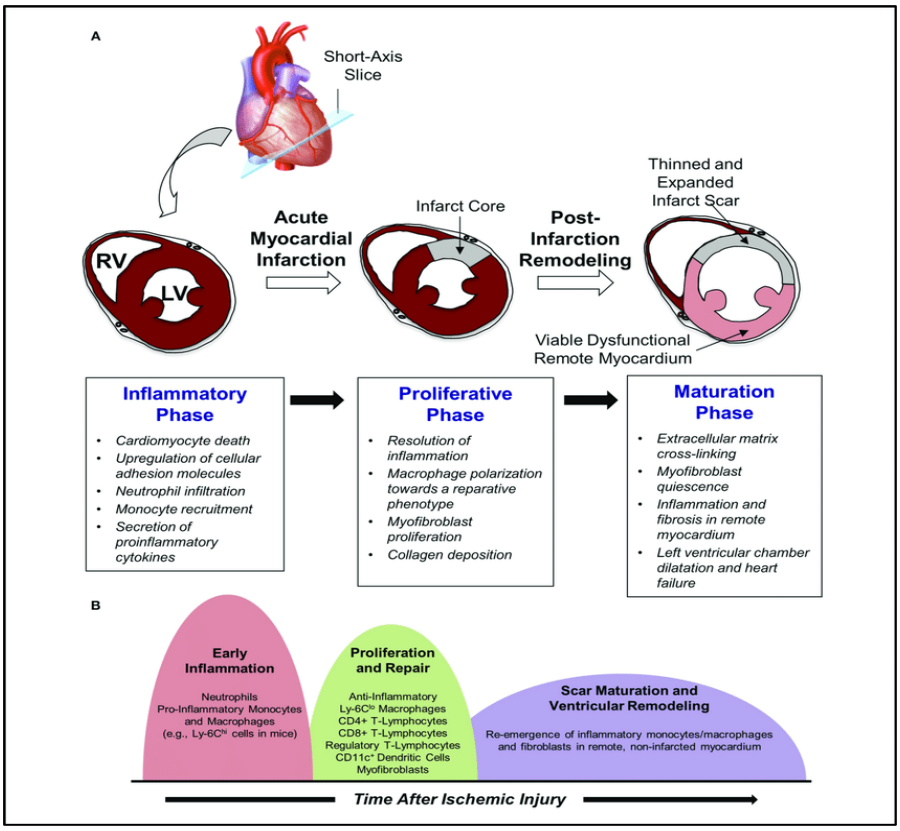

Figure 2. *Myocardial remodeling following AMI: (A) The three phases of repair. (B) Temporal changes in leukocyte populations during repair phase. Figure taken from Weil BR et al. Front Immunol. 2019;10:1-15* [20].

(b) Myocardial Ischaemia reperfusion injury

Myocardial ischaemia is a consequence of an imbalance between oxygen supply and demand and MI is defined as myocardial cells death occurs due to prolonged ischaemia[4]; this imbalance leads to a rapid ATP depletion and accumulation of toxic metabolites. Although systolic dysfunction is almost immediate after an MI[21], histologically, myocardial cells death is not instantaneous but takes a finite period of time - in some animal models this can be as little as 20

minutes[22]. During the first 15-20 minutes early ultrastructural cardiomyocytes changes are evident, but these changes are completely reversible upon rapid restoration of coronary flow[21]. Extending myocardial ischaemia for over 20 minutes is enough to determine a wave-front of dead cardiomyocytes directed from the endocardium to the subepicardium[21,23]. Complete myocardial necrosis requires at least two to four hours and the entire process to a complete, healed infarction usually takes 5-6 weeks[4]. Generally, the presence of sarcolemma disruption and perturbation of the mitochondrial architecture are signs of an irreversible injured cardiomyocyte. The necrosis generates activation of an intense inflammatory reaction and therefore it is common to see a leucocyte infiltration in the infarcted myocardium[21]. The presence of a reperfusion during these periods of time can alter the macroscopic and microscopic appearances of the MI - one common finding is a profound hyperaemia that is particularly evident is the reperfusion is granted after irreversible myocardial damage[21]. Investigating these events is crucial to fully understand the pathophysiology and therefore possible targets for treatment of MI. There is a need for a reliable, reproducible and effective model of cardiac ischaemia-reperfusion injury and acute MI.

Section 1.02 The need for an accurate model of myocardial infarction

Concomitantly to the development of a better understanding of the myocardial changes associated with acute MI (AMI), it is becoming obvious it is critical also to develop and characterize better advanced preclinical AMI models relevant to human so that new treatments can be effectively tested to enhance their translation to bedside. In addition, the advent of primary percutaneous coronary intervention (PPCI) in healthcare systems aiming at reopening the blocked coronary artery within 60-90min from occurrence of AMI has made it obvious that the historical MI model in small rodents with chest opening and permanent coronary ligation is obsolete, and not relevant to the ischaemia-reperfusion injury seen most of the time in humans.

Several in-vitro and in-vivo models have been proposed in the past, but all of them have benefits and limitations. An adequate animal model of MI is very difficult to create for several different factors. First, there is a limitation related to the species used: small animals are easy to use and relatively cheap, but they lack of the adequate anatomical features that are necessary to re-create a reliable model; on the other hand large animals models are more close to the human setting, but they are more expensive and require specialised team of researchers as well as dedicated facilities. Moreover, an adequate animal model should address both the origin of the problem as well as its target[24].

Much information is available on the pig genome[25] as well as housing, feeding, reproductive management and healthcare. The ~2.7 Gb pig genome comprises 18 autosomes and 2 sex chromosomes (X and Y) and is similar to the human genome[26]. The structure and function of the gastrointestinal tract and pharmacokinetics of the pancreas are similar in pigs and humans[27]. Of

note, evidence suggest that the pig genome is much closer to that of human compared to the mice genome with regard to (

Table 1).

	Mean Guanine or Cytosine content in genome			Variance GC content		
Type of sequence	Human	Mouse	Pig	Human	Mouse	Pig
Intron	0.390	0.413	0.407	1.00	0.82	1.02
Coding	0.487	0.500	0.496	1.00	0.69	1.01
3' UTR	0.404	0.426	0.418	1.00	0.77	1.03
5' UTR	0.595	0.593	0.592	1.00	0.81	0.92
Intergenic	0.384	0.399	0.396	1.00	0.91	1.01

Table 1. *Average GC content and the variance among alignments exceeding 40 bp for each species and each functional category. Table taken from Wernersson et al, BMC Genomics (2005)*[28].

This is also confirmed when looking at the evolutionary distances between mouse, pig and human for conserved genome sequences[28].

Pigs have also demonstrated to be a very good animal for the development of a reliable MI model: they have cardiac size, coronary anatomy, baseline heart rate and blood pressure very similar to human, and certainly closer to human than small rodents[24]. The temporal and spatial development of the MI in pigs is also very similar to those of the human. An MI model in these animals can also be conducted with a closed-chest approach and therefore better resemble the events that happen in the PPCI context of an acute MI in the daily clinical practice.

In this thesis we report a large series of myocardial infarction swine models conducted with a closed-chest technique. We will describe the development and characterization of this advanced preclinical model by reporting procedural characteristics, complications as well as the clinical outcomes, biochemical markers and quantification of MI scar measured in-vivo using cardiac magnetic resonance imaging (CMR). We will also show the biochemical, proteomic and histological features of the myocardial infarction.

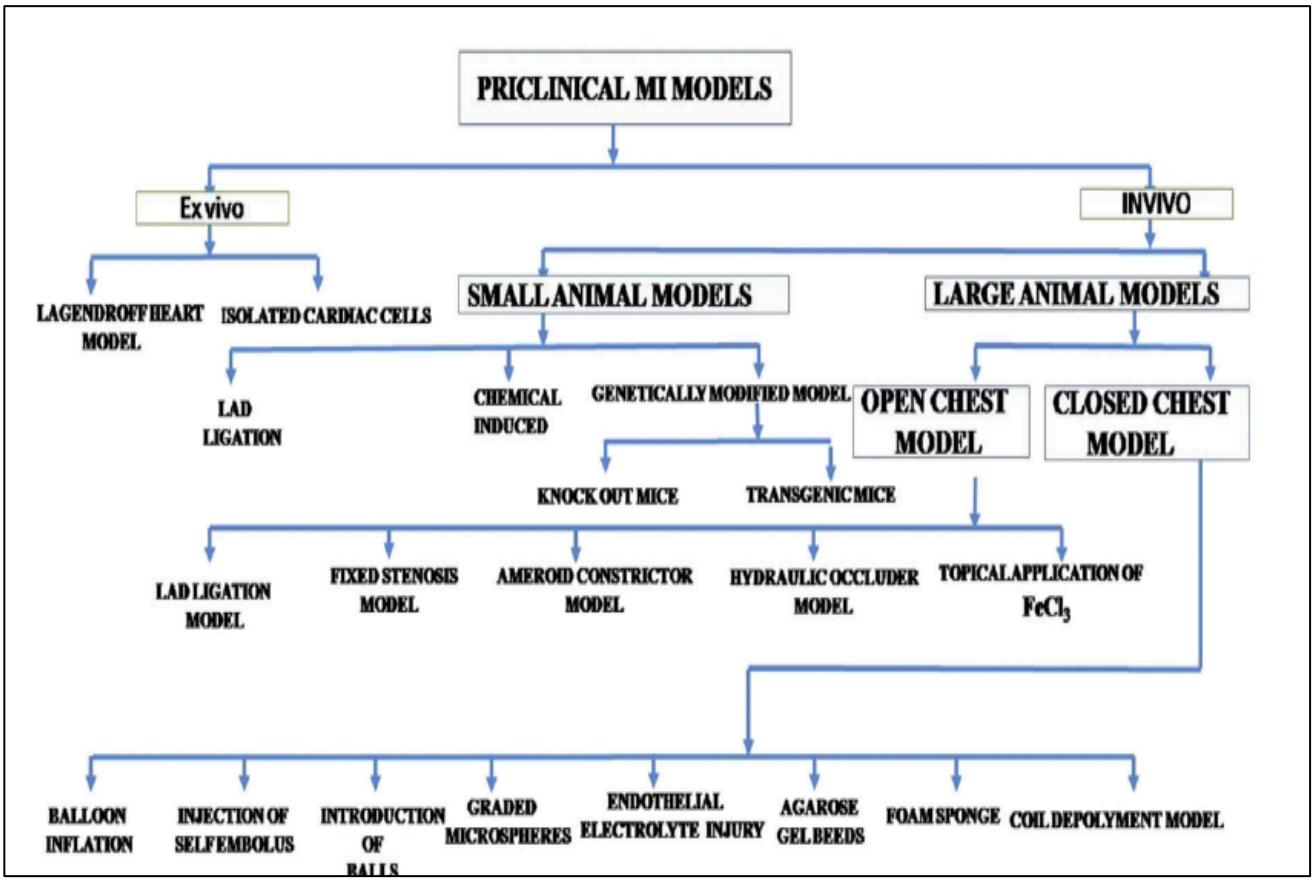

Figure 3. *Schematic representation of preclinical animal models of myocardial infarction. Preclinical models are divided in ex-vivo and in-vivo. In-vivo models are divided in large and small animals' models. Figure taken from Kumar M et al, Regulatory Toxicology and Pharmacology 76(2016) 221-230*[29].

Section 1.03 In-vitro and Ex-vivo models of myocardial ischaemia

(a) Myocyte Cell Culture

Isolated cardiomyocytes have been used as an in-vitro model for ischaemia reperfusion (I/R)[30] and hypoxia re-oxygenation (H/R) of the myocardium. This approach allows a researcher to have full control of the cellular and extracellular environment without confounding effects of other cells or circulating factors. At the same time detailed analysis of the cardiomyocytes can be conducted such as morphology, contractile function, intracellular Ca^{2+} handling and action potentials[31,32]. These models are highly reproducible but cardiomyocyte source and H/R conditions should be carefully considered[30] - generally fresh, isolated adult cardiomyocytes are considered the gold standard for these type of experiments as ischaemic heart disease almost exclusively occur in adults, but they are more difficult to collect and have a technically challenging culture methods affected by a short life of these cells[30]. Neonatal cardiomyocytes, cardiac progenitor cells, induced pluripotent stem cell-derived cells and other cell lines have also been considered[30]. The in-vitro models also are limited by the fact that cannot reliably predict changes in infarct size in-vivo.

(b) Isolated Perfused Heart

Isolated perfused heart models are convenient and reproducible[33]. Using this technique, the heart is removed from the donor animal and connected to an external system that perfuses the heart. It is a model that is ideal for pharmacological and biochemical reasons but can be also used for imaging projects using magnetic resonance imaging (MRI). In the Langendorff model the

perfusate is delivered to the coronaries antegradely via the aorta to perfuse and oxygenate the heart permitting it to beat while a fluid-filled balloon placed into the left ventricular cavity and connected to external transducer will record cardiac indices and function. In this setting the heart does not produce external work. In the working heart mode, the perfusate reaches the heart via the left atrium at a specific filling pressure and the heart pumps perfusate against a hydrostatic pressure set to different levels[34]. These methods are easily to reproduce, can study ischaemia and reperfusion, can accurately measure the infarct size and eliminate confounding effects of intervention on systemic blood pressure or circulating factors[30]. Their limitations are related to tissue oedema, the presence of limited stability, excessive coronary flow and the glucose as only substrate.

Section 1.04 In-vivo models of myocardial ischaemia

(a) Small animal models

Initially, myocardial IR injury and coronary ischaemia models were conducted in large mammals[35] (dogs, pigs etc.), but because of perceived costs, ethical implications and complexity of procedural undertaking requiring skilled operators, these models were replaced by smaller animals models carried out generally with the use of open chest techniques and permanent coronary ligation. Small animals like mice, rats and rabbits have represented a relatively inexpensive option for these models in addition to relative ease in handling and maintenance[29].

Unfortunately over the years it has become obvious that the use of small animal models present major limitations[35] as well as very low reproducibility and high mortality rates as shown by the results of an important survey among 1,500 basic scientists published recently in Nature lifting the lid on result reproducibility and the ‘crisis’ rocking research[36,37]. In addition, the MI

model in small rodents include confounding factors including the surgical stress of a thoracotomy and the related inflammatory response and the resulting physiological thoracic changes. This is usually done in a permanent fashion with surgical ligation of a coronary artery but can be done by temporary snaring around the coronary [38] by the use of snaring devices[39] or a system of sutures[40]. All these procedures carry the risk of an open chest procedure and involve an elevated procedure-related mortality in the first 24 hours[41]. Most of all, those procedures involving permanent coronary ligation negate the key pathophysiological detrimental effects associated with the ischaemia-reperfusion injury seen regularly in the NHS with the advent of the PPCI approach.

The restrictions of small animals are not only limited to the procedural aspects highlighted here. There are other key factors that make these small animal models poorly relevant to human including the major differences in heart rate, coronary anatomy and cardiac size. For instance, in the rat the left sided coronary tree consists of a single vessel with few branches[35] and therefore the size and the characteristic of the infarct could be quite different to those presented in the human. The conduction system is also different from human[42]. An alternative model in small animals could be represented by rabbit[43] although even this model requires a surgical approach and has technical challenges: the left anterior descending artery (LAD) is buried in the heart muscle and the surface of the epicardium is covered by significant fatty tissue[43] and the obtuse marginal (OM) of the left coronary artery is preferable compared to the LAD. This type of model has demonstrated some advantages compared to rat model as rabbits have a third coronary artery and the mortality rate of the model is relatively small. Importantly, rabbits lack collateral blood flow after MI and there is a minimal occurrence of fatal arrhythmias[43].

The difference in cardiac size (Figure 4) has major implications on the translational potential to bedside of treatments. There are differences in scar size observed across preclinical models (from few micrograms in mice to 20-25 gr in pig/humans), the need for scaling up the dose as well as differences in pharmaco-dynamics and pharmaco-kinetics and mode of delivery of the novel treatments. As an example, in mice the new treatments can be delivered only via the intraperitoneal or tail vein route, with no direct approach to central veins or into the coronaries – these are modes of delivery used regularly in humans and can be replicated easily in a pig model.

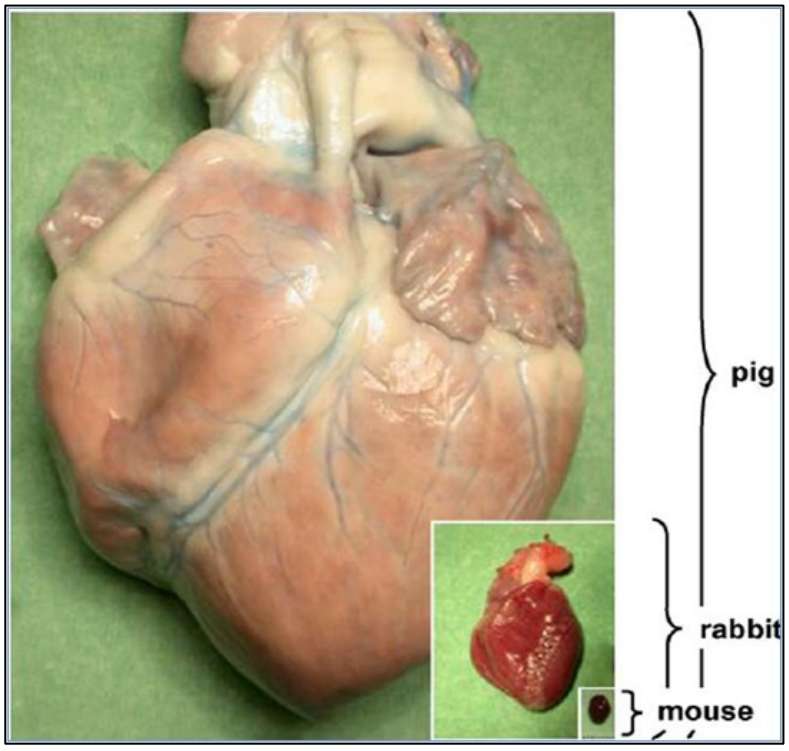

Figure 4. *Difference in size and anatomy between pig, rabbit and mouse hearts. Figure taken from Markannen et al. Cardiovasc Res. 2005, 656-64*[44].

(b) Large animal models

Large animals provide a model of MI that is closer to human, but they are expensive and require more specialised operator expertise and facilities. Most large animal MI models are open chest (surgical) conducted via coronary artery surgical ligation, use of ameroid constrictors or hydraulic occluders, or topical application of $FeCl_3$.

In large animals models the use of ameroid constrictor has been proposed since the fifties[29] especially to create chronic ischaemia: these ameroids consist of casein enclosed in a steel jacket. Once inserted around the coronary, the casein swells and progressively constrict the coronary and induces ischaemia over a period of weeks. These devices are extensively used in porcine models to evaluate cell therapies, gene therapy, pro-angiogenic therapies and collateral circulation physiology[29]. Alternative devices like hydraulic occluders have been also proposed: this model was initially introduced in 1992 by Bolukoglu and colleagues[45] and consist of an expandable silicone membrane within a polyester stretch-resistant cuff that can generate a progressive coronary stenosis via the injections of fluid into the subcutaneous injection port of device. Another open chest method involves the application of $FeCl_3$ (concentration 20-50%) as a strip around the LAD for a period of 45 minutes and then removed. $FeCl_3$ produce perturbation of the endothelial layer and triggers intravascular thrombosis and platelet adhesion, activation, aggregation, granule release and coagulation cascade activation. Generally open chest models carry an elevated mortality risk and are affected by complications like infections. Moreover, they generally need skilled surgeons, anaesthetistand expensive instrumentations.

Different large animals have been used. Primates like rhesus monkeys (Macaca Mulatta) have been used to conduct a surgical model of MI[46]: in this type of model the ligation of the coronary artery (LAD) was completed via a median sternotomy incision in 24 animals. All the animals

survived to the procedure and with a very low rate of ventricular fibrillation (8.3 %). The authors were able to follow-up the animals for 6 months after the MI. Non-human primates (Macaca Mulatta and Macaca Fascicularis) have also been used as model of diet-induced atherosclerosis and consequently MI[47]. Dogs have been also used for the purpose of replicating MI and mostly to replicate a transmural infarct and left ventricular aneurysm[48] and LV remodeling. Open chest ligation of the LAD in swine is a well-established model since the seventies [49].

An alternative approach to this open chest model is represented by the balloon inflation model. In this type of model there is no need to open the chest with the potential to undertake the procedure completely via a percutaneous approach, or with a very small surgical incision at the groin or neck to secure safely vascular access. Once vascular access is obtained, occlusion of the coronary artery is performed by advancing a coronary wire into the targeted coronary artery over which an adequately size coronary balloon is delivered under fluoroscopy guidance. Once in position, the balloon is inflated, then subsequently deflated at predefined timepoints. This technique can be performed in several different large animals including swine and dogs[29] and resembles the ischaemia-reperfusion injury that is thought to be one of the key damage-triggering factors during AMI and associated with the percutaneous treatment of acute myocardial infarction via PPCI. This method requires advanced percutaneous skills by the operator, a minimal surgical approach and precise control of the location and the timing of occlusion of the coronary artery[50].

Other closed-chest models have been also developed; In 2007 Liu and colleagues described an AMI model whereby MI was induced in 12 miniature swine by injecting a strip-shaped clot directly into the LAD. All the animals survived after the procedure and showed large thrombus 6 days after the MI induction[51]. Similar studies have used alternative embolic devices such as platinum or stainless coils[52] or thrombi fibrinogen mixtures into the coronary artery[53]. All these models have

the advantages of replicating in a very close manner the events occurring during MI and providing similar size anatomy, but at significant expensive cost, with associated difficulties in handling and husbandry of the animals, ethical concerns, and the need for sophisticated instruments and a specialised highly skilled team.

Section 1.05 Available methods to measure myocardial damage

One of the issues of undertaking MI in a small animal model was the lack of a reliable and clinically relevant way to measure the infarct size and cardiac function. An ideal preclinical model should allow measurement of these key variables by using methods similar to those used in the NHS. This is a key translational factor as the evaluation of the safety and efficacy of a given new treatment in man. An ideal translational model be would be capable of longitudinal structural evaluation of the heart over time in addition to established biochemical markers - the clinically relevant evaluation of the extent of myocardial scar and of the regional and global left ventricular function is critical. Hence, the accuracy of the methods available to assess these outcome variables in the preclinical setting is paramount to ensure reliability, reproducibility and clinical relevance. Serial circulating release of established biochemical markers of myocardial damage and serial use of Cardiac Magnetic resonance (CMR) imaging and/or echocardiography are the methods used in the NHS to assess patient after AMI. Hence, their use in advanced preclinical models to measure the myocardial damage and how this is affected by new treatment over time is an important consideration.

(a) Biomarkers

(i) Cardiac Damage biomarkers

Biomarkers of cardiac injury have been in use to diagnose myocardial infarction for more than half a century[54] with aspartate transaminase (ALT) identified as the first cardiac biomarker[55] in 1954. Over subsequent years, several different biomarkers have been recognized and found to be more sensitive including creatine kinase (CK), lactate dehydrogenase (LDH) and subsequently CK-MB[54]. However, these biomarkers were lacking specificity to diagnose MI[56]. Cardiac troponins (cTns) are very specific and therefore have become the preferred biomarkers to diagnose acute MI[54,57].

Troponins are relevant for actin and myosin interaction and therefore regulation of the cytoplasmatic contractile function[54]. There are two cardiac specific isoforms of cTn: cTnI and cTnT, while cTnC is also expressed in skeletal muscle and therefore less specific for myocardial damage diagnosis[54]. More recently high sensitivity troponin (hs-cTn) further improved the identification of myocardial injury[58]. Previous investigations have analyzed the role of cardiac biomarkers in a swine model of myocardial infarction[59]: cTnI was found to be the most specific markers and the authors were able to identify a cutoff value of 40 ng/mL at 12 hours after stenosis of the LAD[59], although this study with a longer length and extent of MI compared to our study.In the same study, CK-MB was tested but was found to have a sub-optimal specificity and sensitivity. Myoglobin showed an earlier peak compared to cTnI and CK-MB with an optimal cut-off value of 25 µg/L at 6 hours, but this was a non-significant increase after MI in swine[59]. In human, a contemporary cTnI assay detects plasma cTn levels as low as 0.006 ng/mL with an assay range that spans 4 orders of magnitude (0.006-50 ng/mL) and the most recent diagnostic cut-off of TnI-

Ultra is > 0.04 ng/mL[60]. In this project described in this thesis, we have tested the serum concentration of cTnI at different timepoints as a specific marker of myocardial damage.

(ii) Other biomarkers

The initial ischaemic injury to the heart triggers an inflammatory response that contributes to the pathogenesis of LV remodeling after MI[61]. Several inflammatory markers have being used as biomarkers in acute myocardial infarction[61], but there are no specific inflammatory markers currently used in the standard management of patients with MI[62]. Leukocytosis after MI has shown to have a predictive role in terms of prognostic outcome having an independent association with failure of reperfusion, thrombus resistance, incidence of heart failure and mortality[63]. Other inflammatory markers linked to MI are progenitors cells like CD34+ stem cells[64], myeloperoxidase[61], C-reactive protein[65], growth factors[61], matrix metalloproteinases[61]. Cytokines and chemokines have also shown an important correlation with MI: IL-1β levels in patients with MI increases within 2 hours of presentation[66], while IL-33 receptor has been correlated with HF and mortality after MI[61]. IL-6 is a key secondary cytokine produced by inflammatory cells in response to various stimuli[61] and is elevated after MI with a peak one day after the infarct. Furthermore, the level of IL-6 after MI has been correlated to prognosis, short and long term mortality[61] and LV dilatation at 6 months[67] and specifically elevated IL-6 (> 20 pg/dl) in the first 24 hours after MI has been identified as a predictor of mortality[68]. IL-10 is an anti-inflammatory cytokine - its levels at day 3 after MI correlates with LVEF at 6 months[61] with higher IL-10 predicting better LV function[61], with some authors reporting elevated levels IL-10 as predictor of mortality[61]. Serum TNF-α are elevated in patients with MI[69], but do not correlate well with LV remodeling or infarct size[61]; however level of TNF-α receptor type 1 (sTNFR1) was associated with infarct size[69]. BNP is synthesized mostly by ventricular cardiomyocytes as the preprohormone

consisting of 134 amino acids[70]: measures of plasma BNP is used for diagnosis and risk stratification in patients with HF and rapid increase in BNP secretion has also been found after MI[71]. In a previously published study[72], Omland and colleagues have found a plasma concentration of BNP of 33.1± 3.8 pmol/L three days after MI in human. More recently in another study[73], the authors measured the serum concentration of BNP in 75 patients within 48 hours from an acute MI recording a value of 462.875 ± 405.878 pg/ml. In this thesis we have analysed the plasma concentration of IL-6 and BNP in 5 experiments.

(b) Proteomics

The molecular mechanisms behind ventricular remodeling after myocardial infarction remain poorly understood[74]. In this sense, proteomics analysis might be helpful to determine the processes that contribute to post-infarction remodeling and therefore identify possible molecular pathways and potential therapeutic targets. Previous studies have already quantitatively evaluated proteomics in the context of both small and large animal MI models[74,75] proving the efficacy of such technique in improving the knowledge of the molecular events after MI. Several different changes in proteins expression have been identified by these studies with some peculiar patterns being discovered. Using this technique, Yang et al[74] noted a global mitochondrial dysfunction and impaired shuttling and utilization of high-energy phosphate in the infarct borderzone (BZ)[74]. In another swine model, Binek and colleagues[76] characterized proteins dynamics in ischaemic and remote myocardium at timepoints up to one week after MI. The authors were able to describe molecular processes at different timepoints after the myocardial infarction showing that at early reperfusion the ischaemic area showed a coordinated upregulation of inflammatory processes,

while interstitial proteins, angiogenesis and cardio-renal signaling processes increased at later stages[76].

(c) Echocardiogram

Transthoracic echocardiogram (TTE) is a non-invasive diagnostic tool that is largely used in human cardiovascular medicine to assess cardiac function and hemodynamics[77], but in swine can be challenging[78] because of the keel-shaped chest and cannot be reliably used when the chest is open[78]. Therefore its use is very limited in this context and alternative methods like trans-oesophageal echocardiogram (TOE) are generally preferred as they provide better quality images[78]. Previous studies have used this methodology mostly to evaluate left ventricular function, hemodynamics and valvular apparatus[78] and has been considered an adequate imaging technique for these purposes. However, echocardiography is a generic imaging modality not able to provide detailed tissue characterisation. In addition, the segmental wall motion of the left ventricle and the ejection fraction reported with these methods can be measured less accurately compared to the CMR. Specifically, echocardiography does not allow direct measurement of myocardial scarring.

(d) Cardiac Magnetic Resonance (CMR)

Cardiac magnetic resonance is the most advanced imaging modality used in modern healthcare systems for the assessment of the damage following MI in patients. In clinical studies it is frequently the method of choice to evaluate the efficacy of novel therapies after acute MI. In addition, it is the gold standard imaging for quantifying MI size[79]. Generally, the size of an MI is quantified using late gadolinium enhancement. Gadolinium is an extracellular agent - after acute myocardial necrosis, the cells membranes are damaged, permitting the contrast agent to enter these cells. Therefore, since the contrast agent would redistribute from the vascular compartment to the interstitial space, its concentration is related to the area damaged by the MI[80] (

Figure 5).

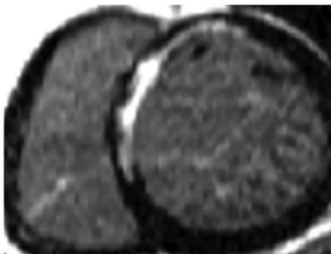

Figure 5. *Cardiac magnetic resonance imaging showing a transverse view of the mid left ventricle with extensive anterior septum scarring (white area).Figure taken from Captur et al, Heart 2016;102:1429-1435*[81].

Other CMR methods of scar assessment have been proposed in the recent past including native T1 mapping[82]: this is a novel technique that can perform quantitative determination of the myocardium without contrast agent[83]. It has been tested in swine model and was able to determine the location of the scar with high specificity however appeared to underestimate the size of myocardial infarction when compared to histopathology[83]. We have conducted a full CMR examination with a 3T MRI in all the animals at different timepoints (early and late follow-up after MI). Table 2 shows the normal values for ventricular measures in adult human.

	Men		**Women**	
	Mean (SD)	**LL-UL**	**Mean (SD)**	**LL-UL**
LVEF(%)	63(6)	49-79	66(7)	52-79
LVEDV(ml)	145(31)	95-215	112(21)	78-167
LVESV(ml)	53(18)	25-85	39(12)	21-64
LVEDVi(ml/m2)	77(15)	50-108	69(12)	50-96
LVESVi(ml/m2)	29(9)	11-47	24(7)	10-40
SV(ml)	103(21)	61-145	83(16)	52-114
SVi(ml/m2)	52(10)	33-72	49(8)	33-64
CO(l/min)	5.6(1.1)	3.4-7.8	4.5(0.9)	2.7-6.3

LVEF: Left ventricular ejection fraction; LVEDV: Left ventricular end diastolic volume; LVESV: left ventricular end systolic volume; LVEDVi: left ventricular end systolic volume indexed; LVESVi: left ventricular end systolic volume indexed; SV: stroke volume; SVi: stroke volume indexed; CO: Cardiac output. LL: Lower Limit; UL: upper limit.

Table 2. Ventricular measurements in adult humans, reference ranges ("normal values") by gender for cardiovascular MRI. Modified from Kawel-Boehm et al.

Few studies have investigated the size of acute myocardial infarction over time in humans reporting a great variance between the different timepoints and the location of the scar. Table 3 shows the scar size as percentage of LV mass in human at different timepoints.

	Timepoint			
Reference	**Early**	**Intermediate**	**Late**	**Very late**
Ingkanisorn(2004)[84]	16 ± 12 (0-5 days)			11 ± 9(2 months)
Hombach(2005)[85]		11.9 ± 7.3 (6.1 ± 2.2 days)		7.8 ± 5.3(6-9 months)
Ibrahim(2010)[86]	18.3[1.5-45.2] (1 day)	12.9 [1.3–37.4] (7 days)	11.3[1.0-40.5](35 days)	11.6[0.9-37.3](6 months)
Dell'armellina(2011)	27 ± 15(12-48 hours)			21 ± 11 (6 months)
Mather(2011)[87]	27.2 ± 13.9(2 days)	21.6 ± 17.5(7 days)	21.1 ± 13.7(30 days)	19 ± 13.9(3 months)
Ganame(2011)[88]		17.7 ± 10.4(7 days)	12.3 ± 8.1(28 days)	10.7 ± 6.2(1 year)

Table 3. Scar size (as percentage of total LV mass) in human at different timepoints. Data are reported as mean and SD or as median and range (in square brackets). The precise timepoint for each study is reported in brackets.

Chapter II. GENERAL METHODOLOGY

The aim of this research project was to develop and characterize a porcine model of closed-chest balloon MI with ischaemia-reperfusion injury in order to replicate a typical NHS clinical scenario of MI treated with an emergency PPCI. This work was conducted at the Translational Biomedical Research Centre (TBRC) of the University of Bristol (http://www.bristol.ac.uk/health-sciences/research/tbrc/), which is staffed by expert veterinary and clinical NHS specialists as well as animal interface technicians overseeing the animal welfare before, during and after the specialist procedures.

The experimental procedures were conducted between 1st November 2016 and 8th March 2018 and involved 65 Yorkshire swine (weight range 55 to 65 kg). All the experiments were conducted according to and regulated by the Animal (Scientific Procedure) Act (ASPA) 1986 under the PPL 70/8975. I conducted all the MI percutaneous procedures having gone through a formal training process involving initially passing Home Office course (Modules 1-4 and Pig bolt) to gain a Personal License. Subsequently I underwent training in percutaneous coronary procedures under supervision by an expert NHS Interventional Cardiologist till I was signed off to work independently. During the MI procedures there was a team of 5 veterinary/NHS expert clinician involved to oversee different aspects of care/animal wellbeing with myself being responsible for the undertaking of the MI procedure and the clinical management including the treatment of intraoperative complications. All those involved in these experimental procedures in this research project have been trained in line with ASPA guidelines and were in possession of a valid Home Office Personal License at the time of conducting the experiments. The animal husbandry was in

accordance with Home Office regulations and the 3R (Refinement, Reduction and Replacement) rules have been applied throughout the research project.

The goal of this project was to develop and characterize this model and to evaluate the efficacy, reliability and reproducibility of a closed-chest MI model of myocardial ischaemia-reperfusion injury in a large animal. Moreover, we wanted to evaluatethe impact of shorter (60 minutes) versus longer (90 minutes) ischaemia time as well as the impact of immunosuppression on scar size and post-operative outcome.

Section 2.01 Benefits of the model

We decided to opt for this model because it provides several clinical and translational advantages. First, the coronary and heart anatomy of the pig is very similar to the human anatomy. The size and the position of the heart in the chest is very close to the human: the coronary anatomy comprise two main coronary arteries (RCA and LCA) and they arise from the aortic root in a very similar position to that of the human. The LAD anatomy is also very similar providing septal and diagonal branches. Second, the size of a Yorkshire pig at 4-5 months of age (approx. 50 – 60 kg) permitted us to use the same equipment and the same instruments used in an adult cardiac catheter laboratory. Third, the use of a closed-chest model reduces to the minimal the surgical incisions and therefore the stress correlated to it. Moreover, the reason to chose pigs is that they can be easily bred, are reasonably inexpensive and easy to keep. They can also be subjected to long term protocols including diet, development of atherosclerosis, collateral growth, neovascularization, myocardial hibernation, postinfarction remodeling and heart failure models. The swine MI model has demonstrated that via steerable catheters a localized damage can be generated in a selected

area of the myocardium and therefore use it as ideal model to understand the development, the structure and the possible treatment pathways of the MI. This model has also been used to deliver stem cells into the infarcted area[89] through catheter based or direct surgical techniques.

Section 2.02 Technical aspects and model's challenges

The closed-chest model for myocardial ischaemia-reperfusion and myocardial infarction has several technical aspects and possible difficulties to consider. First, it requires familiarity with the percutaneous coronary techniques and their relative technical aspects. The first part of these experiments was intended to acquire these essential skills. The open chest model, for certain aspects, might be more approachable by a surgeon or a researcher with surgical background, while the swine closed-chest model requires mastering of both surgical and catheter-based skills. As the swine arteries are prone to spasm, surgical exposure of the target artery for vascular access may be required in order to safely conduct this procedure. Once vascular access is gained, there is the need for a competency in catheter-based coronary procedure and this might be not always practicable in an ordinary research facility. The learning curve for the entire model is steep and one way to overcome this problem is the integrative approach of two different operators, one with surgical background and one with catheter-based background, until at least one of the operators has gained both competencies. This has been our approach: in the first part of the study, the vast majority of the procedures were conducted by two operators (myself and an expert NHS interventional cardiologist), while subsequently the procedures were conducted by a single researcher/operator. Another important technical consideration is related to the prevention of complication and mortality. During the induction of the MI with ongoing ischaemia the occurrence of severe ventricular arrhythmias is elevated. The prevention or treatment of these complications

requires several different preventive measures, similar to those implemented in the NHS. In our approach, we have used Amiodarone and magnesium infusion in the attempt to prevent/reduce ventricular arrhythmic events. In addition, we have also developed a cardio-pulmonary resuscitation (CPR) algorithm, based on the one used in the NHS, that has been successfully used during the entire project and permitted us to achieve an intra-operative mortality rate of less than 5%. One aspect that is also important to consider is that the size of the myocardial scar obtained can be vary - this is due to the variability of the anatomy of the swine coronaries and specifically of the left anterior descending (LAD) coronary artery, which we targeted, with several different variants in relation to the diagonal/ septal branches as seen in humans. Compared to humans, pigs have shorter but larger LCA trunks and diagonal or obtuse marginal branches with slightly higher variability of coronary anatomy[90]. During the experiments reported in this thesis we consistently occluded the mid-portion of the LAD (except for two animals in which we have occluded the mid portion of the circumflex) just distal to the first diagonal branch. Despite this consistency in approach we noted that the number of diagonals and septal branches was variable from animal to animal and reasoned that this factor might have led to some variability in scar size obtained after the MI. However, this limitation would apply also to alternative approaches like the open thoracotomy approach, while reflecting the variability also seen in humans.

The model described in this thesis has also the advantage of a transient coronary blood flow occlusion, hence mimicking the ischaemia-reperfusion injury seen in the NHS in patients with ongoing AMI blue-lighted to the Cath Lab for emergency PPCI to re-open an acutely blocked coronary artery within 60-90min. Accordingly, in the vast majority of the experiments we kept the coronary balloon inflated to occlude the coronary artery for 60 minutes to obtain an obvious myocardial scar while preventing procedure-related malignant arrhythmias/mortality. For model

characterization, in a study sub-group we performed a longer coronary occlusion (90 minutes) and then we undertook comparative evaluations vs the 60 minutes coronary occlusion group.

Section 2.03 Anaesthetic procedures

The animals were all admitted to our research maintenance facility one week prior to intervention to let them adapt to the surrounding environment as per Home Office acclimatization regulations. During this period, a single daily dose of Aspirin (75 mg) was given orally with food for 5-7 consecutive days prior to admission into the clinical interventional facility. The night before the MI induction procedure, the animals were starved for 8 hours with continuous access to drinking water.

The following morning, they were then transferred into the anaesthetic induction room of the TBRC. An intramuscular injection of Ketamine (10 mg/Kg) and Dexmedetomidine (15 mcg/kg) was given in the superior aspect of the neck. Oxygenation was granted via facemask with an oxygen flow of 5 l/min. Next, an intravenous (IV) catheter was positioned in an ear vein. The ear veins are branches of the caudal auricular vein and the superficial cervical vein and usually are easily visible and prominent on pigs of any size - we generally cannulated the lateral more prominent vein using a 22-gauge needle peripheral vein cannula. The induction of general anaesthesia was carried out by expert veterinary anaesthetists and achieved via IV infusion of Propofol at 1.0 mg/Kg boluses until loss of palpebral reflex. After induction, the airways were secured with appropriate size endotracheal tube. The intubation was mostly conducted in sternal position and a size 6.5 to 7.5 mm endotracheal tube was used in most cases. The anaesthesia was maintained by Isoflurane in oxygen with the vaporizer set at 2%. The animals were mechanically ventilated using a target of Vt of 10-20 ml/Kg and a RR of 10-20 breaths per minute. Setting were

adjusted to maintain ET-CO2 between 35 and 45 mmHg. An accurate shaving and cleaning of the skin in the neck region (or groin region if percutaneous approach) was achieved in preparation for the surgical field.

Continuous monitoring of the vital parameters was established by using different monitoring devices including an electrocardiogram (ECG), an invasive arterial blood pressure catheter, a peripheral oxygen saturation probe, a temperature probe and a urinary catheter. Three ECG leads were connected following the standard ECG lead positioning: yellow lead on the left upper limb, red lead on the right upper limb and green lead on the lower left limb. A null lead was positioned to the right lower limb. The leads were then connected to a cardiac monitor for real-time ECG monitoring. A peripheral oxygen saturation probe was applied on the tail to monitor oxygen saturation throughout the entire procedure. A urinary catheter was also placed as soon as the animal was anaesthetized. Once full monitoring was achieved, the animal was moved to the TBRC hybrid surgical theatre also featuring a floor-mounted Artis Zee Siemens Cath Lab. Before proceeding with the experiment, the animal was secured to the surgical table in a supine position and two external defibrillator pads were applied on the superior part of the right side of the chest and on the lower part of the left side of the chest and connected to a semi-automatic defibrillator (Lifepack 20e, Physio-Control, Inc., Redmond, WA). The defibrillator device was used in case of major arrhythmias (Ventricular Fibrillation or Ventricular Tachycardia) occurring during acute ischaemia period where immediate DC defibrillation/cardioversion was required.

On completion of this basic setting up and having used CMR compatible materials, the animal was returned in the hybrid theatre for the closed-chest MI procedure.

Section 2.04 Vascular access and setting up

Different vascular access approaches can be used for this closed-chest MI model. A small surgical incision (4-5cm) approach to the groin or neck for femoral or carotid artery direct exposure is the most used approach to consistently access to the vasculature. This is supported by previous reports by other authors[91] suggesting that access to peripheral arteries in pigs may require surgical exposure to minimize the risk of arterial spasm/severe bleeding. For this reason, in this project we used a small surgical exposure in the neck or groin (mostly commonly neck) to enhance direct arterial cannulation. To explore other options, we have also explored access via a percutaneous US-guided femoral approach (experiments not included in this research project). The small surgical incision in the neck was favored to femoral incision as it permitted the contemporaneous direct cannulation of the jugular vein for a central venous line to provide infusion of antiarrhythmic and inotropic drugs during the MI model procedure. Moreover, this approach is technically less challenging, provides better animal welfare as the groin incision might affect the mobilization of the animal and can be exposed to higher risk of infection, while providing a more direct a shorter route to the aortic root/coronary arteries.

(a) Closed-chest balloon MI procedure

Following general anaesthesia, full invasive monitoring and acquisition of baseline MRI scan, the animal was secured in dorsal recumbent position on the operating table with legs were retracted caudolaterally. To reduce the risk of displacement of the animal during the procedure and/or during possible DC cardioversions, a further securing elastic strap was positioned around the abdomen. The animal was positioned differently depending on the vascular approach used: in

case of carotid approach the head of the pig was directed towards the bed control station as this would permit an easier catheter procedure, whereas the position was the opposite in case of femoral approach (Figure 6).

Surgical preparation of the access area was then conducted using 2% chlorhexidine gluconate (CHG) in 70% isopropyl alcohol (IPA) (ChloraPrep®, Carefusion, El Paso, TX 79912, USA) to disinfect the neck and the superior part of the chest. A surgical draping was then completed using a coronary angiographic drape (Kimal SurgiGuard®, Kimal PLC, Uxbridge, UK) .

Figure 6. *The animal is positioned on the Cath-lab table, fully anaesthetized, artificially ventilated and fully monitored. In the picture we see the C-Arm used for the X-ray procedure as well as the monitor used for the catheter-based procedures*

Next, a longitudinal incision (~ 5 cm long) of the left side of the neck three cm laterally to the trachea was made: after skin incision, the platysma muscle was exposed and incised longitudinally using thermocautery. Blunt dissection of the muscular plane posterior to the planes of the sterno-cephalic and brachiocephalic muscles and anterior to the sternomastoideus, on the lateral side of the neck, was used to expose the external jugular vein for cannulation with the aid of a self-retaining retractor: Figure 7 shows the surgical approach to jugular vein via a 5 cm longitudinal incision of the left side of the neck.

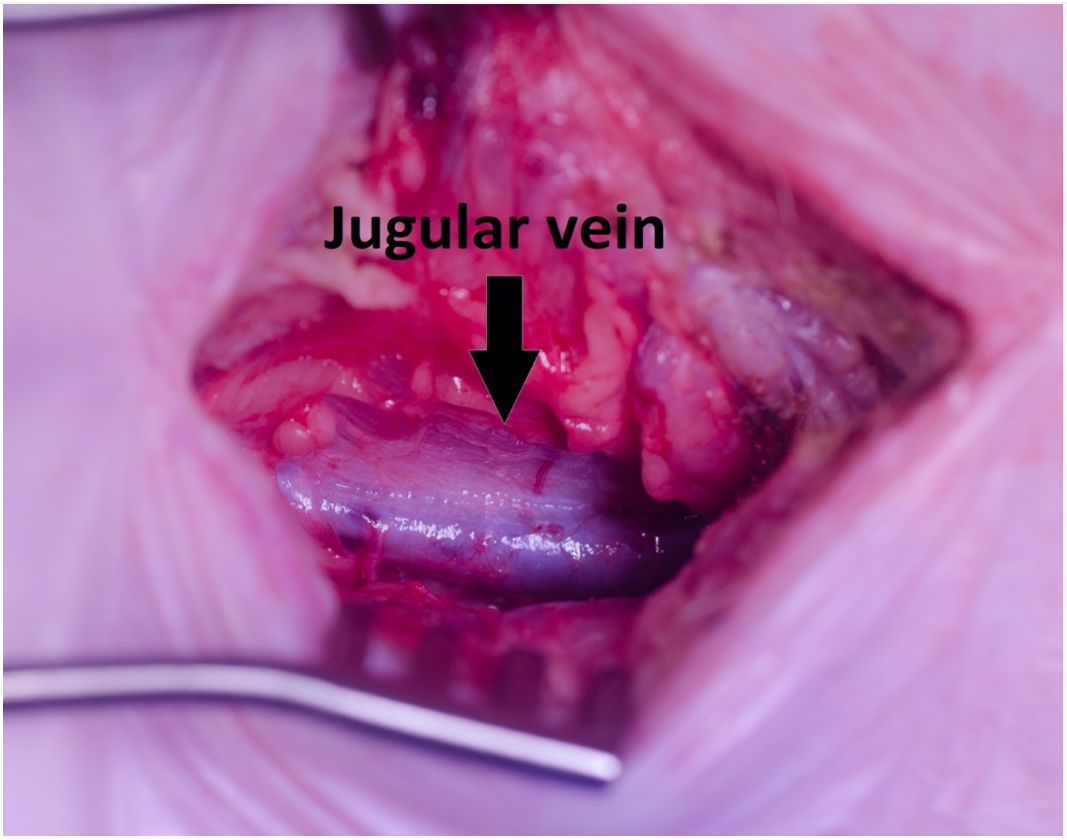

Figure 7. *Surgical Exposure of the jugular vein*

The jugular vein was then cannulated using a double lumen central venous catheter (Figure 8)and secured to the skin with 2-0 polyglactin sutures (Vicryl®, Ethicon Inc. Sommerville, NJ, USA). The cannulation was conducted using the Seldinger technique - after puncture of the vein under direct vision, a guidewire was introduced into the vein lumen and the venous line was positioned over the wire. Two fluid lines were connected to both ends of the venous cannula to provide infusion of Amiodarone (300 mg over 4 hours) and saline solution (1 ml/kg/hour) during the MI procedure.

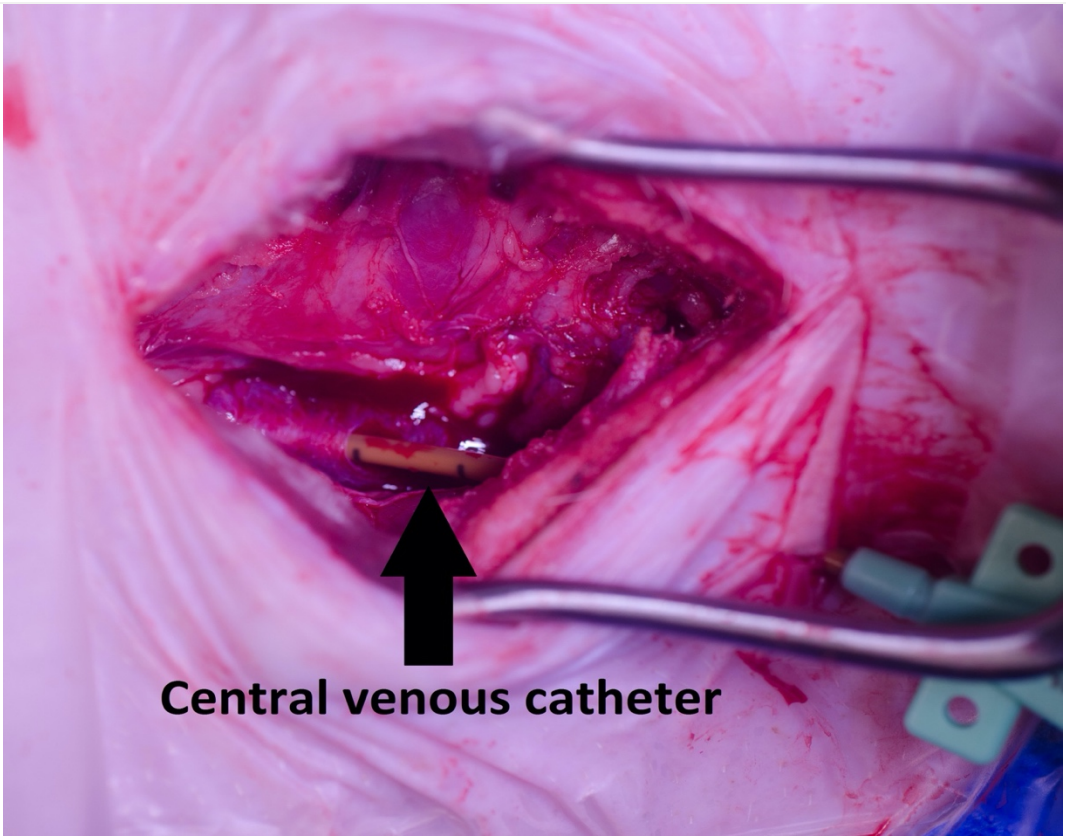

Figure 8. *Central venous catheter inserted into the left internal jugular vein*

After exposure and cannulation of the jugular vein, heparin was administered with an initial dose of 150 IU/Kg aiming for an activated clotting time (ACT) above 250 seconds. This was checked every 15-20 minutes with Hemochron 801® (Soma Technologies Inc, Bloomfield CT, USA). The

use of heparin was indicated to reduce the risk of thromboembolic complication during the cannulation of the carotid artery and the coronary occlusion by prolonged balloon inflation.

After heparin, dissection of the facial plane between the trachea and the sternomastoideus on the medial aspect of the neck permitted palpation of the carotid arterial pulse. Careful exposure of the anterior aspect of the carotid artery was conducted without using thermocautery, but only with the use of scissors to minimise spasm of the artery. Figure 9 shows the left carotid artery exposed and prepared for cannulation.

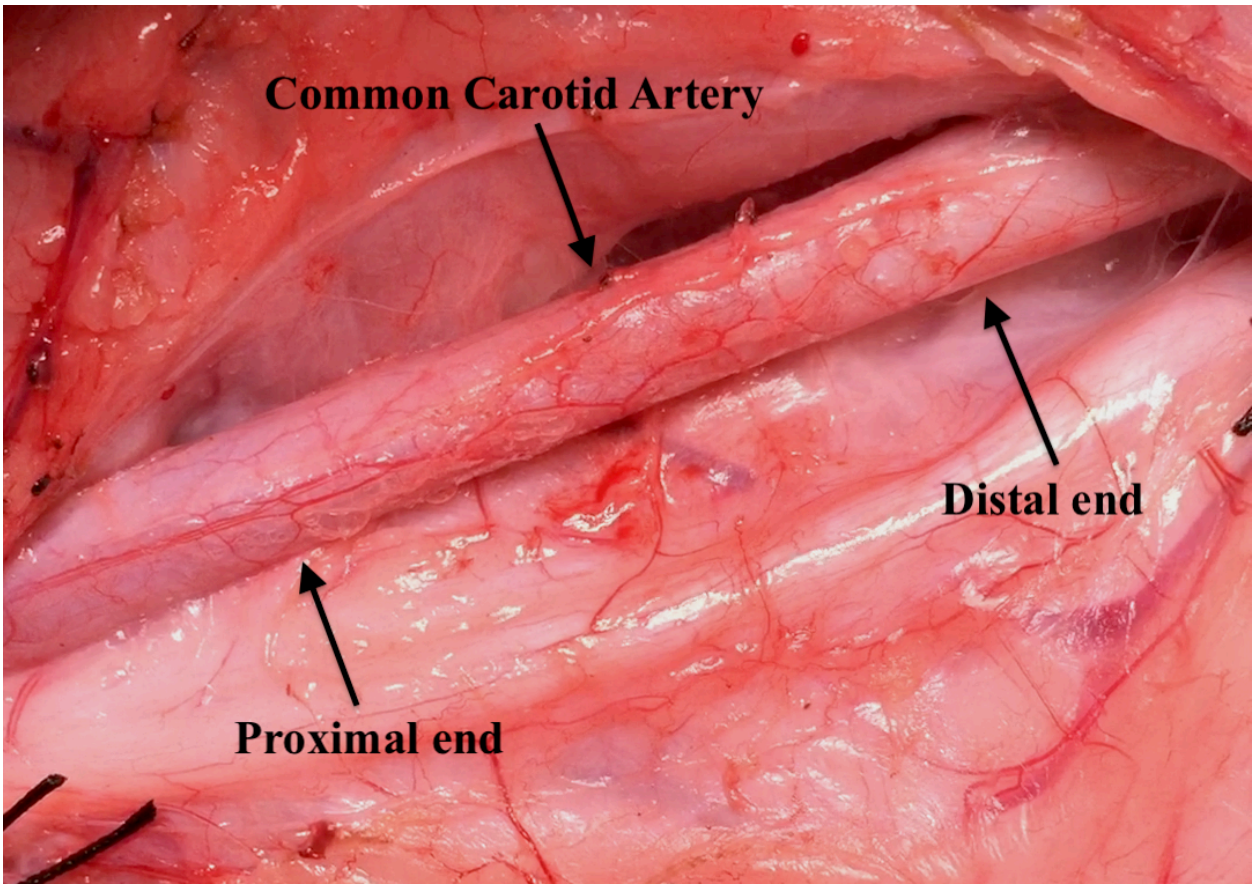

Figure 9. *Left carotid artery exposed and prepared for cannulation*

Differently from other authors[91,92] to minimize the exposure and keep the manipulation of the carotid artery to the minimum we avoided the use of vessel loops excessive manipulation could cause spasm. As previously reported,[91,92] careful exposure should be conducted to avoid a damage of the vagus nerve and related Horner's syndrome.

The common carotid artery was then cannulated using the Seldinger technique using a 5 F introducer (Glidesheath Slender ®, Terumo Europe NV, Leuven, Belgium) secured to the skin with 2/0 polyglactin suture (Vicryl ®, Ethicon Inc. Sommerville, NJ, USA). Figure 10 shows the arterial cannulation at the end of this procedure.

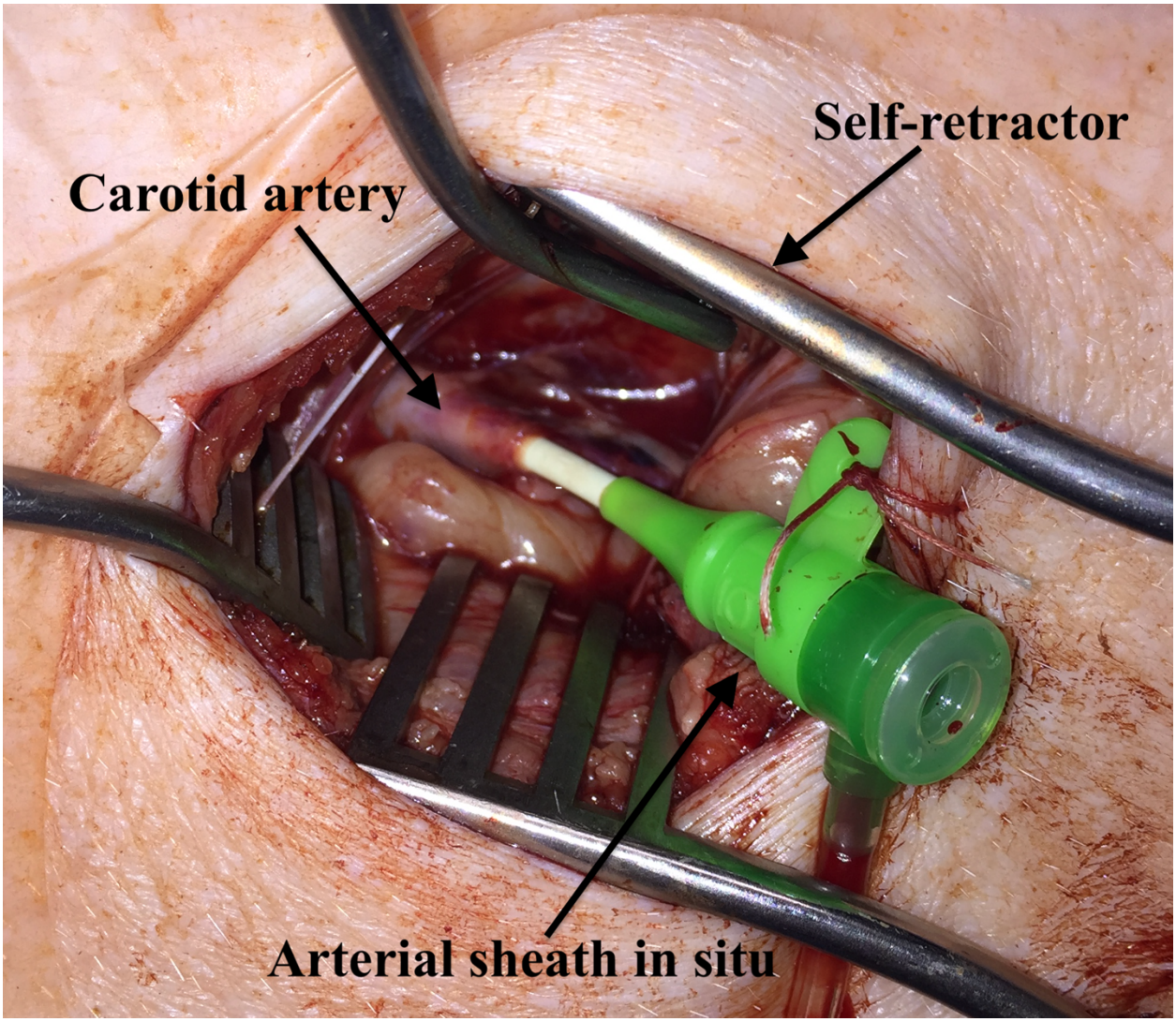

Figure 10. *Arterial catheter inserted in the left carotid artery. In this case I have used a 5F arterial sheath (green catheter showed).*

In some cases, a completely percutaneous approach was used using the femoral artery and conducting the arterial cannulation under vascular ultrasound guidance (Figure 11). This type of approach has the potential to reduce the surgical trauma and the pain for the animal but requires an additional level of technical skills as the coronary catheter management is more complicated than using the carotid approach. Moreover, there is a risk of arterial pseudoaneurysm and or

haematoma at the end of the procedure. This approach cannot be conducted via carotid cannulation due the very high risk of spasm and the small size of the vessel and moreover, cannulation under vascular US in the neck can be challenging.

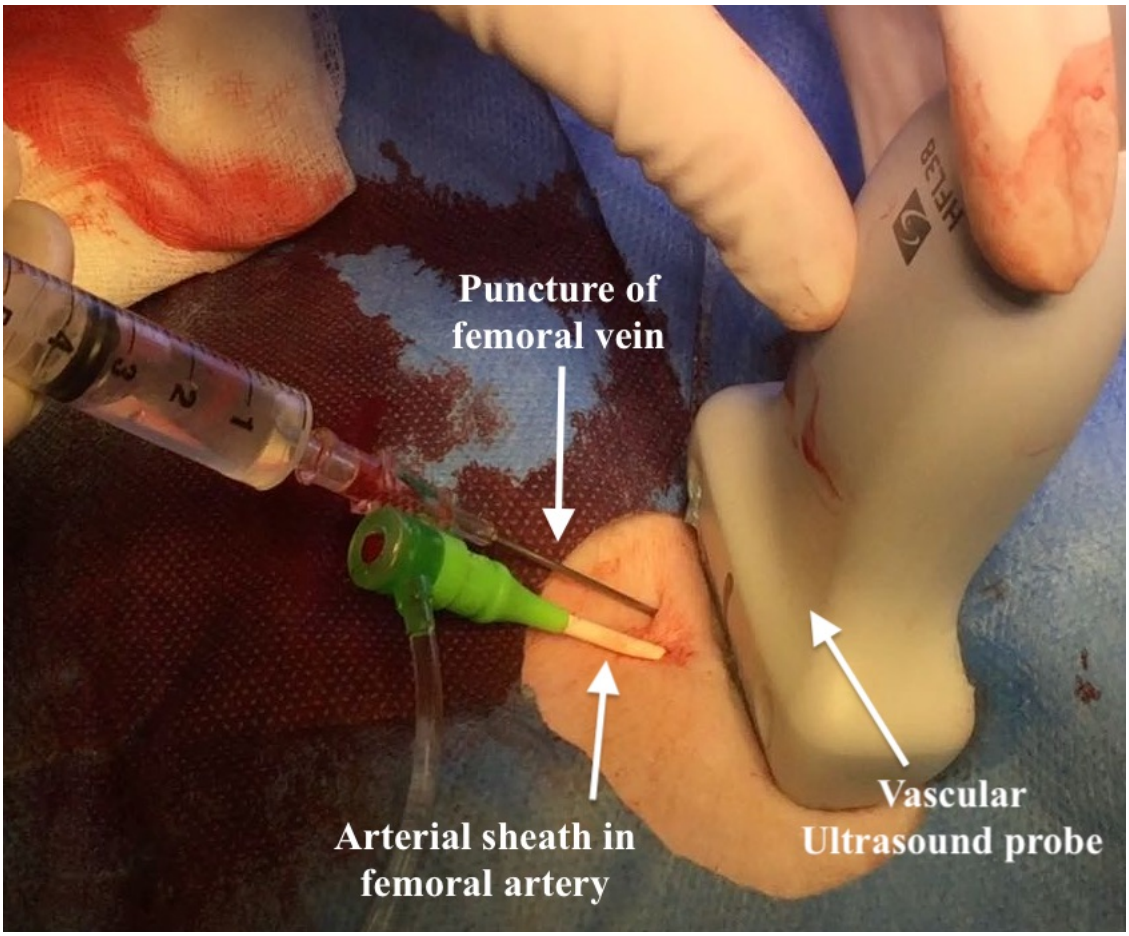

Figure 11. *Percutaneous approach to femoral vessels under vascular ultrasound guidance. An arterial sheath has been inserted using vascular ultrasound guidance and a venous puncture is performed.*

(b) Catheter Based MI procedure

After obtaining stable vascular access, under fluoroscopic guidance (Siemens Artis Zee biplane angiography system - Siemens Healthcare limited, Erlangen, Germany) a guidewire 0.038-inch J-tip exchange wire (Abbott, Illinois, USA) was advanced through the arterial introducer and driven into the aortic root followed by a 5F guiding catheter over the wire; next, a Judkins Left 3.5 (Convey™ JL 3.5 – Boston Scientific, Marlborough, MA, USA) catheter was used to visualize the right coronary artery and the left coronary artery. In our experience this type of catheter can be used for the visualization of both coronary arteries when a carotid approach is used. In case of a femoral approach a femoral right an FR4 catheter (Convey™ FR4 - Boston Scientific, Marlborough, MA, USA) was preferred as it provides a better engagement of both the left coronary artery (LCA) and right coronary artery (RCA). The cardiac silhouette was then imaged on antero-posterior (AP) to confirm the correct position of the JL 3.5 catheter in the aortic root(Figure 12). The RCA ostia was visualized in right anterior oblique (RAO), left anterior oblique (LAO) cranial and caudal views. The LCA ostia was also visualized with the same standard views (Figure 13).

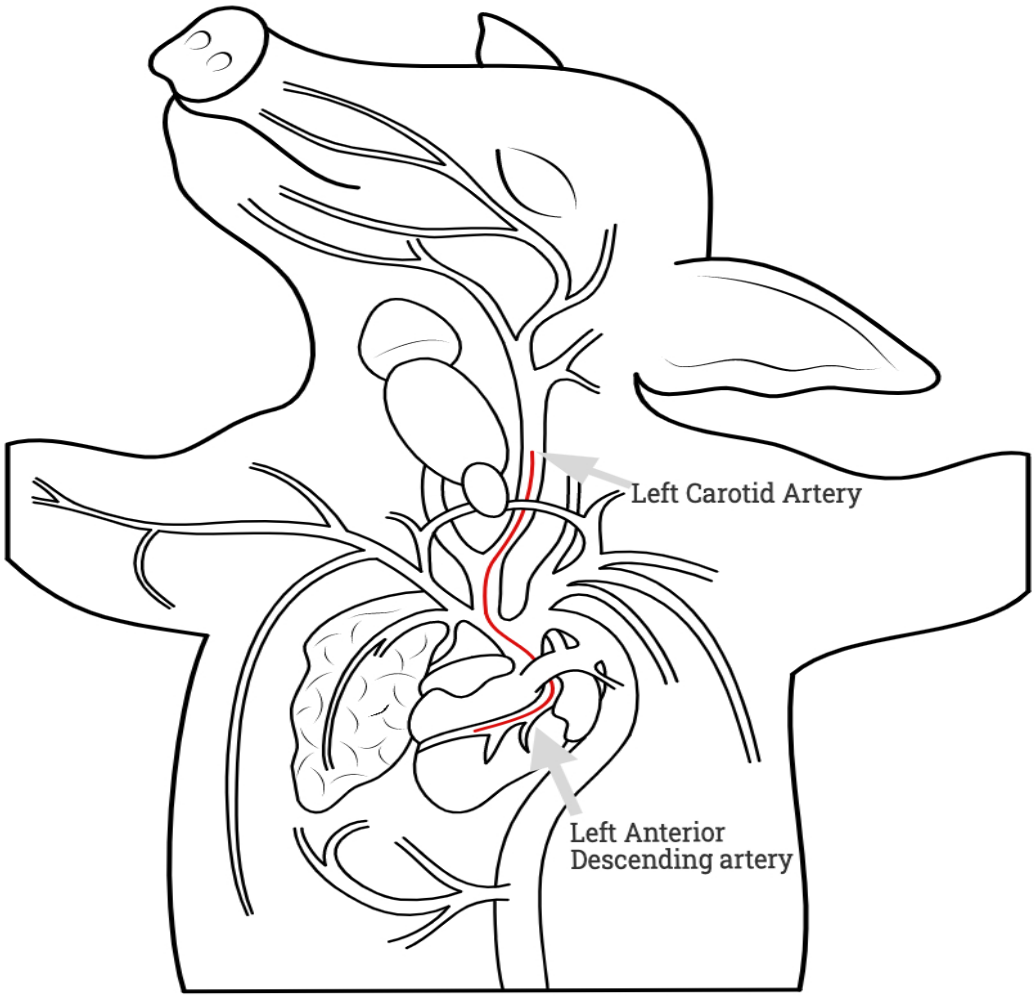

Figure 12. Schematic draw of the swine vasculature. In red: percutaneous coronary guidewire from the left carotid artery to the left anterior descending artery.

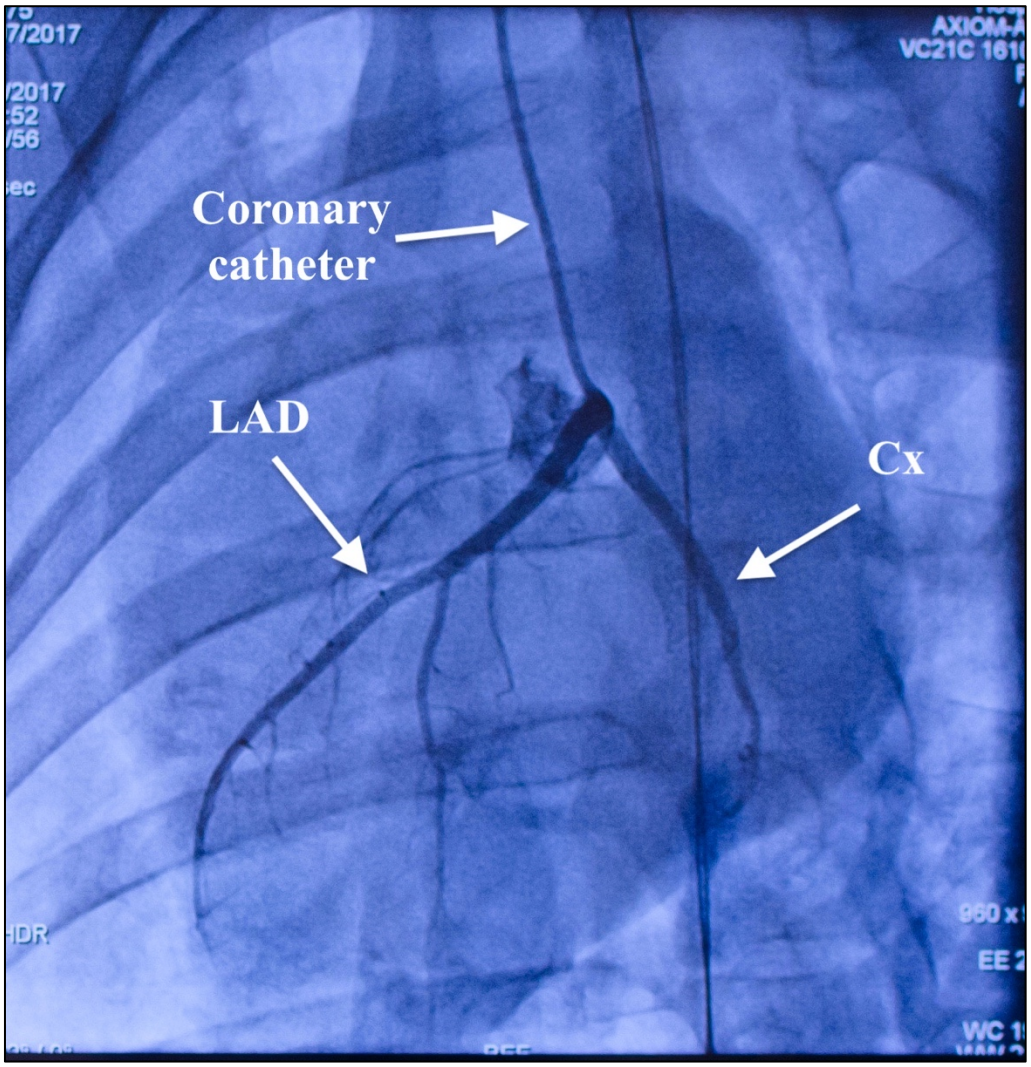

Figure 13. *Direct catheterization and X-ray visualization of the left coronary artery (LCA): the coronary catheter is engaging the left main stem of the LCA allowing the visualization of the Left anterior descending artery (LAD) and the circumflex artery (Cx).*

Next, under fluoroscopy guidance a hi torque balance middleweight guide wire 0.014-inch (Abbott, IL, USA) was introduced into the left anterior descending (LAD) artery followed by a Trek® coronary dilatation catheter (Abbott, IL, USA). Balloon size was decided based on visual assessment of the coronary artery size while the landing zone of the PTCA balloon was chosen

based on the anatomy and the presence of diagonal branches of the LAD: in most cases the occlusion was achieved in the mid-portion of the LAD after the 1st diagonal branch of the LAD. We generally select a straight section of the coronary and avoid bending segments to reduce the risk of partial coronary balloon occlusion or complication. Next, the balloon was inflated within the range of nominal and rated pressure (range 6 – 16 atm) (Figure 14).

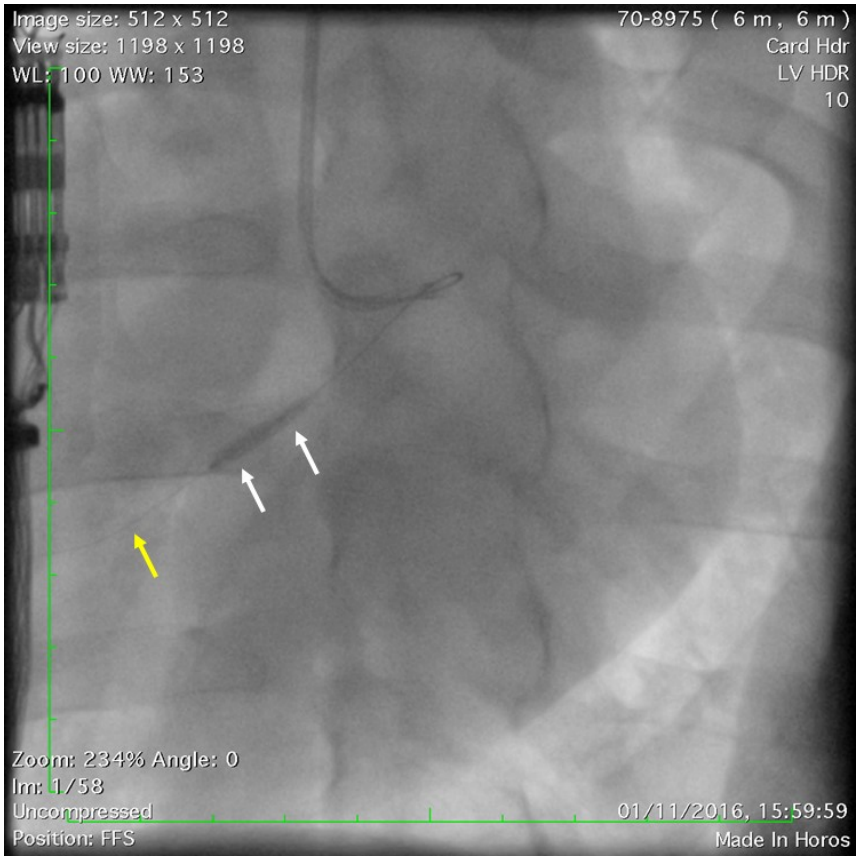

Figure 14. *Representative experiment showing the balloon MI occlusion of the left anterior descending artery: inflated balloon shown by white arrows; guidewire driven through the LAD shown by yellow arrow (X-ray visualization).*

The median pressure for a size 2.5 mm balloon was 12 atm (range 8-16), while for a size 3 mm balloon was 10 atm (range 6-12) and for a size 3.5 mm balloon was 8 atm (range 6-12). The time

of ischaemia was 60 minutes for 44 swine, while 21 had the coronary artery occluded for 90 minutes.

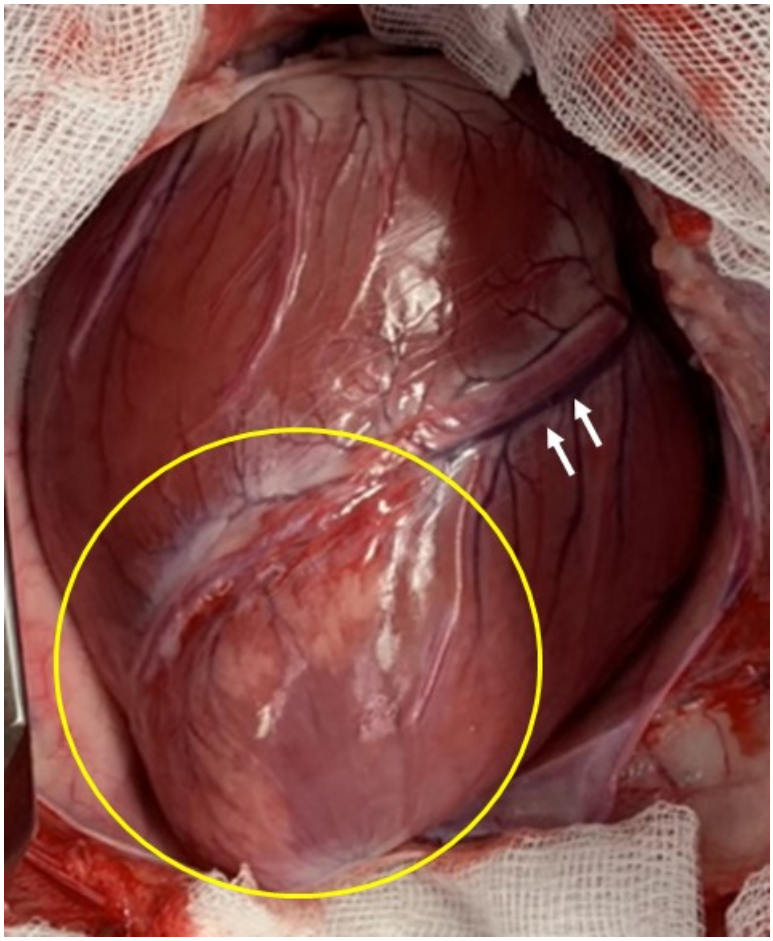

Figure 15. *Porcine heart exposed before termination 24 hours after induction of closed-chest balloon MI procedure: Anterior myocardial infarction seen in the distal antero-apical LAD territory (white arrows); approximative site of previous coronary balloon inflation indicated by yellow arrow after 1st diagonal branch.*

(c) Management of major arrhythmias during the acute MI model

Continuous monitoring of the vital parameter was in place throughout the MI procedure. Significant ECG changes were always observed after inflation of the balloon. Several arrhythmic events were recorded in almost every experiment conducted. Following the balloon inflation and related occlusion of a coronary artery, ventricular arrhythmias develop as a consequence of focal as well as non-focal mechanisms respectively related to automatic and non-automatic ectopic excitation and reentry.[93] As previously reported by other authors cardiac dysrhythmia represents one of the most common complications during these experiments[91] and they are often cause of out-of-hospital arrest in patients suffering acute MI. In a previous canine model of anterior AMI the incidence of Ventricular Fibrillation (VF) or Ventricular Tachycardia (VT) was 72%[93].

To reduce the possibility of major or fatal arrhythmic events and related mortality we used a pre-defined anti-arrhythmic protocol. This protocol included the continuous infusion of Amiodarone (300mg over a period of 2 hours in central venous line) started 10minute before induction of ischaemia and kept throughout the entire ischaemic procedure, the subsequent reperfusion and the following recovery period. This infusion was delivered via the central venous line in the jugular vein. In addition, we also used an infusion of Magnesium Sulphate (8mmol over 2 hours in peripheral line).

Furthermore, we used a predefined anti-arrhythmic treatment involving an emergency bolus of additional Amiodarone to be given in case of major arrhythmic event. Figure 16 describes the predefined algorithm that we have used in case of major or life-threatening arrhythmias: the first episode of VT/VF was treated with a single DC-shock at 300 Joules in association with a bolus of Amiodarone (300 mg IV). If sinus rhythm and reasonable blood pressure was re-instituted the

protocol would be stopped, otherwise a further 300 Joules DC-Shock was given in association to a further bolus of Amiodarone IV (300 mg). If this second attempt to cardioversion would not be enough, an external Cardiopulmonary Resuscitation would be started and a final DC-Shock at 300 Joules would be provided. The resuscitation procedures were stopped if this final DC-shock was not successful in achieving sustainable heart rhythm or if the overall time of re-animation was exceeding 10 minutes. Additional IV medication used during these maneuvers were Lignocaine, Atropine and/or Metaraminol: these were at discretion of the anaesthetist. Figure 17 shows an example of a VF arrest converted into sinus rhythm after DC-shock at 300 J. At the end of the resuscitation protocol, the position of the angioplasty balloon was checked to confirm its position and to check persistence of occlusion of the target coronary vessel.

At the end of the ischaemic time, the balloon was deflated to start reperfusion under fluouroscopic the guidance. Coronary flow was re-assessed and confirmed with direct contrast coronary injection. In some cases, we found a mild coronary spasm at the site of balloon location but none of these were occlusive.

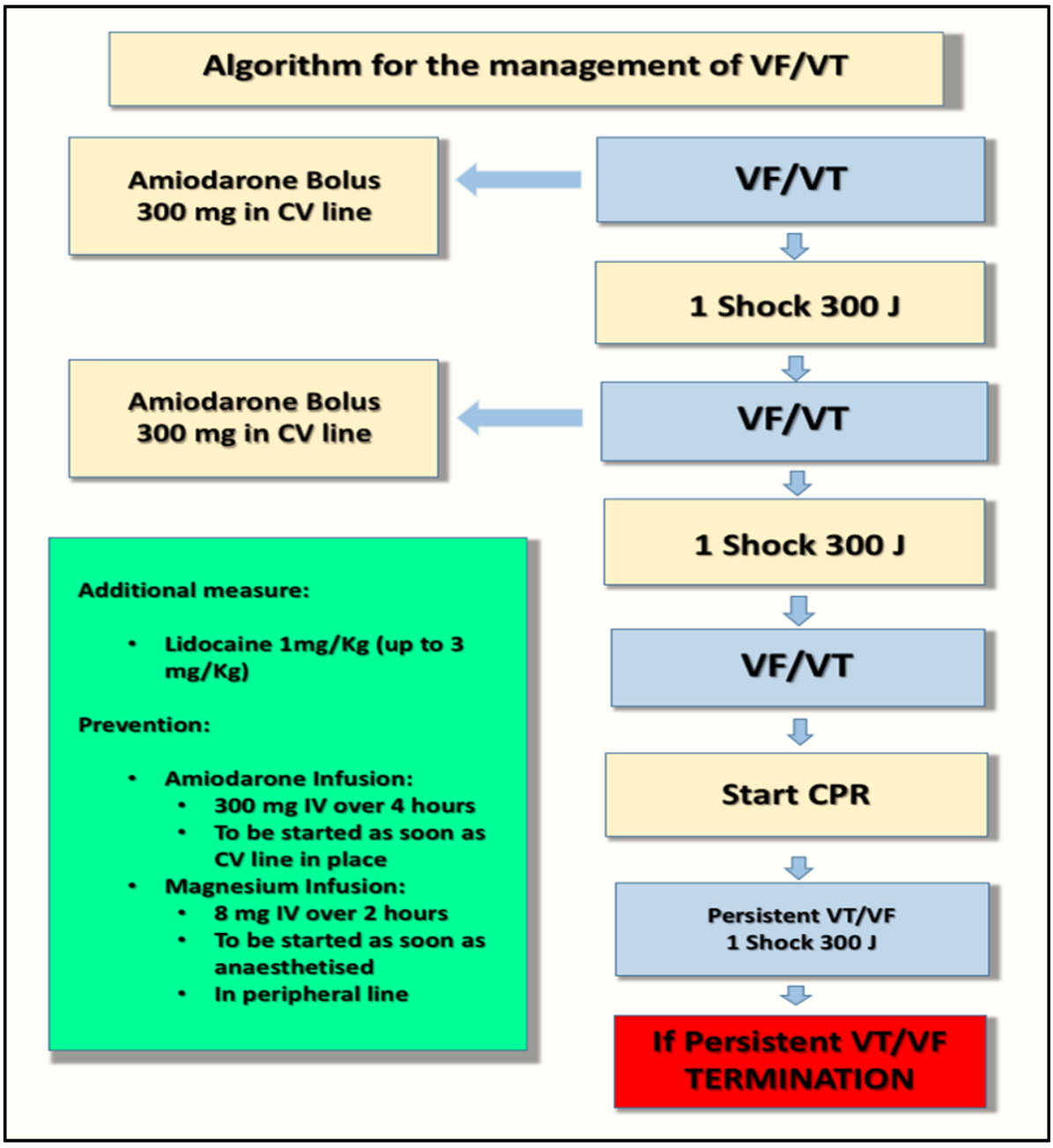

Figure 16.*Algorithm for the treatment of major arrhythmias during the Myocardial Infarction model.*

During reperfusion, several arrhythmias were found, although none of these was major nor was significantly affecting the circulation.

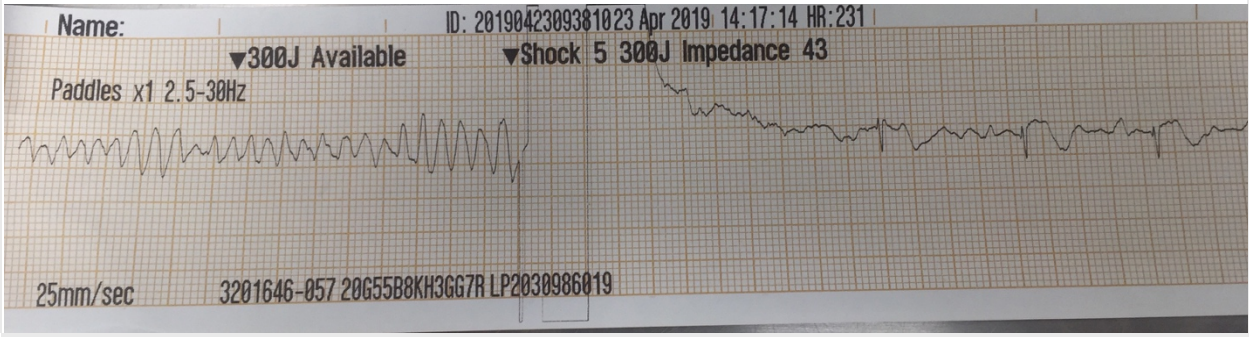

Figure 17. *An example of VF arrest converted to sinus rhythm after a 300 J shock*

The time of occlusion was 60 minutes for vast majority of the animals (n= 43) while in a smaller group (n=21) the LAD was occluded for 90 minutes. In a single case the occlusion was maintained after 30 minutes of occlusion. The target artery was always the LAD at its mid portion except for two cases in which the circumflex artery at its mid portion was targeted to characterize the model in a different coronary territory.

Section 2.05 Methods of assessment of myocardial damage

(a) Clinical and procedural data

Clinical data were collected at several different time-points during the procedures including baseline weight. In addition, hemodynamic parameters were collected manually by the anaesthetist during each phase of the procedures and recorded in the clinical anaesthetic form/chart. These data included systolic and diastolic pressure, heart rate, temperature, saturation, ACT levels, blood gas

analyses, ECG/ST level changes, drug and fluid replacement used and clinical events such as major arrhythmias or other complications. Procedural data regarding the surgical and the catheter-based procedure were also collected prospectively.

(b) Hemodynamic parameters

Blood pressure was measured invasively using an arterial cannula placed in a saphenous artery or directly connected to the carotid artery sheath. The measured blood pressure and all the other vital parameters were recorded continuously and automatically on the monitor display which was set up with predefined alarm ranges; and collected by the anaesthetic team at each specific timepoints on the chart. The heart rate (HR) was visualized continuously on the same monitor using the ECG leads directly connected to the animal and recorded on the anaesthetic chart at predefined time-points including any ST changes with time and duration.

(c) Biochemical and Molecular parameter

Serial blood samples were taken at different timepoints during the experiments: these were used in all pigs to monitor markers of myocardial ischaemia (Troponin I) and in a sub-group of 5 pigs to determine the concentration of specific markers of inflammation (IL-6). To standardize the samples, blood collection was always done after the administration of heparin, in 10 ml aliquots collected in a sterile manner from the central venous catheter. The sample were then handed to the lab technician for processing. The samples were collected at baseline, at reperfusion, 10, 20, 30 minutes; 1, 4, 24 hours and 4 weeks after reperfusion. Once in the laboratory, the blood was immediately transferred into a set of EDTA collection tubes (BD Vacutainer, UK) and centrifugated 1000g at 4℃ for 10 minutes. The separated plasma from all the tubes was pooled together into a

30ml sterile tube (ThermoFisher, CA) and after being mixed was dispensed into the 1.5 Eppendorf tubes (Hamburg, Germany). The tubes were stored at -80℃ until analysis[94].

(i) Cardiac troponin I assay.

An ultra-sensitive pig cardiac troponin enzyme-linked immunosorbent assay (CTNI-9-US Life Diagnostics, PA) was used to detect cardiac troponin-I circulating in plasma. This test is a sandwich assay with a rabbit cardio specific cTnI polyclonal antibody in the solid phase immobilization and a goat anti-cTnI peptide-specific polyclonal antibody conjugated to a horseradish peroxidase (HRP) and is used for detection. This kit has got a range of detection from 0.0156 – 1 ng/ml. From the different plasma samples, a 1/40 and 1/80 dilution were performed according to the manufacturer recommendations. The timepoints 10, 20, 30 minutes and 24 hours for the former and timepoints 1 hour and 4 hours respectively. The rest of the samples were used undiluted. All measurements were performed in duplicate with a 96-microplate reader (Opsys MR™, DYNEX Technologies,Inc. VA)[94].

(ii) Inflammatory and heart failure markers test.

In the very first series of experiments (n=5), we performed inflammatory marker evaluation to investigate the inflammatory response to the experiments. We tested the plasma concentration of interleucin-6 (IL-6) at different timepoints. The collected blood was centrifuged at 1000g for 10’ at 4^{O} C and the plasma was aliquoted to Eppendorff and stored at ≤ -20^{O} C. The assessment of the plasma concentration was done with a quantitative fluorescent immunoassay SMC™ Human Interleukin 6 (Merck KGaA, Darmstadt, Germany).

In the same group of experiments, we have analyzed the concentration of Brain natriuretic peptide (BNP) at different timepoints. BNP was determinate with AxSYM assay (Abbott Laboratory) from venous blood collected in EDTA plastic tubes (Ethylenediaminetetraacetic acid)

(iii) Proteomics analysis.

A subgroup of four animals was utilized for myocardial tissue proteomics analysis. At the time of termination, which was mostly at 28 days post MI, myocardial samples were collected to include the scar tissue, borderzone and transition zone from the infarcted coronary territory and from remote myocardium from a non-infarcted region of the same heart. The frozen tissues of the porcine ventricles collected from the infarcted and remote areas were placed in a tight-fitting glass homogenizer with RIPA lysis and extraction buffer contained: 150 mM NaCl, 50 mM Tris-HCl (pH 8.0), 1% NP-40, 0.5% sodium deoxycholate, 0.1% SDS, complete protease inhibitor cocktail (Roche Diagnostics) and phosphatase inhibitor cocktail 3 (Sigma). The samples were homogenized, transferred into siliconized tubes, incubated for 10 min to maximize protein solubilization and centrifuged at 17,000g for 10 min. All these procedures were carried out on ice or at 4°C. Protein concentration was adjusted to 5 mg·ml-1 using BCA Protein Assay (Thermo Fisher Scientific, Loughborough, UK). Since Sus scrofa gene and protein annotation is not complete, the results of the MSA/MSA scans were compared with both S. scrofa and Homo sapiens protein databases, even though this study focused on S. scrofa proteins. The fractionated peptides were analysed by nano-liquid chromatography-tandem mass spectrometry analysis (nanoLC-MSA/MSA) using a Q-Exactive hybrid quadrupole orbitrap mass spectrometer.

(d) Cardiac MRI

The animals were subjected to in-vivo cardiac MRI imaging after the MI (and in some cases also at baseline before MI) with a 3T cardiac magnetic resonance.

(i) Animal Preparation for cardiac MRI

Cardiac MRI was always undertaken with the animal under general anaesthesia with propofol and maintained using isoflurane 2% with ketamine, morphine and midazolam prior to induction. The animals were constantly monitored and mechanically ventilated throughout the MRI scan. The images were acquired with a 3 Tesla system (Magnetom Prisma® 3T – Siemens Healthcare Ltd, Erlangen, Germany) using the integrated spine coil posteriorly and the Siemens "Body 13" coil anteriorly. During MRI the animal was positioned in supine position with the surface coil positioned centrally on the sternum (Figure 18).

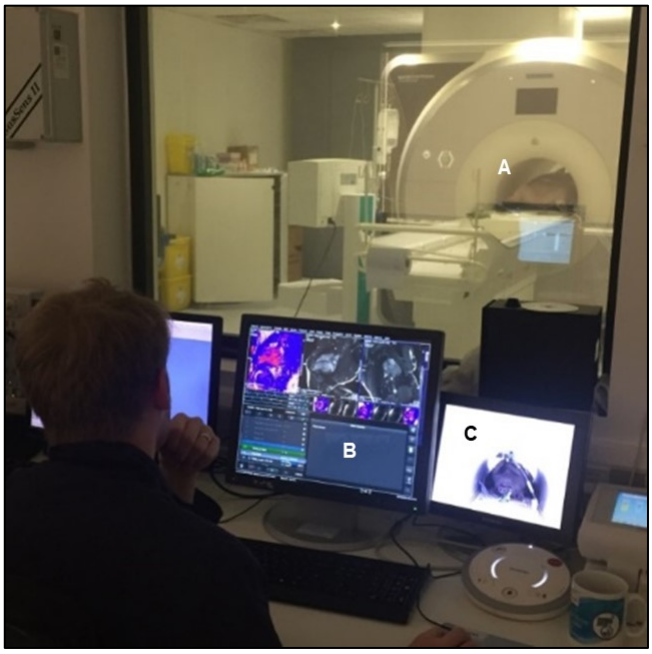

Figure 18. *TBRC MRI suite seen from the control room. Animal under anaesthesia positioned in the scanner (A and C); cardiac image acquisition ongoing (B)*

Cardiac gating was obtained using ECG interface or peripheral pulse monitor. These MRI procedures were conducted without the use of neuromuscular block and therefore breath-hold required repeated short temporary interruption of ventilation to conduct some part of the MRI image acquisition without artefacts. Adequate recovery between breath holds was granted to maintain adequate oxygenation and saturation throughout. In some animals a baseline pre-MI MRI scan was undertaken just before the MI induction and under the same general anaesthesia. Post-operative MRI scans were done in the acute phase (between 4 and 24 hours) after MI and in the chronic phase (24-41 days after MI).

(ii) Cardiac MRI protocol

After acquisition of localizer images, True–FISP functional cinematic images were acquired in the three long axis planes (2-,3- and 4- chamber orientation) of the left ventricle and in a contiguous stack of short axis slices from base (at the level of the mitral valve) to the apex. The acquisition parameters are as follows: slice thickness 8mm, base resolution 208, phase resolution 80%, TE 1.39 ms, TR 46.5 ms, flip angle 45o, bandwidth 1335 Hz/Pixel, calculated phases (temporal resolution) 30, data segments per R-R 15. This allowed for the visual assessment of the 17 American Heart Association (AHA) myocardial segments. To minimize off resonance and center frequency artefacts a True-FISP Frequency Scout was acquired. After reviewing the resulting images, the optimal frequency was subsequently used in the cinematic images. Arrhythmia rejection (acceptance window 200-300ms) was applied where necessary. After cine imaging, a dose of 0.2mmol/kg body weight of Gadobutrol (GadovistTM, Bayer) contrast agent was administered. Early enhancement images were acquired 2 minutes post contrast injection in the three long axis using 2D FLASH, (slice thickness 8mm, base resolution 256, phase resolution 83%, flip angle 15o, TE 2ms, TR 750ms, TI 500ms) and the short axis using a single shot 3D FLASH (slice thickness 8mm, base resolution 256, phase resolution 57% slice resolution 70% slice partial Fourier 6/8, flip angle 15o, TE 1.31ms, TR 700ms, TI 500ms). Late gadolinium enhancement images were acquired after 8-10 minutes in line with the Society for Cardiovascular Magnetic Resonance (SCMR) guidelines. Images were acquired in the long axis and short axis using a 2D FLASH PSIR pulse sequence (slice thickness 8mm, base resolution 256, phase resolution 64%, TE 1.55ms, TR 750ms, TI 300-350ms - based on TI scout images (Figure 19).

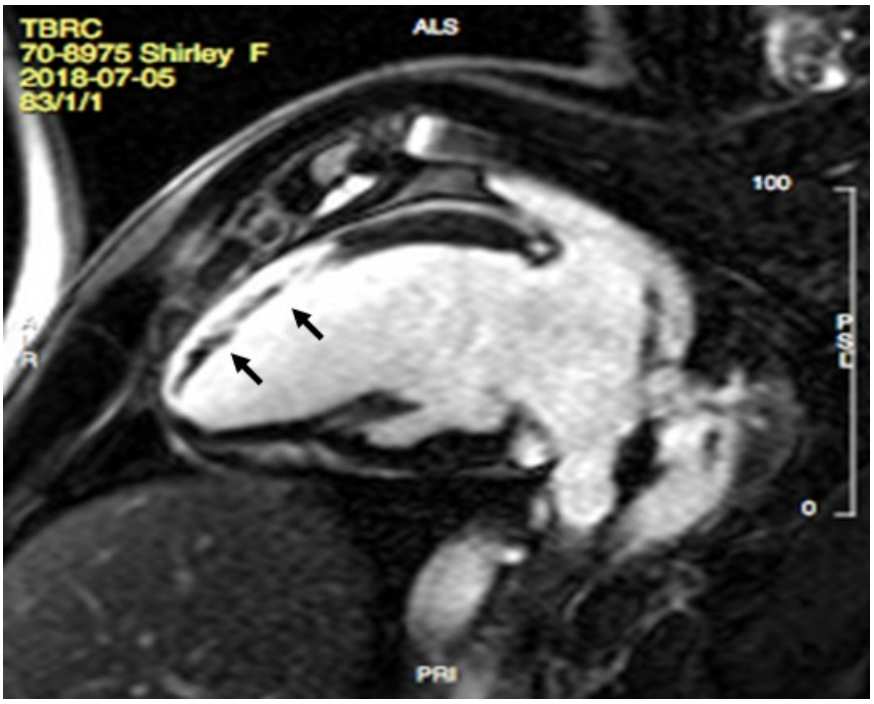

Figure 19. *Representative Cardiac MRI scan showing the distribution and size of the induced MI in one of the animals: Longitudinal view of the left ventricle showing late gadolinium enhancement (black arrows) at the antero-apical LAD territory 30 days after closed-chest balloon MI*

The left ventricular volumes and mass were analysed by manually delineating the ventricular end diastolic and systolic contours in the short axis stack. Papillary muscles and trabeculations were included in blood pool as per SCMR guidelines (Kramer et al JCMR 2013). Left ventricular volumes and ejection fractions were calculated automatically according to Simpson's rule. Values were normalized to body surface area. Left ventricular mass was measured in end-diastole and expressed as percentage of total myocardial mass. Late gadolinium enhancement images were analyzed quantitatively using the 5-Standard Deviation (5SD) or Full Width Half Maximum (FWHM) method – this is a semi-automatic analysis which involves manual

drawing of a region of interest (ROI) onto the scarred or remote region. The analysis was conducted using CVI42, v5.1.1, (Circle Cardiovascular Imaging, Calgary, Ontario, Canada).

Section 2.06 Statistical analysis

Continuous numerical variables are reported as mean and standard deviation (SD) unless otherwise specified. Categorical variables are reported as count and percentages of the total. Numerical variables have been investigated for normality using the Shapiro-Wilk Normality Test. Comparative inferential analysis between numerical variables has been conducted using two sample t-test or Mann-Whitney test according to the distribution of the variable. When more than two groups have been compared an analysis of Variance model was used. Comparison between categorical variables was conducted using Pearson's chi-squared Test for count data or with Fisher's Exact test, as appropriate. Correlation analysis was conducted using Pearson's product moment correlation. Repeated measure analysis has been conducted with linear mixed effect models.

(a) Statistical analysis for proteomics

For each protein, an abundance ratio between infarcted and non-infarcted samples was calculated. Proteins found to be expressed in the infarcted myocardium at an amount two folds or more than in the remote normal myocardium were selected for further analysis. The normalized expression of each of these proteins was correlated with the mechanical endocardial strain and strain rate data of the acute phase with those showing the strongest correlation ($R2 \geqslant 0.95$) being more closely evaluated; a series of univariate linear regression models were performed to correlate each identified protein to each mechanical variable. All tests were two-sided and alpha

error was set at 0.05. The data were collected and tabulated in Excel©(Microsoft Inc, USA) and subsequently processed and analyzed with R version 3.6.0 (2019-04-26) (The R Project for Statistical Computing, Vienna, Austria [https://www.R-project.org/]).

Chapter III. RESULTS

Section 3.01 Clinical and procedural outcomes.

Table 4 shows the clinical and procedural outcomes for the entire cohort. A total of 65 animals underwent the closed-chest MI model procedures in the main part of the project. The mean weight of the animals at the time of the MI model was 61.8 ± 3.4 kg while the average weight 4 weeks after the infarct was 76.8 ± 6.3 kg. Twenty-six pigs had a malignant arrhythmia during the induction of MI (40 %): four of these animals had a refractory ventricular fibrillation (VF) which could not be restored to a sustainable rhythm within the predefined anti-arrhythmias protocol including DC-Shock and Amiodarone infusion. Hence, the overall intra-operative mortality rate was 6.1%. Attempts to further resuscitation were not attempted beyond the predefined protocol to avoid confounding bias in relation to the development and characterization of this experimental model and its use in the future to develop and test new treatments.

Most part of the malignant arrhythmias were represented by VF and 17 animals experienced this complication (26.2 %). Other arrhythmic complications were ventricular tachycardia (6 pigs, 9.2%), supraventricular tachycardia (1 pig, 1.5%) and a combination of VT and VF in 2 pigs (3.1%). A minor arrhythmia was represented by a self-terminating ventricular bigeminy that occurred in one animal (1.5%).

All animals experiencing a major arrhythmia were resuscitated following the resuscitation protocol as previously described: the average duration of the resuscitation was 1.3 ± 2.8 minutes (range 1 -12 minutes). Most of the resuscitations required only a single shock to reinstitute sinus rhythm (7 pigs, 10.8%). The vast majority of the pigs demonstrated ischaemic ECG changes during

and after ischaemia - these were represented by ST depression in 54 cases (83%) and by ST elevation in 3 cases (4.6%). The remaining 6 pigs did not develop evident ECG changes (9.2%). Ventricular ectopics were recorded in 57 (87.7%) of the cases.

The size of the occlusive balloon was decided on table based on visual evaluation of the coronary size. The average size of the occluding balloon was 2.8 ± 0.31 mm: a size 2.5 mm balloon was used in the majority of cases (31 cases, 47.7%), while a size 3 mm was chosen in 29 cases (44.6 %) and a 3.5 mm was used in the remaining 5 cases (7.7%). The inflation pressure was on average 10.7 ± 2.5 atm. In one case the balloon was repositioned distally few seconds after initial inflation to reduce the risk of major complications. In another case the balloon was immediately replaced due to rupture on inflation to an above rated (20 atm) pressure.

	n = 65
Death (%)	4 (6.2)
Weight at time of MI (Kg)	61.83 (3.38)
Weight at termination (Kg)	76.82 (6.30)
Malignant arrhythmias (%)	26 (40)
Type arrhythmia (%)	
VF	17 (25)
VT	6 (9.4)
SVT	1 (1.5)
VT/VF	2 (3.1)
DC Shock required (%)	19 (29.2)
CPR required (%)	11 (16.9)
Duration of resuscitation maneuvers (min)	1.32 (2.77)
ECG changes (%)	
No	3 (5.0)
ST depression	54 (90.0)
ST elevation	3 (5.0)
Duration ECG Changes (min)	51.00 (24.44)
Ventricular ectopic (%)	
Limited	29 (44.6)
Multiple	29 (44.6)
Multiple and bigeminy	1 (1.5)
none	4 (6.1)
Duration Ventricular ectopic (min)	25.60 (20.26)

Definitions: MI: myocardial Infarction; VF: Ventricular fibrillation, VT: ventricular tachycardia, SVT: supra-ventricular tachycardia, DC: Direct Current, CPR: Cardio-pulmonary Resuscitation; ECG: electrocardiogram.

Table 4.*Clinical characteristics during MI model*

The baseline weight of the animals was similar in the 60 minutes and 90 minutes occlusion groups (61.51 ± 3.76 Kg vs 62.57 ± 2.44 Kg respectively, p= 0.25), but interestingly, at the time of termination, the weight was higher in the 60 minutes group (77.66 ± 6.93 Kg vs 74.56 ± 3.88

Kg respectively , p = 0.081). The occurrence of a malignant arrhythmias was more frequent in the 90-minutes group (52.6% vs 32.6%, p = 0.21) and this group required cardiopulmonary resuscitation more frequently (23.8% vs 11.6%, p = 0.37) as well as more DC-Shock cardioversions (38.1% vs 23.3%, p= 0.35). Moreover, this group required a longer time to re-institute a sustainable rhythm (1.86 ± 3.40 minutes vs 0.98 ± 2.38 minutes, p = 0.20). Table 5 shows the clinical characteristics of the animals during the MI procedures divided by duration of ischaemia.

	60 Minutes occlusion (n= 43)	90 minutes occlusion (n= 21)	p-value
Weight at time of MI (Kg)	61.51(3.76)	62.57(2.44)	0.245
Weight at termination (Kg)	77.66(6.93)	74.56(3.88)	0.081
Malignant Arrhythmias (%)	14(32.6)	11(52.4)	0.21
Type Arrhythmias			
VF	8(18.6)	8(38.1)	
VT	4(9.3)	2(9.5)	
SVT	1(2.3)	0(0)	
VT/VF	2(4.7)	0(0)	
DC Shock required (%)	10(23.3)	8(38.1)	0.345
CPR required (%)	5(11.6)	5(23.8)	0.372
Duration of resuscitation (min)	0.98(2.38)	1.86(3.4)	0.233
ECG Changes (%)			
No	3(7.7)	0(0)	
ST depression	33(84.6)	21(100)	
ST elevation	3(7.7)	0(0)	
Duration of ECG changes (min)	42.79(18.58)	63.9(27.27)	0.001
Ventricular ectopic (%)			
Limited	18(46.2)	9(42.9)	
Multiple	17(43.6)	12(57.1)	
Multiple and bigeminy	1(2.6)	0(0)	
None	1(2.6)	0(0)	
Duration Ventricular ectopic	21.34(15.87)	32.1(24.56)	0.058

Data are expressed as mean and SD for numerical variables and as per count and percentages for categorical variables. Definitions: MI: myocardial Infarction, VF: ventricular fibrillation, VT: ventricular tachycardia, SVT: supra-ventricular tachycardia, CPR: cardio-pulmonary resuscitation.

Table 5. Clinical Characteristics of the experiments divided by time of occlusion.

Section 3.02 Hemodynamic Parameters

(a) Arterial Blood Pressure

The arterial blood pressure was measured at regular intervals during the procedure. The mean systolic blood pressure at baseline was 96.15 ± 10.71 mmHg; the diastolic blood pressure at this timepoint was 53.44 ± 9.08 mmHg. The most significant reduction in blood pressure was found at the time of reperfusion: at this timepoint the systolic arterial blood pressure was 82.23 ± 24.81 mmHg and the diastolic was 44.78 ± 50.45 mmHg. The blood pressure tended to recover in the first 10 minutes after reperfusion, although a persistent reduced blood pressure was noted in the 90-minutes ischaemia group (Figure 20 and Figure 21).

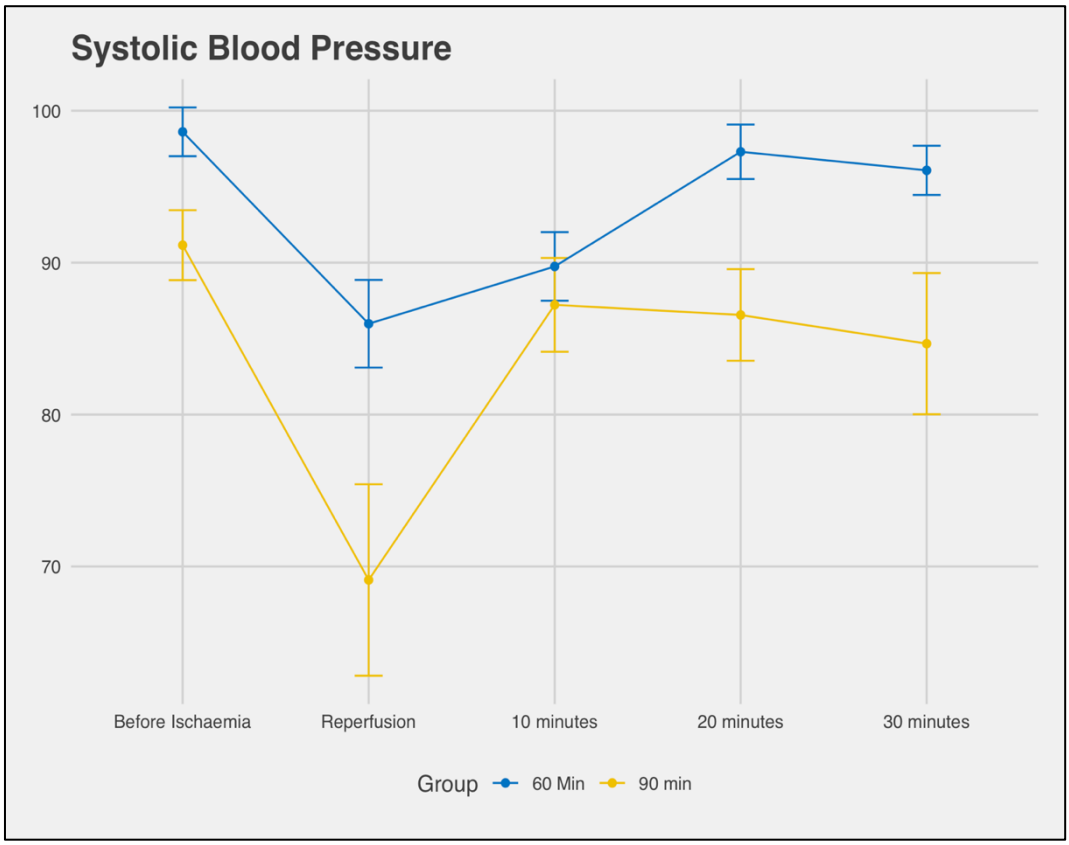

Figure 20. *Systolic blood pressure at different timepoints, divided by time of coronary occlusion. Blue: 60 minutes occlusion. Yellow: 90 minutes occlusion. (n before ischemia=62; n at reperfusion = 60; n at 10 minutes = 59; n at 20 minutes = 56;n at 30 minutes = 36)*

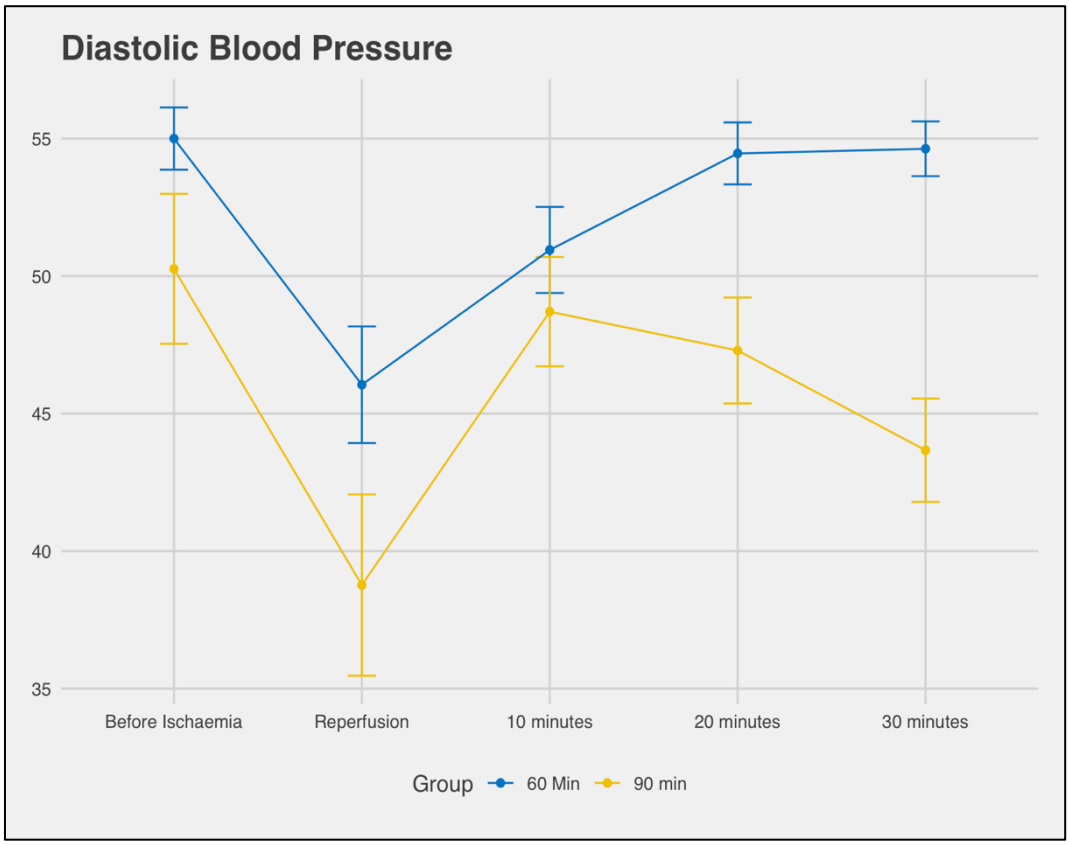

Figure 21. *Diastolic blood pressure at different timepoints, divided by time of coronary occlusion. Blue: 60 minutes occlusion. Yellow: 90 minutes occlusion. (n before ischemia = 61; n reperfusion = 59; n 10 minutes = 58; n at 20 minutes = 55; n at minutes = 36)*

(b) Heart Rate

The heart rate at baseline was 63.5 ± 9.6 bpm; it tended to increase at the moment of reperfusion (83.6 ± 24.5 bpm) and remained elevated during the recovery phase with a mean HR of 91.9 ± 24.7 bpm 10 minutes after reperfusion, 89.9 ± 19.2 bpm 20 minutes after reperfusion and 92.6 ± 18.7 30 minutes after reperfusion. This trend was evident for both groups, although

the HR after reperfusion remained higher in the 90 minutes group with a peak 10 minutes after reperfusion of 105.4 ± 26.2 bpm (vs 86.1 ± 21.9 bpm in the 60 minutes group, $p < 0.01$).

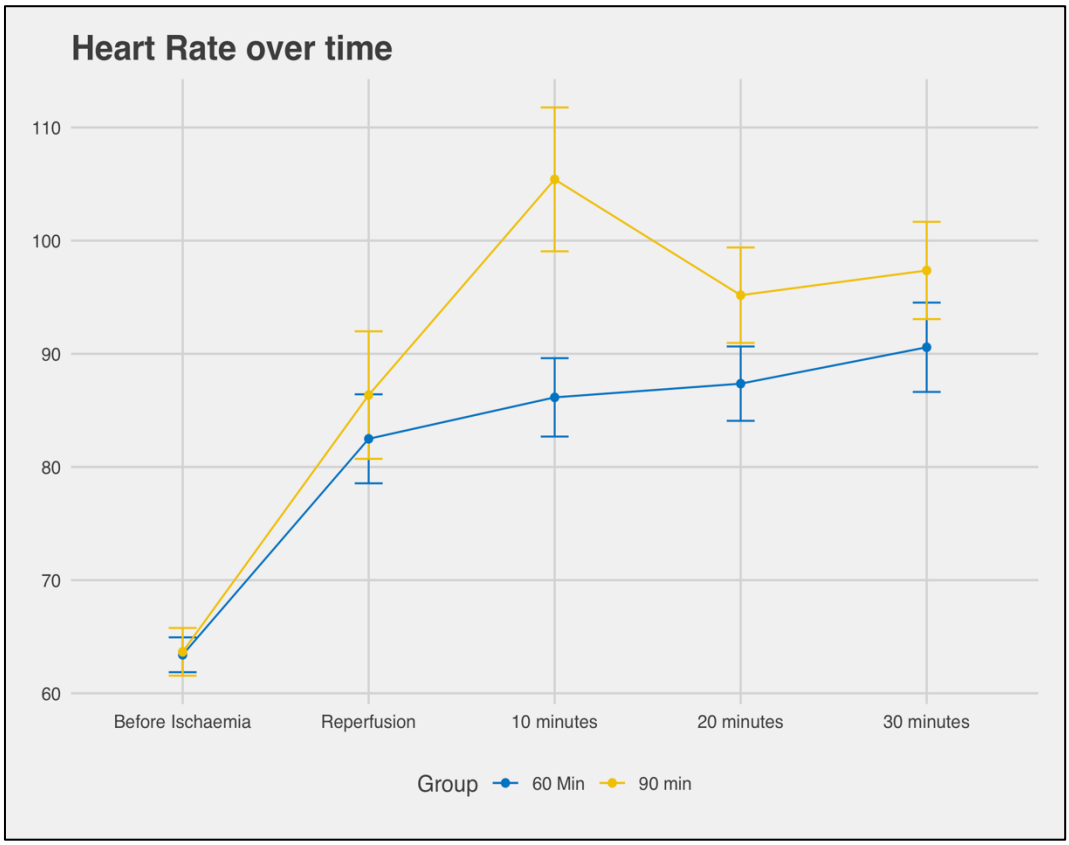

Figure 22. *Heart rate at different timepoints divided by time of coronary occlusion. Blue: 60 minutes occlusion. Yellow: 90 minutes occlusion. (n before ischemia = 61; n at reperfusion = 59; n at 10 minutes = 58; n at 20 minutes = 54; n at 30 minutes = 38)*

Section 3.03 Biochemical and Molecular data

(a) Cardiac Troponin I

To confirm the presence of an acute myocardial infarction by conventional clinical grade biochemical markers and to evaluate the extension of the same, serial repeated sampling of the blood was obtained to estimate the troponin release. These samples were taken before the procedures, at reperfusion time, 10, 20 and 30 minutes after reperfusion and then at 1, 4, 24 hours and 4 weeks after reperfusion. Table 6 shows the mean troponin concentration in the peripheral venous blood. The mean preoperative troponin was 0.04 ± 0.04 ng/mL. At reperfusion, the mean Troponin increase to 0.06 ± 0.11 ng/mL, while the peak Troponin was measured 4 hours after reperfusion with a mean value of 87.47 ± 48.62 ng/mL. The troponin value was back to baseline values when measured at 4 weeks. Table 6 shows the concentration of plasma troponin at each timepoint (expressed and mean and SD).

	Before MI	Reperfusion				After MI			
			10min	20min	30min	1 hour	4 hours	24 hours	4 weeks
Number of samples	62	60	60	60	61	61	57	54	61
Troponin (ng/ml) Mean (SD)	0.04 (0.04)	0.06 (0.11)	1.67 (1.93)	7.18 (10.08)	14.37 (15.81)	40.76 (36.65)	87.47 (48.62)	13.88 (7.67)	0.03 (0.03)

Data are expressed as mean and SD for numerical. Definitions: MI: myocardial Infarction, min: Minutes, ng: nanograms, ml: millilitres, SD: standard deviation.

Table 6. *Plasma concentration of Troponin I at different timepoints.*

Figure 23 shows a spaghetti plot describing the plasma concentration of troponin during time: there is an initial increase in concentration at 30 minutes, but the most significant peaks are measure at 1 and 4 hours after balloon deflation.

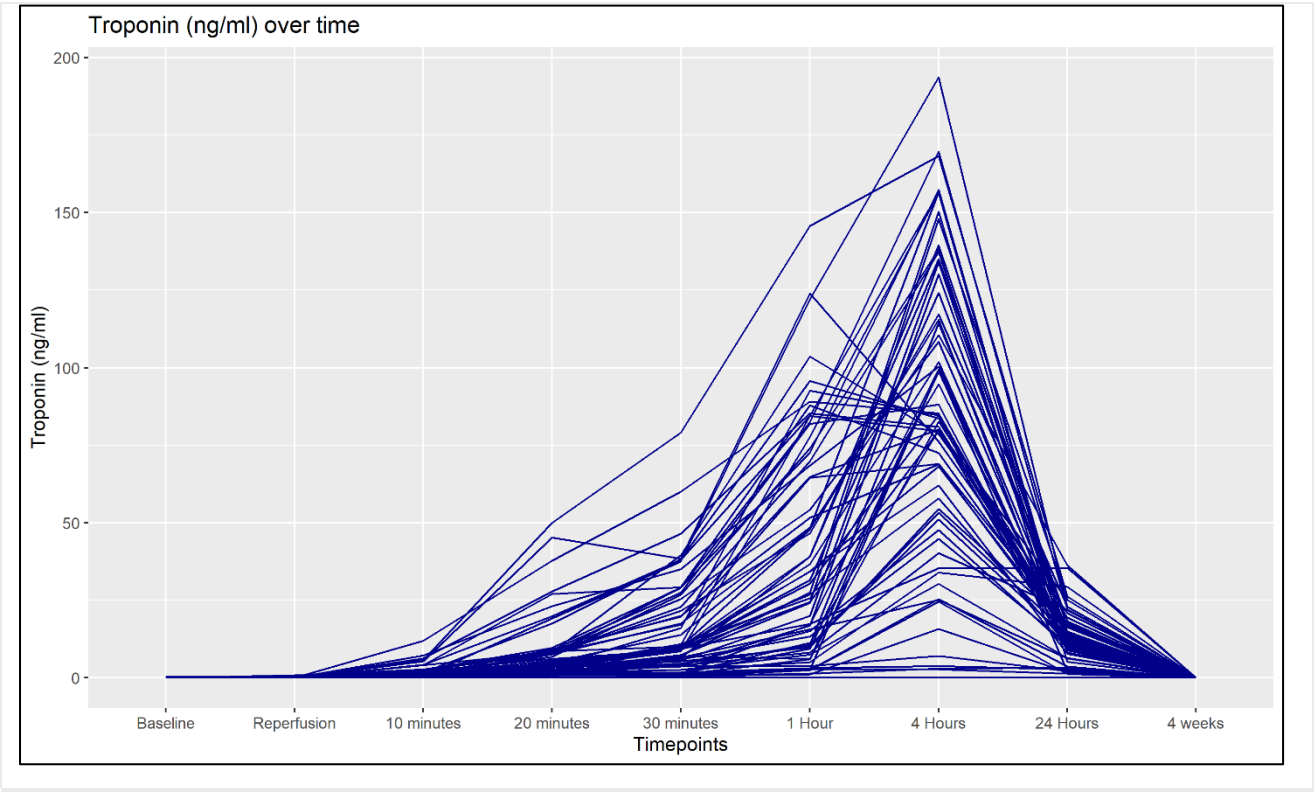

Figure 23. *Spaghetti plot showing the Troponin plasma concentration (ng/ml) at different timepoints for each individual experiment.*

Figure 24 shows the troponin release according to the different time of coronary occlusion. The most significant troponin concentration was found in the 90 minutes occlusion group: 1 hour after reperfusion the mean troponin concentration was 42.6±49.8 ng/ml in the 90 minutes occlusion group (vs 35.2 ± 32.3 ng/ml in the 60 minutes group , $p < 0.01$) and at 4 hours it was 100.2 ± 50.3 ng/ml vs 83.7 ± 46.2 ng/ml respectively ($p = 0.005$). A much lower value of troponin was found in the only animal that had a coronary occlusion time of 30 minutes (1.45 ng/ml at 1 hour and 3.1 ng/ml at 4 hours).

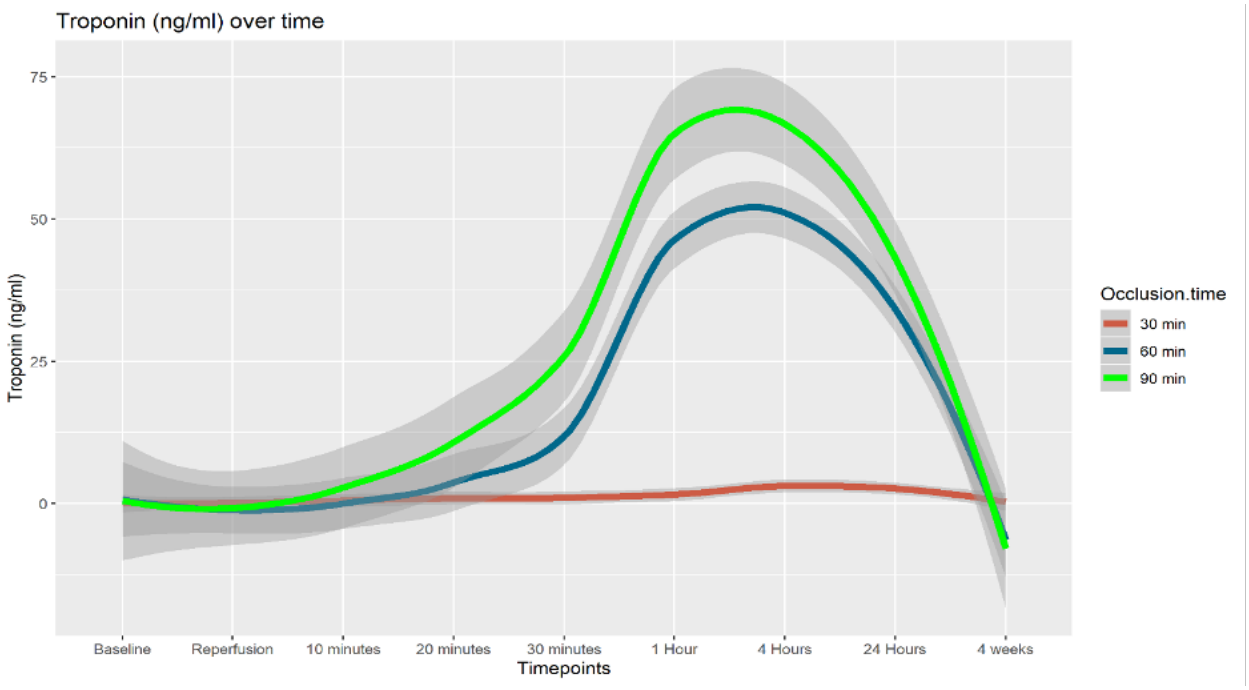

Figure 24. *Mean troponin plasma concentration (ng/ml) with confidence intervals (Loess smoothing) at different timepoints for different time of occlusion. In Blue: 60 minutes of occlusion, Green: 90 minutes occlusion, Red: 30 minutes occlusion.*

(b) Other Biomarkers

(i) Brain (B-type) natriuretic peptide (BNP)

The peak of BNP concentration in plasma was found at 1 hour after MI induction at 39.56 ± 39.2 pg/mL.

The BNP concentration tended to reduce quickly 24 hours after MI and remained very small even at 4 weeks (8.93 ± 8.69 pg/mL). Figure 25 shows the BNP concentration at different timepoints.

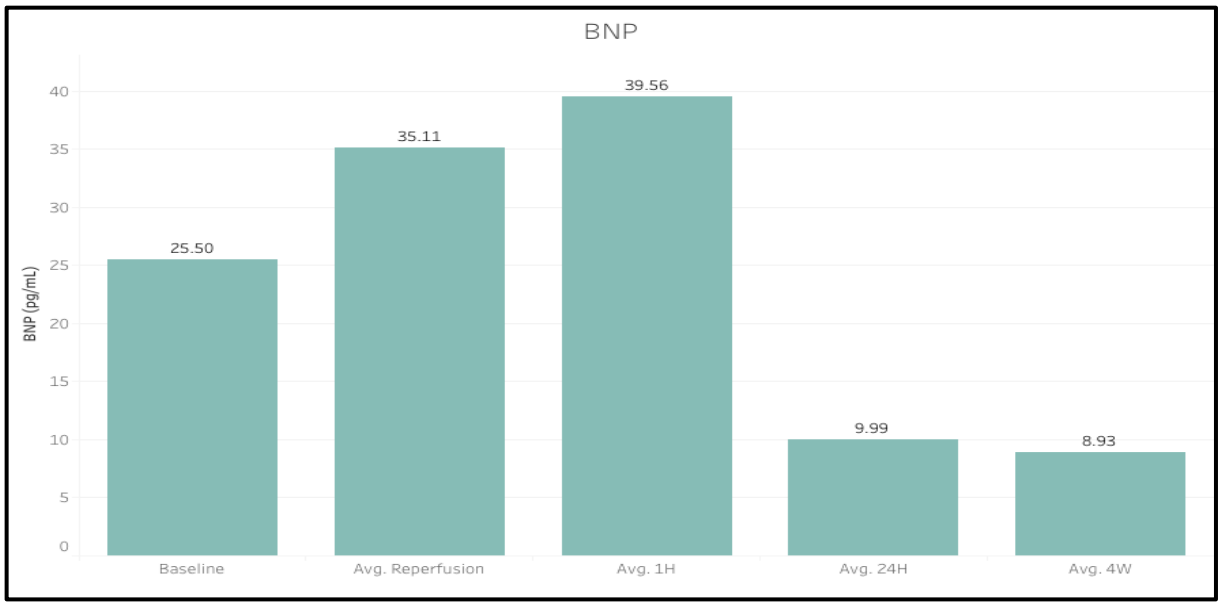

Figure 25. *BNP plasma concentration (pg/mL) at different timepoints (n= 5).*

(ii) Interleukin 6 (IL-6)

The IL6 concentration did not have a specific correlation with the timepoint, with a peak measured at 1 hour (0.13 ± 0.11 ng/mL). The baseline values (0.11 ± 0.06 ng/mL) appeared to be higher than the post-MI values (except 1 hour after MI), showing the lack of correlation with the infarction. Figure 26 shows the concentration of IL6 at different timepoints.

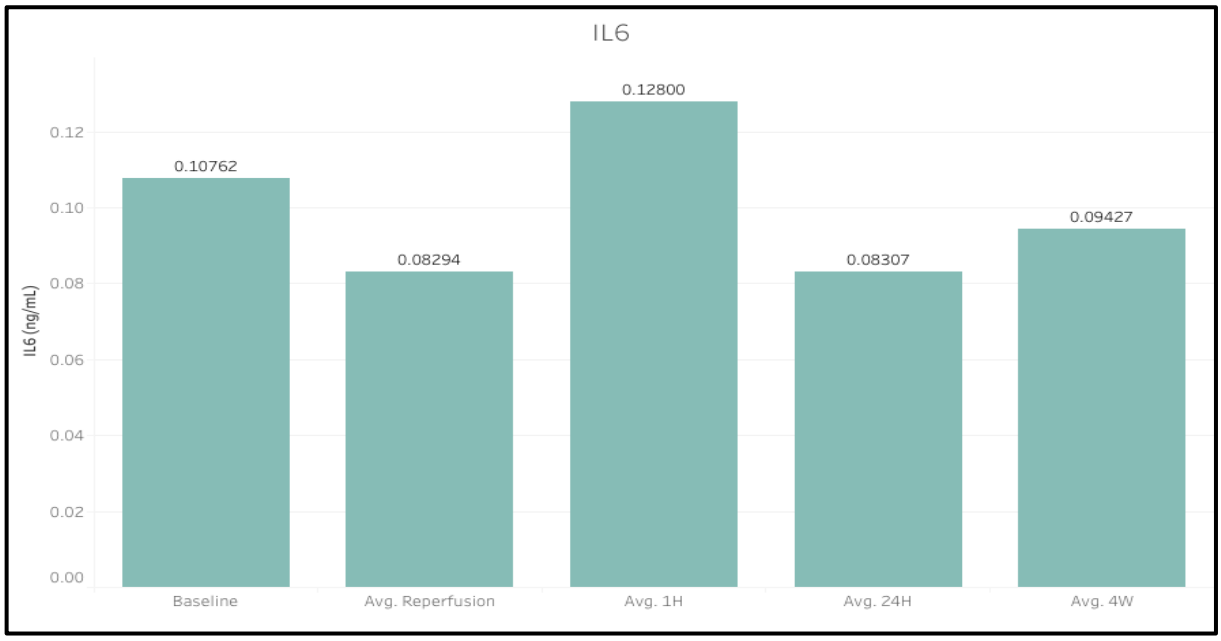

Figure 26. *IL6 plasma concentration (ng/mL) at different timepoints (n= 5).*

(c) Proteomics Analysis

This part of the work has been done in collaboration with the Department of Mechanical Engineering, University of Bath, Bath, UK (Dr. D.S.Mansell, Prof. A.N. Cookson).

To further investigate potential molecular pathways in our model, we have collected myocardial samples from 5 animals at the time of terminations. These samples were collected from the central portion of the infarcted area and from a remote area of the left ventricle. After proteomics analysis, 5981 proteins were identified, and 39 proteins were over-expressed (at least two folds) in the myocardial scar tissue.

We have correlated the expression of these proteins with left ventricular strains data: in this sense this analysis was conducted on only 4 hearts was used as strains were only available for these experiments[94]. Significant linear correlations were found between endocardial circumferential strain rate (ECSR) and 21 of the proteins increased in the infarcted territories. The proteins showing the strongest correlation ($R2 \geqslant 0.95$) with the ECSR were: D-3-phosphoglycerate dehydrogenase (D-3PGDH, $R2 = 0.96$, $p = 0.01$), cysteine and glycine-rich protein-2 (CG-RP, $R2 = 0.95$, $p = 0.02$), and secreted frizzled-related protein 1 (sFRP1, R2 0.96, $p = 0.01$)[94]. Western blotting for D-3PGDH and sFRP1 confirmed that the level of D-3PGDH and sFRP1 protein in the infarcted myocardium was significantly increased compared to the non-infarcted myocardium (both $P<0.05$). Western blotting for CG-RP showed no difference[94].

Section 3.04 Cardiac Magnetic Resonance

We have conducted a full 3T cardiac MRI (CMR) at two different timepoints: early phase (24-48 hours after MI) and late phase (4-6 weeks) in most of the experiment to undertake in-vivo evaluations of this model that are similar to those done in AMI patients.

The CMR were conducted under general anaesthesia by a trained MRI radiographer and reported by a trained cardiologist with specialist interest in CMR. Figure 27 shows a typical transverse late gadolinium enhancement CMR image of a myocardial scar in swine, 24 hours after induction: the scar is clearly visible on the distal part of the septum as well as the apex of the left ventricle, while the posterior aspect of the LV and the proximal part of the septum are not involved by the degenerative process.

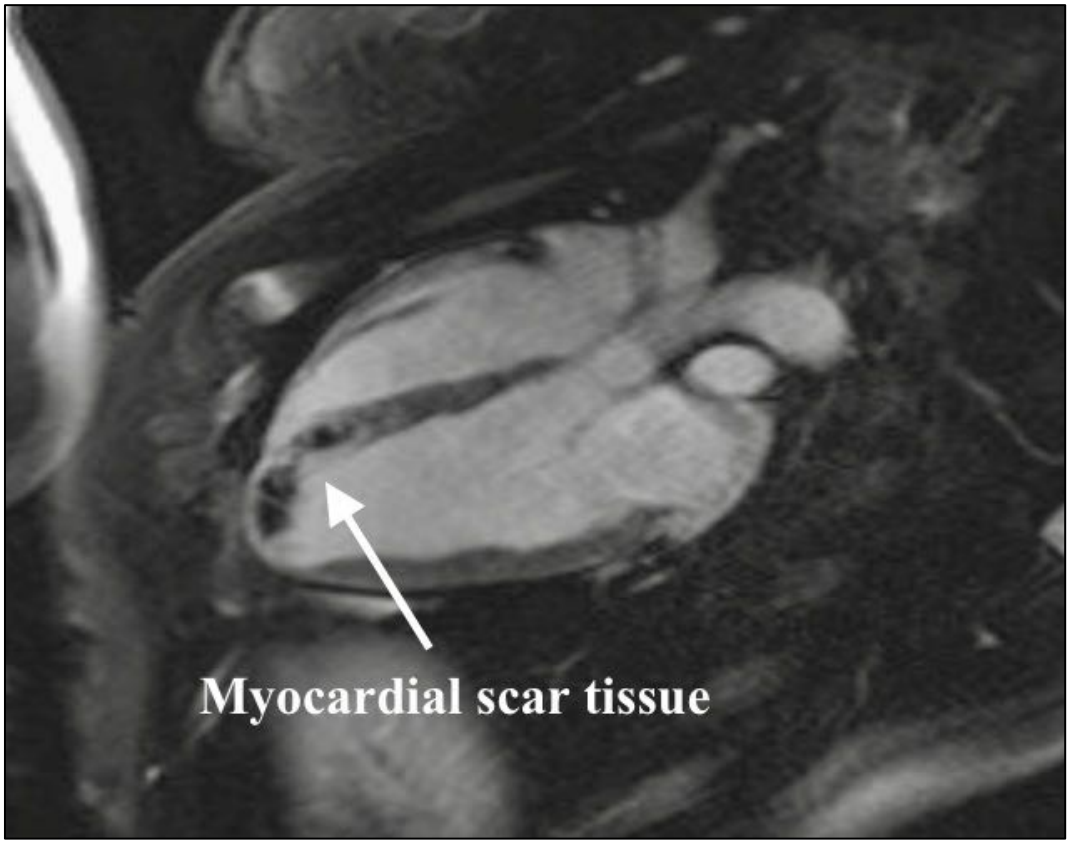

Figure 27. *CMR evidence of a myocardial scar at the acute CMR on the distal portion of the septum and the apical portion of the left ventricle (longitudinal view).*

At the chronic time point, CMR demonstrated thinning of the myocardial tissue in the corresponding region with disappearance of the microvascular obstruction with enhancement demonstrating fibrotic replacement. (Figure 28).

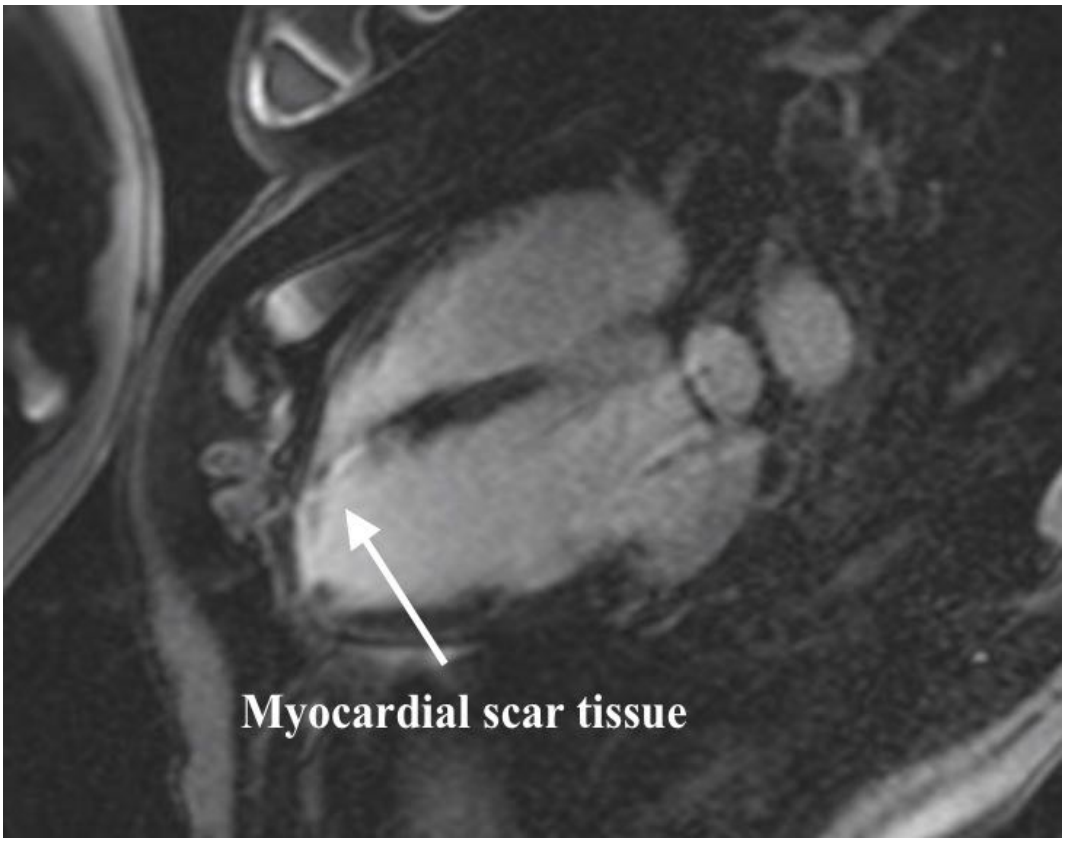

Figure 28. *CMR evidence of a myocardial scar at the chronic CMR: the scar tissue appears to be thinner and more delineated, bit still involving the distal portion of the ventricular septum and the apical portion of the left ventricle.*

(a) Left ventricular measures

In terms of left ventricular function (LVEF), there was a reduction on LVEF on day 2, with a mean value of 43.21±8.62 %. The measurement at 4 weeks were slightly better with an average LVEF of 48.32±5.84 %. There was no difference between 60 and 90 minutes of occlusion in terms

of LVEF on day 2 (43.33± 8.78 % vs 43.11±8.92 respectively, p = 0.93), while the function was better in the 90 minutes group (47.27±5.84 vs 50.22±5.3 %, p = 0.03) at late CMR.

LV volumes tended to be progressively bigger over time: at early MRI the left ventricular end diastolic volume (LVEDV) was 138.38±16.67 ml (LVEDVi = 85.36±9.09 mm/m^2) while the left ventricular end systolic volume was 78.36±16.5 ml (LVESVi = 48.59±9.85 mm/m^2). Four weeks after the MI, the volume increased with a LVEDV of 195.88±24.19 ml (LVEDVi = 106.44±13.52 mm/m^2) and a LVESD of 102.26±17 ml (LVESVi = 55.84±10.22 mm/m^2). There was a significant difference in terms of LVEDD and LVEDVi at four weeks between 60- and 90-minutes groups (LVEDV = 191.64 ± 23.26 mm vs 207.47 ± 22.67, p = 0.022; LVEDVi = 104.15±13.20 vs 112.94 ±11.82 ml/m^2, p = 0.022).Figure 29 shows the LVEDV at the different timepoints for the two groups of occlusions.

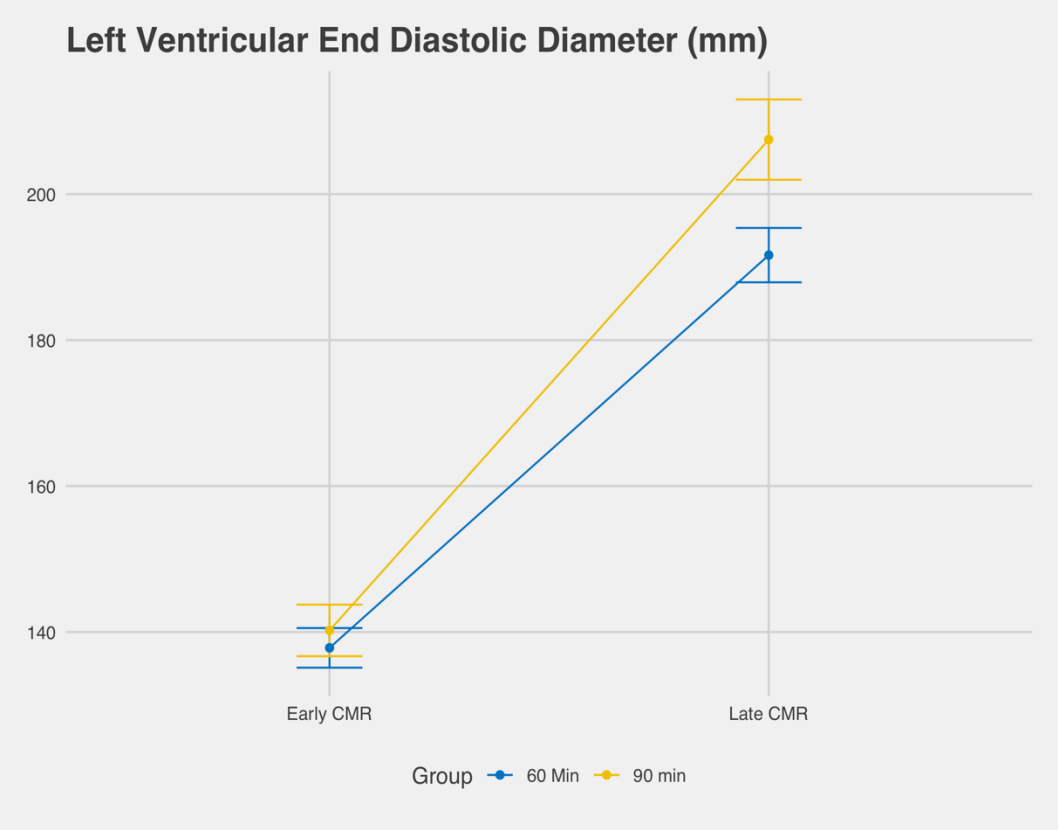

Figure 29. *Left Ventricular End Diastolic volume (n at early CMR = 61; n at late CMR = 57)*

(b) Scar size

As previously described, two methods of quantitative assessment of late gadolinium enhancement images were used: the 5-Standard Deviation (5SD) or Full Width Half Maximum (FWHM) method. These two techniques of measurement were reporting significant different values at each timepoint, when smaller size scar measured with the FWHM method. When measured using the 5SD method, the average scar mass on the early CMR scan was 23.07±8.25 grams representing 24.05±8.13 percent of the entire left ventricular mass. At late CMR the scar size was smaller with a mass of 10±3.61 grams (9.38 ± 3.49 percent of the LV). Using the FWHM method the scar mass was smaller than the 5SD method being 20.70±7.24 grams (percentages of LV mass = 21.61 ± 7.58 %, $p < 0.01$ compared to 5SD method) at early CMR, and 8.38±3.5 grams (percentages of LV mass = 7.93±3.36 %, $p < 0.01$ compared to 5SD method) at late CMR.

(i) Impact of occlusion time on scar size

The degree of late gadolinium enhancement appeared to be bigger at early CMR in the animals that had a coronary occlusion of 90 minutes, while appeared smaller in this group at late CMR. Figure 30 is showing the scar mass (in grams) measured at the two different timepoints using the 5SD method, while Figure 31 shows the scar mass (in gram) measured using the FWHM method.

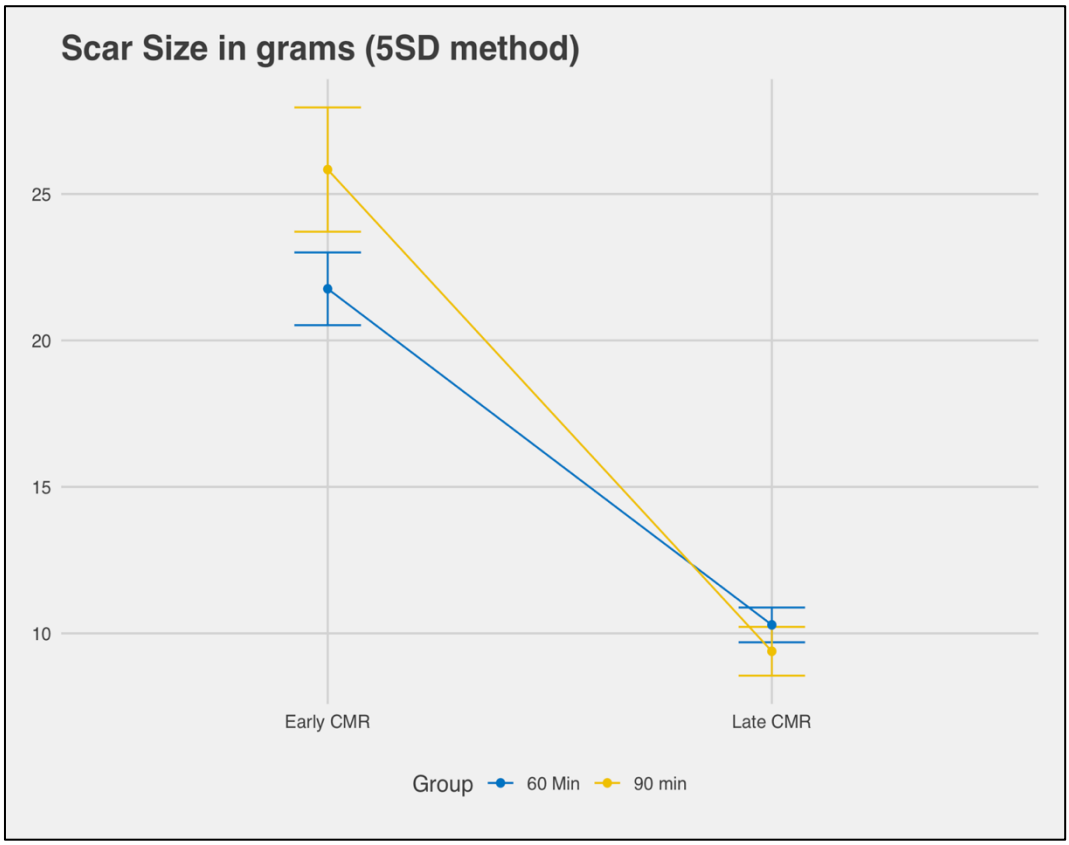

Figure 30. *Scar size weight (in grams) at early and late cardiac MRI depending on the time of coronary occlusion. Blue: 60 minutes occlusion, Yellow: 90 minutes occlusion. Scar size measured with 5SD (5 Standard Deviation) method. (n at Early CMR = 56; n at Late CMR = 56)*

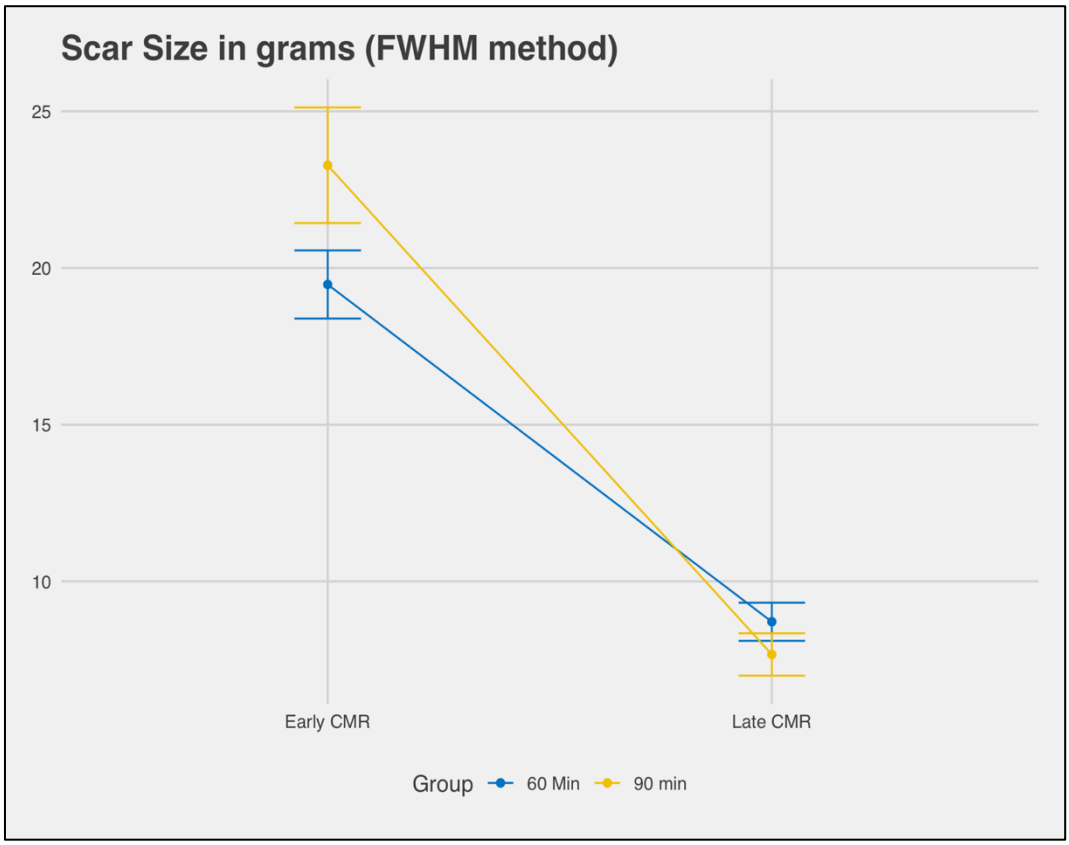

Figure 31. *Scar size weight (in grams) at early and late cardiac MRI depending on the time of coronary occlusion. Blue: 60 minutes occlusion, Yellow: 90 minutes occlusion. Scar size measured with FWHM (Full width at half maximum) method. (n at Early CMR = 56; n at Late CMR = 56)*

The 90 minutes occlusion provided a larger scar at early CMR (confirmed with both methods of assessment), but a smaller scar at late CMR. The scar mass at early CMR was 21.8 ± 7.7 grams in 60 min vs 25.8 ± 9 grams in 90 min when measured with 5SD ($p = 0.04$) and 19.5 ± 6.7 grams vs 23.3 ± 7.9 grams with the FWHM method ($p=0.02$). This difference was not present at late CMR with a 5SD scar mass of 10.3 ± 3.7 grams vs 9.4 ± 3.5 grams ($p = 0.16$) and a FWHM scar mass

of 8.7 ± 3.8 grams vs 7.7 ± 2.9 grams ($p = 0.32$). Table 7 is showing the CMR results in the overall cohort and divided by time of ischaemia.

Table 7. *Cardiac MRI results at early and late timepoints in the overall population and both groups.*

	Overall		60 Minutes occlusion		90 minutes occlusion	
	Early CMR (n = 60)	Late CMR (n = 58)	Early CMR(n = 42)	Late CMR(n = 40	Early CMR(n = 18)	Late CMR(n = 18)
Scar Size						
5SD %	24.05(8.13)	9.38(3.49)	23.79(8.17)	9.84(3.69)	24.61(8.27)	8.39(2.87)
5SD mass(gram)	23.07(8.25)	10(3.61)	21.76(7.66)	10.29(3.65)	25.83(9)	9.39(3.53)
FWHM %	21.61(7.58)	7.93(3.36)	21.26(7.52)	8.42(3.67)	22.33(7.87)	6.89(2.37)
FWHM mass (gram)	20.70(7.24)	8.38(3.5)	19.47(6.7)	8.71(3.75)	23.28(7.83)	7.67(2.87)
LV measures						
LVEF	43.21(8.68)	48.32(5.84)	43.33(8.78)	47.27(5.84)	43.11(8.92)	50.22(5.30)
LVEDV (ml)	138.38(16.67)	195.88(24.19)	137.83(17.59)	191.64(23.26)	140.22(14.98)	207.47(22.67)
LVESV (ml)	78.36(16.50)	102.26(17)	78.43(17.57)	101.97(18.48)	78.33(14.70)	104.71(11.71)
LVEDVi (ml)	85.36(9.09)	106.44(13.52)	85.55(9.36)	104.15(13.20)	84.39(8.60)	112.94(11.82)
LVESVi (ml)	48.59(9.85)	55.84(10.22)	48.69(10.52)	55.79(11.24)	47.89(8.43)	57(6.62)
SV	59.52(13.63)	93.75(15)	59.21(13.06)	89.85(13.32)	60.67(15.47)	102.82(15.55)
SVi	36.95(8.69)	50.78(8.02)	37.18(8.71)	49.19(6.85)	36.44(8.87)	54.24(9.42)
CO	5.06(1.40)	6.18(1.39)	4.84(1.12)	5.99(1.27)	5.52(1.82)	6.68(1.59)

CMR: Cardiac MRI; 5SD: 5 Standard deviations, FWHM: Full width at half maximum; LV: left Ventricle; LVEF: left ventricular ejection fraction; LVEDV: left ventricular end diastolic diameter; LVEDVi: indexed left ventricular end diastolic diameter; LVESV: left ventricular end systolic diameter; LVESVi: indexed left ventricular end systolic diameter; SV: stroke volume; SVi: indexed stroke volume; CO: cardiac output. Data are expressed as mean and SD (in brackets).

(ii) Reliability of CMR late gadolinium assessment

The two methods of assessment of the scar size used during CMR analysis provided a slightly different size of the scar. In the overall population the scar was bigger with the 5SD method at both acute and chronic timepoints. At the acute CMR the mean scar size with 5SD was 23.07±8.25 grams vs 20.7 ± 7.24 grams with FWHM ($p = 0.04$); this difference was even more significant when measured in percentage of the LV mass (24.05±8.13% vs 21.61±7.58%, $p = 0.02$). At the late CMR the mean scar was still bigger in the 5SD being 10±3.61 grams vs 8.38±3.5 grams ($p < 0.01$) and 9.38±3.49% vs 7.93±3.36% ($p <0.01$). When correlated with the peak troponin (at 4 hours) the scar mass measured with 5SD showed a marginally better correlation (Pearson's product moment correlation: $R= 0.44$, $p = 0.001$) compared to FWHM ($R=0.42$, $p =0.002$) as shown in Figure 32.This demonstrate that the size of the scar was proportionally greater when the troponin release was higher.

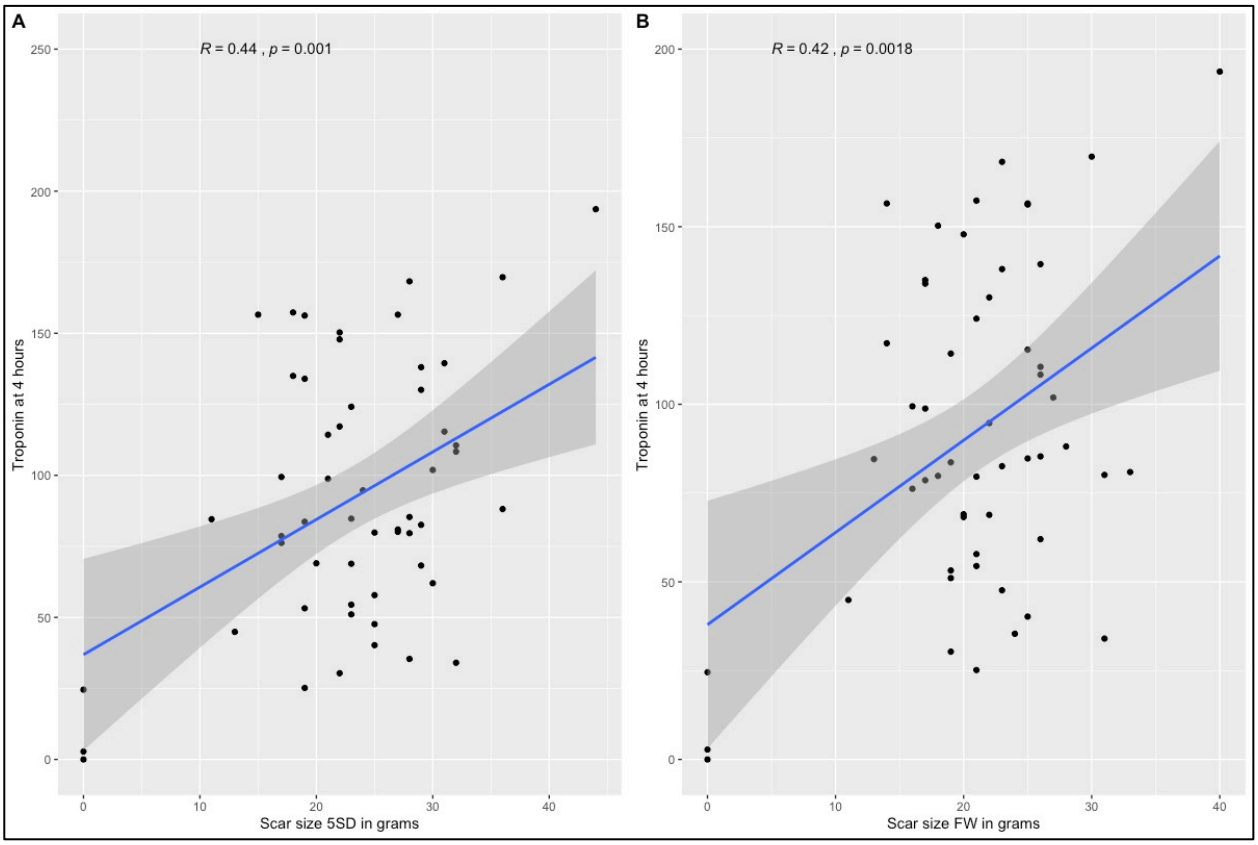

Figure 32. *Correlation between troponin peak and scar size by method of measurement in the acute CMR (A: 5SD method, B: FWHM method): the x-axis represent the scar size weight measurement done with both techniques, while the y-axis represents the peak serum troponin measured 4 hours after the induction of the myocardial infarction; the blue line is a graphical representation of the linear model (with relative confidence intervals: grey shadowed area; n = 56).*

(iii) Impact of ventricular fibrillation on myocardial scar size and ventricular size

Malignant ventricular arrhythmias are a severe complication of the acute MI causing often the occurrence of out-of-hospital arrest: ventricular fibrillation prior to hospitalization have been reported to occur in more than 10% of all MI cases in turn affecting MI survival rates[95]. In our MI model we observed ventricular arrhythmias in a large proportion of our experiments, which is a good reflection of what is seen in humans during AMI. We wanted to understand the impact of VT/VF and the relative DC-shock on the scar size after MI. An additional procedural factor is that DC-Shock/cardioversion, due to abrupt movement of the wired animal on the operating table, might trigger the displacement of the inflated coronary balloon and therefore lead to a possible reperfusion before the end of the pre-established ischaemia time. To avoid this possibility, we checked the position of the balloon after any successful DC-Shock/cardioversion once stable clinical conditions were re-established. For these reasons, we wanted to ascertain the impact of VT/VF and related DC cardioversion on the scar size.

The scar size at the acute timepoint was similar in these two groups: when measured with 5SD method the average scar size was 22.33±8.51 grams in the uncomplicated experiments (vs 24.4±7.81 grams in case of major ventricular arrhythmias, $p = 0.21$). Similar results were found when measured with the FWHM method: in this case the scar size at acute timepoint was 20.31±7.63 grams vs 21.40 ± 6.60 respectively ($p = 0.59$). Even at the chronic timepoint we did not find significant differences in terms of scar between these two groups. At this timepoint the 5SD method showed a scar of 10.06±3.65 grams in the not-complicated group vs 9.90±3.63 in the

arrhythmic group (p = 0.59). The FWHM method also showed similar scar size at the chronic CMR with a 8.53±3.71 grams vs 8.10±3.16 grams respectively (p = 0.74).

Interestingly, we have noticed a trend toward a larger size of the LV at the chronic timepoint in those animals that had an arrhythmia: in this group, the left ventricular end diastolic volume was 260.55±17.90 ml (vs 190.83±25.34 ml, p = 0.02). The same analysis done at the acute CMR did not showed significant differences (138.13±18.29 ml vs 139.27 ±14.11 ml, p =0.80). Similar figures have been seen when considering indexed measurements - at the acute phase the indexed left ventricular end diastolic volume was again similar between uncomplicated and complicated experiments (84.71±9.5 vs 86.5±8.44 respectively, p = 0.59) with near statistical significance at the chronic time point (104.28±13.76 ± 111.40±11.4, p =0.06). This finding might represent an important factor to consider when developing a heart failure model.

Chapter IV. – GENERAL DISCUSSION AND FUTURE WORKS

Section 4.01 Discussion

This work demonstrates the importance and relevance of an appropriate model of myocardial infarction to understand the pathophysiology behind this pathophysiology and to investigate potential targets for treatments with the ultimate aim for translation and improvement in prognosis. Animal models of MI play an important role in translation of new approaches to management of human MI[96] and therefore this thesis provides important information that is helpful in improving the knowledge and refining the quality and reproducibility of these models.

Ischaemic heart disease is the single most common cause of death and its frequency is increasing , now accounting for almost 1.8 million annual deaths[97]. Myocardial infarction is the most severe end of the clinical spectrum in the setting of ischaemic heart disease and it is defined as a abrupt interruption of coronary flow leading ischaemic death of myocardial tissue[21]. Mortality after MI remains substantial with acute mortality varying between 4 and 12 % in European countries while reported 1-year mortality among STEMI patients in angiographic registries is approximately 10%[97]. Moreover, patients who survive to an heart attack have an increased risk of developing heart failure[98] and the improved survival in the last few years has determine an increased number of patients living with HF[21]. Though there have been some improvements in the therapy of HF in recent years, the prognosis remains poor and further understanding and treatment of the adverse remodelling seen in ischaemic HF is needed. It is obvious that deeper understanding

the pathophysiology of the MI is crucial to identify new biomarkers and therapeutic targets and reduce the heavy healthcare and societal burden associated with the condition.

The role of large animal research in this field is undoubtedly important as they resemble to human physiological and pathophysiological processes[99]. This is particularly obvious in an era when significant issues have been identified with research in small animal in relation very high rates of procedural mortality (at times > 50%) and approx. 90% or poor or lack of results reproducibility reported recently in Nature[100].

With this background, we have planned this project to deliver a model with high reliability and reproducibility and importantly, one relevant to the human setting. With this work we have been able to develop extensive expertise of a swine model of myocardial infarction. Using a minimally-invasive closed-chest model clinical approach and through the multi-disciplinary team expertise available at our facility we have been able to achieve a clinically relevant model with a high procedural success rate of 94%, and a low complication and mortality rate. We have used clinical NHS standards to develop and implement every step of this model and the entire project has been carried out through the supervision of fully trained cardiologists and cardiac surgeons to replicate what it is currently done in clinical practice. We have taken every opportunity to optimise our techniques and protocols allowing refinement and standardisation – a crucial factor when planning studies aiming to develop novel therapies. We developed and implemented a strict resuscitation protocol involving no further resuscitation after 3 cycles. The development of the arrhythmias protocol is one of these improvements that allowed us to treat vast majority of the severe ventricular arrhythmias that we have faced during the experiments - despite observing a 40% incidence of major ventricular arrhythmias, the mortality rate was only 6.2%: this was possible through a protocol that included infusion of Amiodarone and Magnesium throughout the

procedure. This experience signifies that this model can also be used to understand the development and occurrence of ventricular arrhythmias during AMI and to develop potential therapeutic measures in future work. Interestingly we have noticed a constant pattern of development of major arrhythmias with vast majority of the animals experiencing this complication between minute 25 and minute 35 of coronary occlusion - we believe this could be a potential cut-off time indicating important underlying cellular changes which warrant further investigation in future work.

The additional strength of this work is that we have been able to characterize the model fully using clinically-relevant biomarkers and reference standard CMR scanning for structural and functional assessment. The heart shape and size of the Yorkshire pig are very similar to the human and most of the cardiac MRI measures in this swine model (Table 7) are very close to those obtained with the human heart (Table 3).

In terms of myocardial scar, this model of antero-apical MI showed an average scar size similar to that observed in patients suffering anterior MI. Although human these studies are affected by a certain variability of timings and techniques of assessment (Table 2), the scar size measured in the early phase after an MI has been reported between 16 % and 27.2% of the entire LV mass. In our model, in the early phase, we have measured an average scar size of 21.6 % (with FWHM method) and 24.5 % (with 5SD method): these values are in keeping with those reported in table 2. Differently from the acute phase, the scar size in the late phase was smaller in our model: in Table 2 we can see that the scar size in human at this timepoint is comprised between 11.3 % and 21.1%: in our model we have measured an average scar of 9.38 % (with the 5SD method) and 7.93% (with the FWHM method).

These are important findings as they mean that when using this model to develop or test new treatments for MI there will be no need for scaling up when translating new treatments to bedside. One other important finding was related to the similar scar size between the 60 minutes and the 90 minutes occlusion time - this discovery represents an important factor when planning future research projects. The observation that occlusion of the coronary artery for 90 minutes resulted in a higher number of complications and greater haemodynamic instability, without gaining an important changes in scar size is crucial for minimizing animal loss in future projects. Taking this forward, we have been able to conclude that occlusion of the coronary artery for 60 minutes is adequate to achieve a reasonable scar size of about 20% of the LV while minimizing complication rate. Finally, we have also compared the different late gadolinium enhancement quantification used in cardiac MRI and were able to demonstrate that there were no significant differences between 5SD and FWHM: both techniques had a significant positive correlation with the serum troponin release and therefore are reliable measurement of scar size. Moreover, though this was an MI protocol, using CMR we have been able to assess for ventricular remodelling and systolic impairment and we would be able to develop this for HF-related as well as MI-related projects in future work.

The ability of our facility and the assembled team to deliver this project means that future research projects can be developed using our refined model and minimal number of animals in line with the 3Rs requirements. The protocols and procedures developed are now readily usable for translation of innovative medications and devices into human clinical research in the setting of MI and HF.

Section 4.02 Future perspectives

This model can be easily replicated in large scale to test potential therapeutic measure for cardiac ischaemia-reperfusion injury, myocardial infarction and heart failure. At the time I am writing this thesis, several different projects are being conducted at the TBRC using this model to develop and test new drugs, cell-based or gene-based new therapy to help reducing scar size and preserve LV function following AMI. With this model we have been able to investigate the potential therapeutic effect of several different medications as well as the impact of stem cells directly injected into the myocardial scar. Moreover, we have been able to start a project using animal subjected to this model and then superimpose a model of cardiac surgery with cardiopulmonary bypass to test a new myocardial protection technique.

The relevance of these applications is important due to the potential for translation to the clinical setting – given the similarities in size, anatomy and clinical characteristics of the swine heart we could anticipate a quick and swift translational effect of positive findings into human first in-man clinical trials.

One of the most significant factors that led this work was related to the high reproducibility and reliability of the model: we are currently in the process of developing a multinational collaboration to gather clinical information from other sites that are conducting MI model in large animals. With this project we aim to create an international network and a registry of MI model in large animals to share knowledge and expertise and therefore further optimise what we have learned with this work.

Through this model I have been able to learn the basics of catheter-based coronary techniques. This is another significant positive aspect of this model that represents a relevant learning procedure for clinicians in training and for healthcare professionasl who wants to develop

different skill-sets. In my case it represented an excellent way of understanding and learning percutaneous coronary interventions that are very relevant to my clinical practice: these new learning points have been extremely useful in my clinical activities and have allowed me to interact with professionals from different specialties. In addition, these skills will be crucial for my plan to develop my clinical academic career in translational work. To this end, I am applying for clinical research intermediate fellowships and research grants based on the experience I have gained during this project.

Section 4.03 Limitations

This study has several limitations mostly related to the technical aspects of the project. First, the size of the scar, although consistent, cannot be entirely predicted at the time of myocardial infarction due to the anatomical variability of the coronary circulation. Several factors appear to have an impact on scar size and some of them are not entirely controllable. The balloon landing zone depends heavily on the anatomy of the coronary to be occluded and a consistent target area is very difficult to reproduce. Generally, the more proximal the occlusion or the larger the myocardial territory affected, the larger the scar, but this comes at the cost of exposing the animal to an elevated risk of complications such as ventricular arrhythmias and therefore increasing the mortality rate. In an attempt to mitigate this limitation, we have tried to standardize the occlusion targeting the same region of the mid portion of the LAD but given variability in branch anatomy, we appreciate further work is needed to address this.

Another important limitation is related to the methods of assessment of the scar size. Since there is not a unique method of CMR evaluation of the MI scar tissue, we have used two of the

most commonly used (5-Standard Deviation - 5SD and Full Width Half Maximum -FWHM): the two methods have showed a slightly different size of scar despite having been analyzed by the same team with the same MRI methods. In the 60 minutes group the 5SD method reported on average a larger scar size at both early and late CMR, while in the 90 minutes group the FWHM have shown a larger size than the 5SD. We have compared the two methods correlating the measurement in the acute phase to the peak of troponin and found no significant difference between these two methods in terms of reliability.

A third significant limitation of this specific group of animals is related to the fact that some of these animals have received a medication that was intended to mitigate the myocardial ischaemia-reperfusion injury and therefore could have had consequences on the scar size.

The cTnI serum concentration was not consistent across the experiments with a wide variance between the animals at the different timepoints. Although this might be due to several factors, including methods of assay, the most likely cause is the variability in myocardial damage, which still remains the main limitation of this model.

Finally, we used healthy animals with no atherosclerosis. Ideally, this model could be easily applied to either genetically modified pigs with a tendancy to develop atherosclerosis or a high fat diet approach – the first seeming preferred as a diet approach would require several months of preparation to obtain a tangible amount of atherosclerosis at considerable animal husbandry cost. It is likely that in a context of diffuse atherosclerosis we would observe a higher incidence of VT/VF during the MI induction as well as a larger scar size. Hence, repeating this study in a porcine model of atherosclerosis would be of great additional value to the results presented in this thesis.

Chapter V. REFERENCES

1. Thygesen K, Alpert JS, White HD. Universal definition of myocardial infarction. *Circulation*. 2007;116(22):2634-2653. doi:10.1161/CIRCULATIONAHA.107.187397

2. Harrington RA. Targeting inflammation in coronary artery disease. *N Engl J Med*. 2017;377(12):1197-1198. doi:10.1056/NEJMe1709904

3. American Heart Association. Understand Your Risks to Prevent a Heart Attack. https://www.heart.org/en/health-topics/heart-attack/understand-your-risks-to-prevent-a-heart-attack. Published 2016. Accessed October 15, 2020.

4. Thygesen K, Alpert JS, Jaffe AS, et al. Third universal definition of myocardial infarction. *Eur Heart J*. 2012;33(20):2551-2567. doi:10.1093/eurheartj/ehs184

5. Kayani WT, Ballantyne CM. Improving outcomes after myocardial infarction in the US population. *J Am Heart Assoc*. 2018;7(4):117-120. doi:10.1161/JAHA.117.008407

6. Emelia J. Benjamin, MD, SCM F, Michael J. Blaha, MD M, Stephanie E. Chiuve S, et al. *Heart Disease and Stroke Statistics—2017 Update*. Vol 135.; 2017. doi:10.1161/CIR.0000000000000485.Heart

7. White HD, Chew DP. Acute myocardial infarction. *Lancet*. 2008;372:570-584. http://www.ncbi.nlm.nih.gov/pubmed/12642064.

8. Kernis SJ, Harjai KJ, Stone GW, et al. The incidence, predictors, and outcomes of early reinfarction after primary angioplasty for acute myocardial infarction. *J Am Coll Cardiol*. 2003;42(7):1173-1177. doi:10.1016/S0735-1097(03)00920-3

9. Torabi A, Cleland JGF, Rigby AS, Sherwi N. Development and course of heart failure after a myocardial infarction in younger and older people. *J Geriatr Cardiol*. 2014;11(1):1-12. doi:10.3969/j.issn.1671-5411.2014.01.002

10. Global Health Observatory data repository. World Health Organization. https://apps.who.int/gho/data/node.home#. Published 2016. Accessed October 15, 2020.

11. Ambrosy AP, Fonarow GC, Butler J, et al. The global health and economic burden of hospitalizations for heart failure: Lessons learned from hospitalized heart failure registries. *J Am Coll Cardiol*. 2014;63(12):1123-1133. doi:10.1016/j.jacc.2013.11.053

12. Townsend N, Williams J, Bhatnagar P, Wickramasinghe K, Rayner. M. *Cardiovascular Disease Statistics 2014*.; 2014.

13. Yancy CW, Jessup M, Bozkurt B, et al. 2013 ACCF/AHA guideline for the management of heart failure: A report of the American college of cardiology foundation/american heart association task force on practice guidelines. *J Am Coll Cardiol*. 2013;62(16). doi:10.1016/j.jacc.2013.05.019

14. Lerman DA, Alotti N, Ume KL, Péault B. Cardiac repair and regeneration: The value of cell therapies. *Eur Cardiol Rev* . 2016;11(1):43-48. doi:10.15420/ecr.2016:8:1

15. Marín-Juez R, Marass M, Gauvrit S, et al. Fast revascularization of the injured area is

essential to support zebrafish heart regeneration. *Proc Natl Acad Sci*. 2016;113(40):11237 LP - 11242. doi:10.1073/pnas.1605431113

16. Narmoneva DA, Vukmirovic R, Davis ME, Kamm RD, Lee RT. Endothelial cells promote cardiac myocyte survival and spatial reorganization: implications for cardiac regeneration. *Circulation*. 2004;110(8):962-968. doi:10.1161/01.CIR.0000140667.37070.07

17. Psaltis PJ, Simari RD. Vascular wall progenitor cells in health and disease. *Circ Res*. 2015;116(8):1392-1412. doi:10.1161/CIRCRESAHA.116.305368

18. Paschalaki KE, Starke RD, Hu Y, et al. Dysfunction of endothelial progenitor cells from smokers and chronic obstructive pulmonary disease patients due to increased DNA damage and senescence. *Stem Cells*. 2013;31(12):2813-2826. doi:10.1002/stem.1488

19. Toshner M, Dunmore BJ, McKinney EF, et al. Transcript analysis reveals a specific HOX signature associated with positional identity of human endothelial cells. *PLoS One*. 2014;9(3):e91334. doi:10.1371/journal.pone.0091334

20. Weil BR, Neelamegham S. Selectins and immune cells in aucte mycardial infarction and post-infarction ventricular remodelings: Pathophysiology and novel treatments. *Front Immunol*. 2019;10(FEB):1-15. doi:10.3389/fimmu.2019.00300

21. Frangogiannis NG. Pathophysiology of myocardial infarction. *Compr Physiol*. 2015;5(4):1841-1875. doi:10.1002/cphy.c150006

22. Jennings R, Ganote C. Structural Changes in Myocardium During Acute Ischemia. *Circ*

Res. 1974;35(Suppl 3):156-172.

23. Hashmi S, Al-Salam S. Acute myocardial infarction and myocardial ischemia-reperfusion injury: a comparison. *Int J Clin Exp Pathol*. 2015;8(8):8786-8796. http://www.ncbi.nlm.nih.gov/pubmed/26464621%0Ahttp://www.pubmedcentral.nih.gov/articlerender.fcgi?artid=PMC4583853.

24. Heusch G, Skyschally A, Schulz R. The in-situ pig heart with regional ischemia/reperfusion - Ready for translation. *J Mol Cell Cardiol*. 2011;50(6):951-963. doi:10.1016/j.yjmcc.2011.02.016

25. Groenen MAM. A decade of pig genome sequencing: a window on pig domestication and evolution. *Genet Sel Evol*. 2016;48:23. doi:10.1186/s12711-016-0204-2

26. Cabot RA, Kühholzer B, Chan AW, et al. Transgenic pigs produced using in vitro matured oocytes infected with a retroviral vector. *Anim Biotechnol*. 2001;12(2):205-214. doi:10.1081/ABIO-100108347

27. Li M, Chen L, Tian S, et al. Comprehensive variation discovery and recovery of missing sequence in the pig genome using multiple de novo assemblies. *Genome Res*. 2017;27(5):865-874. doi:10.1101/gr.207456.116

28. Wernersson R, Schierup MH, Jørgensen FG, et al. Pigs in sequence space: A 0.66X coverage pig genome survey based on shotgun sequencing. *BMC Genomics*. 2005;6:1-7. doi:10.1186/1471-2164-6-70

29. Kumar M, Reddy E, Narendra L, et al. Animal models of myocardial infarction : Mainstay

in clinical translation. *Regul Toxicol Pharmacol*. 2016;76:221-230. doi:10.1016/j.yrtph.2016.03.005

30. Lindsey ML, Bolli R, Canty JM, et al. Guidelines for experimental models of myocardial ischemia and infarction. *Am J Physiol Circ Physiol*. 2018;314(4):H812-H838. doi:10.1152/ajpheart.00335.2017

31. Heinzel FR, Luo Y, Li X, et al. Impairment of diazoxide-induced formation of reactive oxygen species and loss of cardioprotection in connexin 43 deficient mice. *Circ Res*. 2005;97(6):583-586. doi:10.1161/01.RES.0000181171.65293.65

32. Kang PM, Aoki H, Izumo S, Haunstetter A, Usheva A. Morphological and Molecular Characterization of Adult Cardiomyocyte Apoptosis During Hypoxia and Reoxygenation. *Circ Res*. 2012;87(2):118-125. doi:10.1161/01.res.87.2.118

33. Bell RM, Mocanu MM, Yellon DM. Retrograde heart perfusion: The Langendorff technique of isolated heart perfusion. *J Mol Cell Cardiol*. 2011;50(6):940-950. doi:10.1016/j.yjmcc.2011.02.018

34. Bux AS, Lindsey ML, Vasquez HG, Taegtmeyer H, Harmancey R. Glucose regulates the intrinsic inflammatory response of the heart to surgically induced hypothermic ischemic arrest and reperfusion. *Physiol Genomics*. 2016;49(1):37-52. doi:10.1152/physiolgenomics.00102.2016

35. O h-Ici D, Jeuthe S, Dietrich T, et al. Closed-chest small animal model to study myocardial infarction in an MRI environment in real time. *Int J Cardiovasc Imaging*. 2014;31(1):115-121. doi:10.1007/s10554-014-0539-0

36. Baker M. 1,500 scientists lift the lid on reproducibility. *Nature*. 2016;533(7604):452-454. doi:10.1038/533452a

37. Allison D, Brown AW, George BJ, Kaiser KA. A tragedy of errors. *Nature*. 2016;530:7-9.

38. Smith EF, Egan JW, Bugelski PJ, Hill DE, Hillegass LM, Griswold DE. Temporal relation between neutrophil accumulation and myocardial reperfusion injury. *Am J Physiol Circ Physiol*. 1988;255(5):H1060-H1068. doi:10.1152/ajpheart.1988.255.5.h1060

39. Michael LH, Entman ML, Hartley CJ, et al. Myocardial ischemia and reperfusion: a murine model. *Am J Physiol Circ Physiol*. 1995;269(6):H2147-H2154. doi:10.1152/ajpheart.1995.269.6.h2147

40. Himori N, Matsuura A. A simple technique for occlusion and reperfusion of coronary artery in conscious rats. *Am J Physiol Circ Physiol*. 1989;256(6):H1719-H1725. doi:10.1152/ajpheart.1989.256.6.h1719

41. Pfeffer MA, Fletcher PJ, Spadaro J, et al. Myocardial infarct size and ventricular function in rats. *Circ Res*. 1979;44(4):503-512. doi:10.1161/01.res.44.4.503

42. Meijler FL. Atrioventricular conduction versus heart size from mouse to whale. *J Am Coll Cardiol*. 1985;5(2):363-365. doi:10.1016/S0735-1097(85)80060-7

43. TAN M-Y, FAN Z-W, ZHOU H, et al. Development of a new model for acute myocardial infarction in rabbits. *J Vet Med Sci*. 2017;79(3):467-473. doi:10.1292/jvms.16-0114

44. Markkanen JE, Rissanen TT, Kivelä A, Ylä-Herttuala S. Growth factor-induced therapeutic angiogenesis and arteriogenesis in the heart - Gene therapy. *Cardiovasc Res*.

2005;65(3):656-664. doi:10.1016/j.cardiores.2004.10.030

45. Bolukoglu H, Liedtke AJ, Nellis SH, Eggleston AM, Subramanian R, Renstrom B. An animal model of chronic coronary stenosis resulting in hibernating myocardium. *Am J Physiol Circ Physiol*. 2017;263(1):H20-H29. doi:10.1152/ajpheart.1992.263.1.h20

46. Yang P, Han P, Hou J, et al. Electrocardiographic Characterization of Rhesus Monkey Model of Ischemic Myocardial Infarction Induced by Left Anterior Descending Artery Ligation. *Cardiovasc Toxicol*. 2011;11(4):365-372. doi:10.1007/s12012-011-9129-8

47. Bond MG, Bullock BC, Bellinger D a, Hamm TE. Myocardial infarction in a large colony of nonhuman primates with coronary artery atherosclerosis. *Am J Pathol*. 1980;101(3):675-692. http://www.pubmedcentral.nih.gov/articlerender.fcgi?artid=1903666&tool=pmcentrez&rendertype=abstract.

48. Jugdutt BI. The dog model of left ventricular remodeling after myocardial infarction. *J Card Fail*. 2002;8(6 SUPPL.):472-475. doi:10.1054/jcaf.2002.129274

49. Lichtig C, Brooks H, Chassagne G, Glagov S WR. Basic fuchsin picric acid method to detect acute myocardial ischemia. An experimental study in swine. *Arch Pathol*. 1975;99(3):158-161.

50. Krombach G a, Kinzel S, Mahnken AH, Günther RW, Buecker A. Minimally invasive close-chest method for creating reperfused or occlusive myocardial infarction in swine. *Invest Radiol*. 2005;40(1):14-18. http://www.ncbi.nlm.nih.gov/pubmed/15597015.

51. Liu JX, Yu Z, Li XZ, et al. Cardioprotective effects of diltiazem reevaluated by a novel myocardial ischemic model in Chinese miniature swine. *Acta Pharmacol Sin*. 2007;28(1):52-57. doi:10.1111/j.1745-7254.2007.00464.x

52. Dib N, Diethrich EB, Campbell A, Gahremanpour A, McGarry M, Opie SR. A percutaneous swine model of myocardial infarction. *J Pharmacol Toxicol Methods*. 2006;53(3):256-263. doi:10.1016/j.vascn.2005.10.005

53. Koning MMG, Krams R, Xiao CS, et al. Intracoronary trimetazidine does not improve recovery of regional function in a porcine model of repeated ischemia. *Cardiovasc Drugs Ther*. 1993;7(5):801-807. doi:10.1007/BF00878934

54. Chen Y, Tao Y, Zhang L, Xu W, Zhou X. Diagnostic and prognostic value of biomarkers in acute myocardial infarction. *Postgrad Med J*. 2019;95(1122):210-216. doi:10.1136/postgradmedj-2019-136409

55. Karmen A, Wroblewski F, J.S. L. Transaminase activity in human blood. *J Clin Invest*. 1955;34(1):131-133.

56. Nowakowski JF. Use of cardiac enzymes in the evaluation of acute chest pain. *Ann Emerg Med*. 1986;15(3):354-360. doi:10.1016/s0196-0644(86)80584-4

57. Katus HA, Remppis A, Looser S, Hallermeier K, Scheffold T, Kübler W. Enzyme linked immuno assay of cardiac troponin T for the detection of acute myocardial infarction in patients. *J Mol Cell Cardiol*. 1989;21(12):1349-1353. doi:10.1016/0022-2828(89)90680-9

58. Conrad MJ, Jarolim P. Cardiac troponins and high-sensitivity cardiac troponin assays. *Clin*

Lab Med. 2014;34(1):59-73, vi. doi:10.1016/j.cll.2013.11.008

59. Feng YJ, Chen C, Fallon JT, et al. Comparison of cardiac troponin I, creatine kinase-MB, and myoglobin for detection of acute ischemic myocardial injury in a swine model. *Am J Clin Pathol*. 1998;110(1):70-77. doi:10.1093/ajcp/110.1.70

60. Mahajan VS, Jarolim P. How to interpret elevated cardiac troponin levels. *Circulation*. 2011;124(21):2350-2354. doi:10.1161/CIRCULATIONAHA.111.023697

61. Seropian IM, Sonnino C, Van Tassell BW, Biasucci LM, Abbate A. Inflammatory markers in STelevation acute myocardial infarction. *Eur Hear J Acute Cardiovasc Care*. 2016;5(4):382-395. doi:10.1177/2048872615568965

62. Seropian IM, Toldo S, Van Tassell BW, Abbate A. Anti-inflammatory strategies for ventricular remodeling following ST-segment elevation acute myocardial infarction. *J Am Coll Cardiol*. 2014;63(16):1593-1603. doi:10.1016/j.jacc.2014.01.014

63. Barron H V, Cannon CP, Murphy SA, Braunwald E, Gibson CM. Association between white blood cell count, epicardial blood flow, myocardial perfusion, and clinical outcomes in the setting of acute myocardial infarction: a thrombolysis in myocardial infarction 10 substudy. *Circulation*. 2000;102(19):2329-2334. doi:10.1161/01.cir.102.19.2329

64. Porto I, De Maria GL, Leone AM, et al. Endothelial progenitor cells, microvascular obstruction, and left ventricular remodeling in patients with ST elevation myocardial infarction undergoing primary percutaneous coronary intervention. *Am J Cardiol*. 2013;112(6):782-791. doi:10.1016/j.amjcard.2013.04.056

65. Morishima I, Sone T, Tsuboi H, et al. Plasma C-reactive protein predicts left ventricular remodeling and function after a first acute anterior wall myocardial infarction treated with coronary angioplasty: comparison with brain natriuretic peptide. *Clin Cardiol*. 2002;25(3):112-116. doi:10.1002/clc.4960250306

66. Guillen I, Blanes M, Gomez-Lechon MJ, Castell J V. Cytokine signaling during myocardial infarction: Sequential appearance of IL-1β and IL-6. *Am J Physiol - Regul Integr Comp Physiol*. 1995. doi:10.1152/ajpregu.1995.269.2.r229

67. Ohtsuka T, Hamada M, Inoue K, et al. Relation of circulating interleukin-6 to left ventricular remodeling in patients with reperfused anterior myocardial infarction. *Clin Cardiol*. 2004. doi:10.1002/clc.4960270712

68. Borrayo-Sánchez G, Pacheco-Bouthillier A, Mendoza-Valdez L, Isordia-Salas I, Argüero-Sánchez R, Careaga Reyna G. Prognostic value of serum levels of interleukin-6 in patients with ST-segment elevation acute myocardial infarction. *Cir Cir*. 2010;78(1):25-30.

69. Nilsson L, Szymanowski A, Swahn E, Jonasson L. Soluble TNF Receptors Are Associated with Infarct Size and Ventricular Dysfunction in ST-Elevation Myocardial Infarction. *PLoS One*. 2013. doi:10.1371/journal.pone.0055477

70. Bełtowski J. Short-term follow-up BNP level and risk stratification after myocardial infarction. *Int J Cardiol*. 2019;291:173-174. doi:10.1016/j.ijcard.2019.05.012

71. Lee JW, Choi E, Khanam SS, et al. Prognostic value of short-term follow-up B-type natriuretic peptide levels after hospital discharge in patients with acute myocardial infarction. *Int J Cardiol*. 2019. doi:10.1016/j.ijcard.2019.01.026

72. Omland T, Aakvaag A, Bonarjee V V, et al. Plasma brain natriuretic peptide as an indicator of left ventricular systolic function and long-term survival after acute myocardial infarction. Comparison with plasma atrial natriuretic peptide and N-terminal proatrial natriuretic peptide. *Circulation*. 1996;93(11):1963-1969. doi:10.1161/01.cir.93.11.1963

73. Durak-Nalbantić A, Džubur A, Dilić M, et al. Brain natriuretic peptide release in acute myocardial infarction. *Bosn J Basic Med Sci*. 2012;12(3):164-168. doi:10.17305/bjbms.2012.2470

74. Yang L, Gregorich ZR, Cai W, et al. Quantitative Proteomics and Immunohistochemistry Reveal Insights into Cellular and Molecular Processes in the Infarct Border Zone One Month after Myocardial Infarction. 2017;16(5):2101-2112. doi:10.1007/s11065-015-9294-9.Functional

75. Datta K, Basak T, Varshney S, Sengupta S, Sarkar S. Quantitative proteomic changes during post myocardial infarction remodeling reveals altered cardiac metabolism and Desmin aggregation in the infarct region. *J Proteomics*. 2017;152:283-299. doi:10.1016/j.jprot.2016.11.017

76. Binek A, Fernández-Jiménez R, Jorge I, et al. Proteomic footprint of myocardial ischemia/reperfusion injury: Longitudinal study of the at-risk and remote regions in the pig model. *Sci Rep*. 2017;7(1):1-16. doi:10.1038/s41598-017-11985-5

77. Esmaeilzadeh M, Parsaee M, Maleki M. The role of echocardiography in coronary artery disease and acute myocardial infarction. *J Tehran Univ Hear Cent*. 2013;8(1):1-13.

78. Huenges K, Pokorny S, Berndt R, Cremer J, Lutter G. Transesophageal Echocardiography

in Swine: Establishment of a Baseline. *Ultrasound Med Biol*. 2017;43(5):974-980. doi:10.1016/j.ultrasmedbio.2016.12.011

79. Bulluck H, Dharmakumar R, Arai AE, Berry C, Hausenloy DJ. Cardiovascular magnetic resonance in acute st-segment-elevation myocardial infarction: Recent advances, controversies, and future directions. *Circulation*. 2018;137(18):1949-1964. doi:10.1161/CIRCULATIONAHA.117.030693

80. Kim HW, Farzaneh-Far A, Kim RJ. Cardiovascular Magnetic Resonance in Patients With Myocardial Infarction. Current and Emerging Applications. *J Am Coll Cardiol*. 2009;55(1):1-16. doi:10.1016/j.jacc.2009.06.059

81. Captur G, Manisty C, Moon JC. Cardiac MRI evaluation of myocardial disease. *Heart*. 2016;102(18):1429-1435. doi:10.1136/heartjnl-2015-309077

82. Dastidar AG, Harries I, Pontecorboli G, et al. Native T1 mapping to detect extent of acute and chronic myocardial infarction: comparison with late gadolinium enhancement technique. *Int J Cardiovasc Imaging*. 2019;35(3):517-527. doi:10.1007/s10554-018-1467-1

83. Cui C, Wang S, Lu M, et al. Detection of recent myocardial infarction using native T1 mapping in a swine model: A validation study. *Sci Rep*. 2018;8(1):1-10. doi:10.1038/s41598-018-25693-1

84. Ingkanisorn WP, Rhoads KL, Aletras AH, Kellman P, Arai AE. Gadolinium delayed enhancement cardiovascular magnetic resonance correlates with clinical measures of myocardial infarction. *J Am Coll Cardiol*. 2004;43(12):2253-2259.

doi:10.1016/j.jacc.2004.02.046

85. Hombach V, Grebe O, Merkle N, et al. Sequelae of acute myocardial infarction regarding cardiac structure and function and their prognostic significance as assessed by magnetic resonance imaging. *Eur Heart J*. 2005;26(6):549-557. doi:10.1093/eurheartj/ehi147

86. Ibrahim T, Hackl T, Nekolla SG, et al. Acute myocardial infarction: Serial cardiac MR imaging shows a decrease in delayed enhancement of the myocardium during the 1st week after reperfusion. *Radiology*. 2010;254(1):88-97. doi:10.1148/radiol.09090660

87. Dall'Armellina E, Karia N, Lindsay AC, et al. Dynamic changes of edema and late gadolinium enhancement after acute myocardial infarction and their relationship to functional recovery and salvage index. *Circ Cardiovasc Imaging*. 2011;4(3):228-236. doi:10.1161/CIRCIMAGING.111.963421

88. Ganame J, Messalli G, Masci PG, et al. Time course of infarct healing and left ventricular remodelling in patients with reperfused ST segment elevation myocardial infarction using comprehensive magnetic resonance imaging. *Eur Radiol*. 2011;21(4):693-701. doi:10.1007/s00330-010-1963-8

89. McCall FC, Telukuntla KS, Karantalis V, et al. Myocardial infarction and intramyocardial injection models in swine. *Nat Protoc*. 2012;7(8):1479-1496. doi:10.1038/nprot.2012.075

90. Gómez FA, Ballesteros LE. Morphologic expression of the left coronary artery in pigs. An approach in relation to human heart. *Brazilian J Cardiovasc Surg*. 2014;29(2):214-220. doi:10.5935/1678-9741.20140027

91. McCall FC, Telukuntla KS, Karantalis V, et al. Myocardial infarction and intramyocardial injection models in swine. *Nat Protoc*. 2012;7(8):1479-1496. doi:10.1038/nprot.2012.075

92. Koudstaal S, Jansen of Lorkeers SJ, Gho JMIH, et al. Myocardial infarction and functional outcome assessment in pigs. *J Vis Exp*. 2014;(86):1-10. doi:10.3791/51269

93. Di Diego JM, Antzelevitch C. Ischemic Ventricular Arrhythmias Experimental Models and Their Clinical Relevance. *Hear Rhythm*. 2011;8(12):1963-1968. doi:10.1111/j.1547-5069.2010.01344.x.Prenatal

94. Mansell DS, Bruno VD, Sammut E, et al. Regional changes in myocardial strain predict ventricular remodelling after myocardial infarction in a large animal model. *Submitted*.

95. Sattler SM, Skibsbye L, Linz D, Lubberding AF, Tfelt-Hansen J, Jespersen T. Ventricular Arrhythmias in First Acute Myocardial Infarction: Epidemiology, Mechanisms, and Interventions in Large Animal Models. *Front Cardiovasc Med*. 2019;6(November). doi:10.3389/fcvm.2019.00158

96. Wang J, Bo H, Meng X, Wu Y, Bao Y, Li Y. A simple and fast experimental model of myocardial infarction in the mouse. *Texas Hear Inst J*. 2006;33(3):290-293.

97. Ibanez B, James S, Agewall S, et al. 2017 ESC Guidelines for the management of acute myocardial infarction in patients presenting with ST-segment elevation. *Eur Heart J*. 2018;39(2):119-177. doi:10.1093/eurheartj/ehx393

98. Crisóstomo V, Maestre J, Maynar M, et al. Development of a Closed Chest Model of Chronic Myocardial Infarction in Swine: Magnetic Resonance Imaging and Pathological

Evaluation. *ISRN Cardiol*. 2013;2013:1-8. doi:10.1155/2013/781762

99. Lukács E, Magyari B, Tóth L, et al. Overview of large animal myocardial infarction models (review). *Acta Physiol Hung*. 2012;99(4):365-381. doi:10.1556/aphysiol.99.2012.4.1

100. Baker M. Is there a reproducibility crisis? *Nature*. 2016;533:452-454.

101. du Sert NP, Ahluwalia A, Alam S, et al. *Reporting Animal Research: Explanation and Elaboration for the Arrive Guidelines 2.0*. Vol 18.; 2020. doi:10.1371/journal.pbio.3000411

Appendix

Section 5.01 ARRIVE Guidelines conformity

In this section I report the ARRIVE guidelines 2.0 checklist: The ARRIVE guidelines (Animal Research: Reporting In-vivo Experiments) were developed in 2010 to help authors and journals identify the minimum information necessary to report in publications describing in-vivo experiments[101].

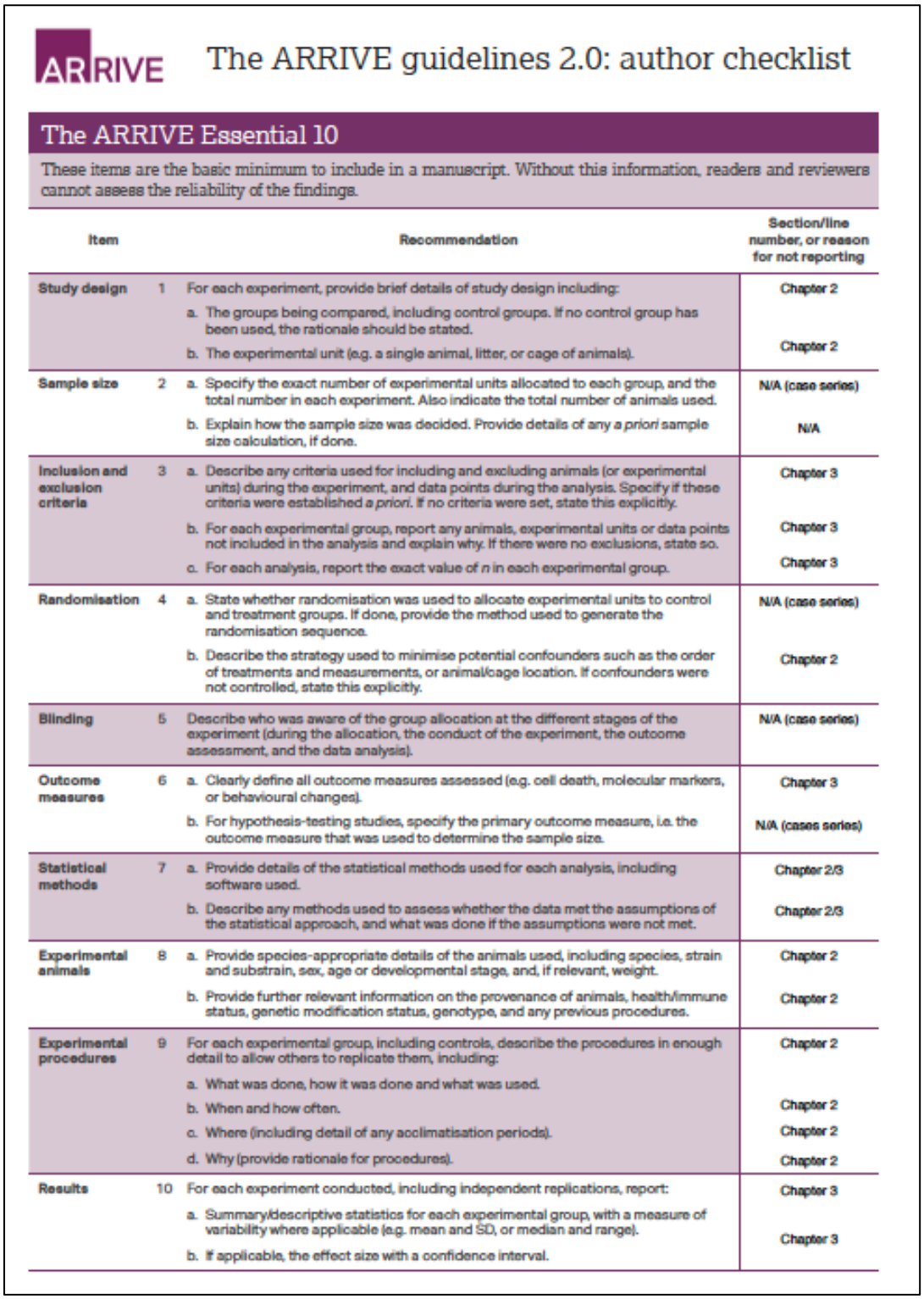

ARRIVE The ARRIVE guidelines 2.0: author checklist

The ARRIVE Essential 10

These items are the basic minimum to include in a manuscript. Without this information, readers and reviewers cannot assess the reliability of the findings.

Item		Recommendation	Section/line number, or reason for not reporting
Study design	1	For each experiment, provide brief details of study design including:	Chapter 2
		a. The groups being compared, including control groups. If no control group has been used, the rationale should be stated.	
		b. The experimental unit (e.g. a single animal, litter, or cage of animals).	Chapter 2
Sample size	2	a. Specify the exact number of experimental units allocated to each group, and the total number in each experiment. Also indicate the total number of animals used.	N/A (case series)
		b. Explain how the sample size was decided. Provide details of any *a priori* sample size calculation, if done.	N/A
Inclusion and exclusion criteria	3	a. Describe any criteria used for including and excluding animals (or experimental units) during the experiment, and data points during the analysis. Specify if these criteria were established *a priori*. If no criteria were set, state this explicitly.	Chapter 3
		b. For each experimental group, report any animals, experimental units or data points not included in the analysis and explain why. If there were no exclusions, state so.	Chapter 3
		c. For each analysis, report the exact value of *n* in each experimental group.	Chapter 3
Randomisation	4	a. State whether randomisation was used to allocate experimental units to control and treatment groups. If done, provide the method used to generate the randomisation sequence.	N/A (case series)
		b. Describe the strategy used to minimise potential confounders such as the order of treatments and measurements, or animal/cage location. If confounders were not controlled, state this explicitly.	Chapter 2
Blinding	5	Describe who was aware of the group allocation at the different stages of the experiment (during the allocation, the conduct of the experiment, the outcome assessment, and the data analysis).	N/A (case series)
Outcome measures	6	a. Clearly define all outcome measures assessed (e.g. cell death, molecular markers, or behavioural changes).	Chapter 3
		b. For hypothesis-testing studies, specify the primary outcome measure, i.e. the outcome measure that was used to determine the sample size.	N/A (cases series)
Statistical methods	7	a. Provide details of the statistical methods used for each analysis, including software used.	Chapter 2/3
		b. Describe any methods used to assess whether the data met the assumptions of the statistical approach, and what was done if the assumptions were not met.	Chapter 2/3
Experimental animals	8	a. Provide species-appropriate details of the animals used, including species, strain and substrain, sex, age or developmental stage, and, if relevant, weight.	Chapter 2
		b. Provide further relevant information on the provenance of animals, health/immune status, genetic modification status, genotype, and any previous procedures.	Chapter 2
Experimental procedures	9	For each experimental group, including controls, describe the procedures in enough detail to allow others to replicate them, including:	Chapter 2
		a. What was done, how it was done and what was used.	
		b. When and how often.	Chapter 2
		c. Where (including detail of any acclimatisation periods).	Chapter 2
		d. Why (provide rationale for procedures).	Chapter 2
Results	10	For each experiment conducted, including independent replications, report:	Chapter 3
		a. Summary/descriptive statistics for each experimental group, with a measure of variability where applicable (e.g. mean and SD, or median and range).	Chapter 3
		b. If applicable, the effect size with a confidence interval.	

Figure 33. *ARRIVE 2.0 guidelines checklist. Duplicated from du Sert et al, PLoS Biology, 2020; 18 (7); 1:65*[101].

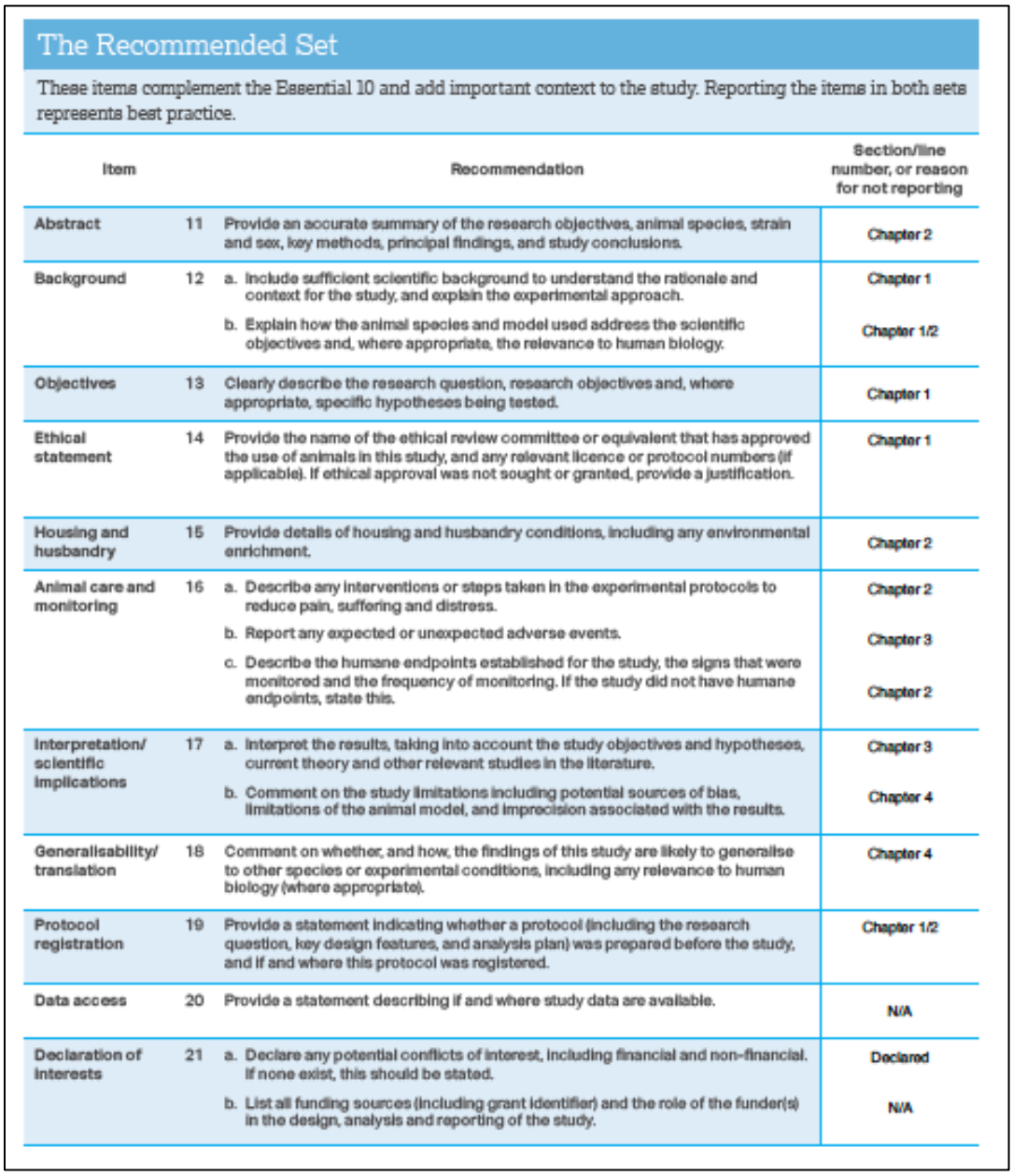

The Recommended Set

These items complement the Essential 10 and add important context to the study. Reporting the items in both sets represents best practice.

Item		Recommendation	Section/line number, or reason for not reporting
Abstract	11	Provide an accurate summary of the research objectives, animal species, strain and sex, key methods, principal findings, and study conclusions.	Chapter 2
Background	12	a. Include sufficient scientific background to understand the rationale and context for the study, and explain the experimental approach.	Chapter 1
		b. Explain how the animal species and model used address the scientific objectives and, where appropriate, the relevance to human biology.	Chapter 1/2
Objectives	13	Clearly describe the research question, research objectives and, where appropriate, specific hypotheses being tested.	Chapter 1
Ethical statement	14	Provide the name of the ethical review committee or equivalent that has approved the use of animals in this study, and any relevant licence or protocol numbers (if applicable). If ethical approval was not sought or granted, provide a justification.	Chapter 1
Housing and husbandry	15	Provide details of housing and husbandry conditions, including any environmental enrichment.	Chapter 2
Animal care and monitoring	16	a. Describe any interventions or steps taken in the experimental protocols to reduce pain, suffering and distress.	Chapter 2
		b. Report any expected or unexpected adverse events.	Chapter 3
		c. Describe the humane endpoints established for the study, the signs that were monitored and the frequency of monitoring. If the study did not have humane endpoints, state this.	Chapter 2
Interpretation/ scientific implications	17	a. Interpret the results, taking into account the study objectives and hypotheses, current theory and other relevant studies in the literature.	Chapter 3
		b. Comment on the study limitations including potential sources of bias, limitations of the animal model, and imprecision associated with the results.	Chapter 4
Generalisability/ translation	18	Comment on whether, and how, the findings of this study are likely to generalise to other species or experimental conditions, including any relevance to human biology (where appropriate).	Chapter 4
Protocol registration	19	Provide a statement indicating whether a protocol (including the research question, key design features, and analysis plan) was prepared before the study, and if and where this protocol was registered.	Chapter 1/2
Data access	20	Provide a statement describing if and where study data are available.	N/A
Declaration of interests	21	a. Declare any potential conflicts of interest, including financial and non-financial. If none exist, this should be stated.	Declared
		b. List all funding sources (including grant identifier) and the role of the funder(s) in the design, analysis and reporting of the study.	N/A

Figure 34. *ARRIVE 2.0 Recommended set. Duplicated from du Sert et al, PLoS Biology, 2020; 18 (7); 1:65*[101]